Vasopressinergic action in the olfactory bulb:

Substrates and impact on social odor processing

DISSERTATION

Zur Erlangung des Doktorgrades

der Naturwissenschaften (Dr. rer. Nat.)

der Fakultät für Biologie und Vorklinische Medizin

der Universität Regensburg

Vorgelegt von

Hajime Suyama

aus Funabashi, Japan

April 2021

Das Promotionsgesuch wurde eingereicht am 21. April. 2021.

Die Arbeit wurde angeleitet von Dr. Michael Lukas.

Unterschrift:

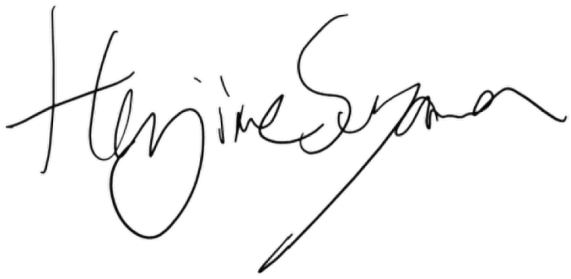

Summary

Social discrimination is a behavioral readout from rats. In the experimental paradigm, rats recognize a rat that they previously interacted with so that they show a preference towards a novel rat over the known one. Since the olfactory bulb is necessary for social discrimination, it is believed to be olfactory discrimination. The intrinsic vasopressin system in the olfactory bulb in the context of social discrimination has been demonstrated with behavioral pharmacology and the discovery of vasopressin expressing cells in the olfactory bulb using a transgenic rat expressing eGFP under the vasopressin promotor. Although it is suggested that bulbar vasopressin cells are a subpopulation of external/superficial tufted cells and vasopressin application reduces firing rates in mitral cells, detailed electrophysiological and morphological properties as well as synaptic inputs to and synaptic outputs from vasopressin cells were undetermined yet.

Chapter 2 demonstrates electrophysiological and morphological properties of vasopressin cells. My data contributes to revealing unique electrophysiological properties in vasopressin cells. Accordingly, vasopressin cells had slower membrane time constants and higher input resistances compared to other glutamatergic bulbar neurons. Further, even though vasopressin cells were initially categorized as a subpopulation of external tufted cells, firing patterns upon somatic current injections showed that vasopressin cells are dissimilar to classical external tufted cells. Biocytin filling during recordings enabled reconstruction neurite projections of vasopressin cells. Biocytin labeling combined with immunohistochemical visualization of neurophysin 2, a peptide co-expressed with vasopressin, demonstrated vasopressin expression in not only the soma but also their apical and lateral dendrites. Moreover, I found two subtypes of innervations depending on the number of axons crossing the mitral cell layer (MCL). Accordingly, type 1 cells with multiple axons crossing the MCL had denser arborization in the superficial layers and shorter branch lengths than type 2 cells that had a single axon crossing the MCL. Most neuron types in the olfactory bulb including both excitatory and inhibitory neurons are excitable following electrical olfactory nerve

stimulation in acute brain slices. Intriguingly, vasopressin cells were highly inhibited following olfactory nerve stimulation. Further, vasopressin bath application reduced amplitudes of olfactory nerve-evoked inhibitory postsynaptic potentials (IPSPs). However, vasopressin application did not alter the amplitudes of excitatory components in the existence of the $GABA_A$ receptor antagonist indicating less inhibition rather than enhanced excitation. These results indicate that olfactory cues alone, i.e., olfactory nerve inputs, are not able to excite vasopressin cells. Therefore, additional inputs than olfactory cues may be required for vasopressin cell excitation.

In chapter 3, inputs that are responsible for activating vasopressin cells were further investigated. First, it was revealed that bulbar vasopressin cells are excitable under the *in-vivo* condition, although no excitation in vasopressin cells was observed *in-vitro*. Furthermore, vasopressin cells are more activated during social interaction with a novel juvenile rat than during investigating cotton with water in the experiment using immunohistochemical visualization of eGFP and phosphorylated extracellular signal-regulated kinase (pERK), as a neural activity marker. Second, centrifugal neuromodulators, i.e., serotonin, noradrenaline, and acetylcholine, were examined if they can alter olfactory nerve-evoked inhibition in vasopressin cells *in-vitro*. Indeed, serotonin and noradrenaline reduced amplitudes of evoked IPSPs. However, acetylcholine showed more prominent effects as inhibition was reversed into excitation, i.e., excitatory postsynaptic potentials or action potentials, in 75 % of examined vasopressin cells. I further showed that the muscarinic cholinergic pathway is mainly responsible for effects on vasopressin cells. Lastly, behavioral pharmacology was performed. Local microinjection of atropine, a muscarinic receptor antagonist, into the olfactory bulb impaired social discrimination and additional microinjection of vasopressin after atropine rescued the impairment. Behavioral results indicate that the impairment by atropine is likely due to the blockade of vasopressin release. In conclusion, I suggest that olfactory inputs and acetylcholine synergistically excite vasopressin cells and presumable vasopressin release from them is involved in social discrimination.

List of Publications

This cumulative dissertation is composed of the following published or accepted manuscripts, in which I am either first or co-author:

A. Lukas, M., **Suyama, H.**, Egger, V. (2019) Vasopressin Cells in the Rodent Olfactory Bulb Resemble Non-Bursting Superficial Tufted Cells and Are Primarily Inhibited upon Olfactory Nerve Stimulation
eNeuro, ENEURO.0431-0418.2019. doi: 10.1523/eneuro.0431-18.2019

B. **Suyama, H.**, Egger, V., Lukas, M. (2021) Top-down acetylcholine signaling via olfactory bulb vasopressin cells contributes to social discrimination in rats
Communications Biology, accepted.

Personal Contributions

Publication A

The research was designed by Dr. Michael Lukas and Prof. Veronica Egger. The experimental work was designed by myself and Dr. Michael Lukas. My contributions were:

(1) Electrophysiological recordings from vasopressin cells and middle tufted cells for the comparison of electrophysiological cellular properties. Analysis was done by Dr. Michael Lukas.

(2) Visualization of biocytin-filled vasopressin cells and double staining with VP-neurophysin 2.

(3) Analysis of neurite structures in biocytin-filled vasopressin cells.

(4) Electrophysiological recordings from vasopressin cells with 50 Hz olfactory nerve stimulation.

(5) Electrophysiological recordings from vasopressin cells and mitral cells during olfactory nerve stimulation on the same brain slice and visualization of the cells with biocytin.

(6) Electrophysiological recordings and pharmacology on vasopressin cells with bicuculline and vasopressin application.

The work was supervised by Dr. Michael Lukas. The publication was written by Dr. Michael Lukas and Prof. Veronica Egger.

Publication B

The research was designed by myself and Dr. Michael Lukas. Electrophysiological recordings and pharmacology and analysis were done by myself. Immunohistochemistry and analysis were done by myself. Behavioral experiments were performed by Dr. Michael Lukas and myself. Analysis of behavior was done by Dr. Michael Lukas. Intracellular Ca^{2+} imaging was performed by Dr. Michael Lukas. The work was supervised by Prof. Veronica Egger and

Dr. Michael Lukas. The publication was written by myself, Prof. Veronica Egger, and Dr. Michael Lukas.

Table of Contents

Chapter 1: General Introduction

In this chapter, I highlight previous neurobiological and zoological findings on different social behavior and vasopressin, the neuropeptide which plays a role in various social behavior. Moreover, the contributions and functions of sensory systems, especially the olfactory system, underlying social behavior in mammals are introduced.

1.1 Social behavior

As living organisms, appropriate responses to the stimuli that we get are important for our survival. Especially in mammals, physical responses are shown as behavior. Among the vast variations of behavior, especially the ones that are associated with other individuals such as conspecifics, are called social behaviors. From birth, mammals find themselves in a social environment, with their mother or their litter mates. As grownups, after their sexual maturation, they get another social context, reproduction. Aside, non-sexual interactions with other adult individuals are still important. In most mammalian species, relationships with other individuals in their territory are directly associated with their safety, food resources, and reproduction. In this chapter, I will dissect different kinds of these social behavior (Dulac et al., 2014; Lukas and de Jong, 2015; Perna and Engelmann, 2015).

1.1.1 Parental behavior

One of the peculiarities in mammals is that offspring receive milk from their mothers and grow up under the protection and care of their mothers and in some species, their fathers. Immediately after birth, mothers lick their newborn offspring to dry them to avoid hypothermia. Further, this mechanical stimulus facilitates offspring's voluntary respiration as well. Mothers lay down next to or even over their offspring to feed them and keep them warm. Moreover, mothers often lick offspring's anogenital regions to promote excretion and for cleaning purposes. Parental behavior is observed not only from mothers but also from fathers in different mammalian species. Male prairie voles and California mice are known to show

paternal behavior which is the same as typical maternal behavior. Interestingly, males of uniparental species raised by close-related biparental species parents showed more paternal behavior than controls raised by their own uniparental species. This finding indicates that environmental factors during early life are important for regulation of paternal behavior in addition to genetic differences (Dulac et al., 2014). Offspring do not just wait for their mothers doing so, but they also emit signs for mothers to take care of them. In rodents, it is known that pups emit ultrasonic vocalizations to attract mothers and promote their maternal behavior typically when they are in social isolation (Dulac et al., 2014). Another mammalian species in which maternal behavior has been investigated is sheep, because of its lamb recognition. Ewes recognize their own lambs according to the lamb's odors and calls, which results in rejecting other's lambs (Baldwin and Shillito, 1974; Searby and Jouventin, 2003). Not only one but multiple sensory systems are involved in promoting parental behavior. Early research studied maternal behavior of female rats that lost some sensations, i.e., removal of eyes, lesion of the olfactory bulb, or anesthesia of the snout and lip region. Intriguingly, although the impairment of one sensation delays the onset of retrieving their pups, they can still retrieve them completely. Even several sensory deficits do not entirely abolish maternal retrieving behavior, however behavioral impairments are stronger (Beach and Jaynes, 1956). Since ultrasonic vocalizations from pups are another crucial factor promoting maternal behavior in rodents, the audition is also obviously involved. Smotherman et al. (1974) examined maternal motivation using a modified Y maze. Stimuli presented were an intact pup, a pup anesthetized by hypothermia (Phifer and Terry, 1986), or playback of taped pup ultrasonic vocalizations. Subject mother rats or mice could explore two arms presenting stimuli beyond a mesh separation. Both, mother rats and mice spend similar time in both arms presenting either taped vocalizations or nothing, indicating that pup vocalization alone is enough for mothers to be motivated to search their pups. However, results further suggest that pup vocalization is not enough to localize their pups. Surprisingly, when a chilled pup and taped vocalizations are presented in each arm, mothers show a preference, even though

rats and mice showed the opposite preference. Accordingly, rats spent a longer time in an arm with taped vocalizations whereas mice spent longer in an arm with a chilled pup. The authors suggested that, even if there is a species-specific difference between rats and mice, the combination of two sensations is essential for successfully establishing maternal retrieval behavior. Moreover, some brain regions involved in maternal behavior show multi sensation-dependent neural activation. The bed nucleus of the stria terminalis and the medial preoptic area in mother mice show increased c-Fos expression levels only when both, pup ultrasonic vocalizations and pup olfactory cues are presented. In contrast, c-Fos expression stays at basal levels when either auditory or olfactory cues alone are presented (Okabe et al., 2013).

1.1.2 Sexual behavior/partner preference

One of the most important goals for organisms is reproduction. Mammals have two sexes, and each produces eggs or sperms. Since in mammals, internal fertilization occurs, copulation is carried out for reproduction. Sexual behavior has been investigated a lot in rodents. Typically, in mice or rats, males approach a female first. They investigate a female with sniffing to obtain information including sex hormone-regulated, hence estrous cycle-dependent olfactory cues. If the female is not receptive, not estrous, she shows rejection, e.g., escaping from the male or standing with facing the male. If the female is receptive, she stays and the male starts the so-called consummatory phase in which the male tries to mount the female from behind and the female reacts with a receptive posture, so-called lordosis. This acceptance from the female allows the male to insert his erected penis, intromission, and finally, sperm is ejaculated (Lukas and de Jong, 2015). Being associated with sexual behavior, sexual preference is measured especially in the research of the vomeronasal system, in which both, male and female animals were presented in different components of experimental apparatus to assess the preference of investigation from the subject animal. If recognition of sex is performed properly, subjects investigate or stay longer with the opposite sex (Pankevich et al., 2004; Baum and Kelliher, 2009).

Sexual behavior is known to be modulated by olfactory cues. Especially pheromones have been investigated as social chemosignals regulating other individual behavior in rodents (Baum and Kelliher, 2009; Asaba et al., 2014a). ESP1 is a pheromone secreted in male mouse tears (Kimoto et al., 2005). This was found through the investigation of male mouse pheromones that activate the vomeronasal epithelium in female mice. Since then, this pheromone has been investigated in detail with its effect on female sexual behavior including the associated neural networks. ESP1 binds to V2Rp5 expressed in vomeronasal sensory neurons projecting to the posterior region of the accessory olfactory bulb (AOB, Kimoto et al., 2005; Haga et al., 2010). Projection neurons, mitral/tufted cells in the AOB send their signals to the medial amygdala which sends its projections further to the ventromedial hypothalamus, a neural center responsible for sexual behavior (Ishii et al., 2017). Female mice exposed to ESP1 show increased receptive behavior, i.e., lordosis, compared to unexposed controls (Haga et al., 2010).

In addition, sexually attractive calls from males towards females are also known. In mice, the ultrasonic vocalizations of males are testosterone dependent (Dizinno and Whitney, 1977) and attract females when olfactory cues are also presented (Asaba et al., 2014b). Asaba et al. (2017) demonstrated that female mice approach intact males more than males who cannot emit vocalization due to surgical lesion of the inferior laryngeal nerve. This finding implies that even though olfactory signaling is predominant, both, olfactory and auditory cues induce female sexual motivation.

Prairie voles are famous in behavioral neuroscience for their monogamy. Both males and females exclusively prefer their mating partners after they form the pair bonding, and even males show aggression towards stranger females which is merely seen in mice or rats. This pair-bonding also depends on olfaction. Extraction of the olfactory bulb (OB) or the vomeronasal organ before mating impairs pair-bonding formation in female prairie voles (Williams et al., 1992; Curtis et al., 2001).

1.1.3 Aggression

Even though aggression is often described as a “bad” or unwanted behavior in human society, it is quite important behavior in nature. Aggression is usually observed in a context where animals have conflicts in their purposes, such as the territory, mating partners, or litters. In territorial mammalian species, such as mice, the most robust intermale aggression can be observed. In the laboratory, the resident-intruder test is carried out for testing this behavior. As soon as a mouse in his home cage, the resident, finds a stranger mouse, he approaches and investigates the intruder and displays aggressive behavior, typically biting the intruder on the back or neck and chasing it away (Hattori et al., 2016). Rats show more variability, such as lateral threat or clinch (Veenema et al., 2010).

Interestingly, olfactory-related neural circuits responsible for aggression are similar to those for sexual behavior in rodents. ESP1, described as a releaser pheromone on female sexual behavior above, influences male aggression as well. ESP1 binds V2Rp5 in the vomeronasal organ, then signals travel through the AOB to the medial amygdala. However, the target regions of the medial amygdala are different. The medial preoptic area and bed nucleus of the stria terminalis show elevated activation with ESP1 stimulation, which is in line with that both brain regions are known to modulate aggression in mice (Haga et al., 2010). Moreover, olfactory bulbectomy reduces rat aggression indicating that olfaction is crucial for aggression (Bandler Jr and Chi, 1972). Rats whose whiskers are surgically removed showed lower aggression, suggesting that tactile stimuli in the snout region are also involved in rat aggressive behavior (Bugbee and Eichelman Jr, 1972).

Females in various species also show aggression especially when they have offspring. Rejection of strange lambs mentioned above is one example. Ewes emit high-pitched bleats and butt the strange lambs. Moreover, in rodents, maternal aggression towards males is known. Like some other mammalian species, male mice and rats tend to kill pups when they are not theirs (Isogai et al., 2018). To prevent this, dams show aggression towards males (Lonstein and Gammie, 2002; Bosch, 2013). This aggression is also found to be regulated by

both olfactory and tactile stimuli. In a context of maternal aggression, the origins of stimuli are not only intruders but also pups. Indeed, when mother rats are separated from their pups for at least four to five hours, maternal aggression is significantly reduced. Unlike maternal behavior or male aggression, it is likely to highly depend on tactile stimuli from pups around the ventral part of mothers. However, olfactory cues from pups also play an important role, as mothers who receive only olfactory cues but no physical stimulation from pups, still show maternal aggression. In addition, of course stimuli from the intruder are essential to promote maternal aggression. Because of mixed odor sources, i.e., pups and the intruder, in a context of maternal aggression, the involvement of olfactory cues from the intruder is only suggested. The olfactory bulbectomy reduces maternal aggression, however as described above, this result still cannot exclude that this surgery impairs maternal aggression by abolishing pup-originated olfactory inputs. Similar to male aggression, the importance of whiskers was reported, as anesthesia of mystacial pads of mothers reduced maternal aggression. Moreover, mothers showing aggression in that experiment sniff the intruder more, indirectly suggesting the involvement of intruder-derived olfactory inputs as well (see review Lonstein and Gammie, 2002).

1.1.4 Recognition

A shared feature of the social behavior explained above is that mammals should firstly investigate other animals. Investigation is crucial for animals to choose which behavior they should show. Proper choice of social behavior is of course essential to enhance their quality of life, such as protecting their territory or their reproductive success (Lukas and de Jong, 2015). To do this, there are characteristics to recognize and distinguish such as sex and individuals. Especially, recognition of individuals is thought to strongly depend on the olfactory system. The following sections convey previous studies related to individual recognition to more extent.

1.2 Social memory

Social memory is often used to describe the phenomenon in which animals recognize a known conspecific or discriminate known and novel conspecifics. As mentioned above, recognition and discrimination of individuals are important for showing proper social behavior towards them. Traditionally, researchers quantify rodent social recognition ability with so-called habituation-dishabituation tests, which can also be used for non-social stimuli. The test is carried out by letting subject animals investigate the same stimulus animal several times, usually 4 sessions, until the subject animals lose their motivation to investigate the stimulus animal through sessions as they recognize the stimulus animal, habituation. Finally, when a novel stimulus animal is introduced, the subject animals show again high motivation to investigate the novel one (Winslow, 2003). In 1995, Engelmann et al. introduced an alternative way to quantify their recognition ability, the social discrimination paradigm (Engelmann et al., 1995). This test is supposed to be a more difficult task for animals since they have to choose one animal from two animals presented. In the first session, the sampling phase, a stimulus animal is introduced to a subject animal for social interaction. After a certain length of an inter exposure interval, usually 30 or 60 minutes for rats and 120 minutes to 24 hours for mice, a known and a novel stimulus animal are simultaneously introduced to the subject animal, the discrimination phase. If the subject recognizes the known one, it investigates rather the novel one than the known one (Engelmann et al., 2011). An involvement of vasopressin or oxytocin in social memory has been revealed. Further, some brain regions are known to be crucial for social discrimination, such as the lateral septum, the hippocampus, and the OB. I the next section, I introduce findings of the role of vasopressin and oxytocin, and about the brain region which I focused on in this thesis, the OB.

1.2.1 Vasopressin and oxytocin in social memory

Vasopressin and oxytocin are neuropeptides consisting of nine amino acids. They are known to have both, peripheral and central effects. Although oxytocin cells are found only in the hypothalamus and bed nucleus of the stria terminalis, vasopressin cells are found in various regions, e.g., the hypothalamus, the bed nucleus of the stria terminalis, the locus coeruleus, the anterior olfactory nucleus, and the OB. Even though they have a different expression distribution, both neuropeptides are known to modulate social behavior. One of such social behavior is social memory in rodents. Intracerebroventricular injection of vasopressin or oxytocin elongates social memory in rats (Dluzen et al., 1998a). Further, oxytocin knock-out (KO), oxytocin receptor KO, and vasopressin receptor KO mice show impaired social memory (Ferguson et al., 2000; Bielsky et al., 2004; Takayanagi et al., 2005). Region-specific data has been demonstrated as well. Microinjection of the vasopressin or oxytocin antagonist into the lateral septum impairs social memory (Bielsky et al., 2005; Lukas et al., 2013). It is also shown that conditional KO of oxytocin receptors in the mouse hippocampus and local application of oxytocin receptor antagonist into the rat medial amygdala impairs social memory (Lukas et al., 2013; Raam et al., 2017).

Most importantly for my thesis, vasopressin and oxytocin systems in the main OB (MOB) are associated with social memory as well.

1.2.2 Anatomy of the MOB

For a better understanding of the microcircuits in the MOB involved in social memory, I briefly summarize the cellular anatomy of the MOB (see Fig. 1). The MOB is the very first brain region that receives olfactory signals from the peripheral sensory organ, the olfactory epithelium in the nasal cavity. Because of the well-organized distribution of different cell types and their innervations, several layers in the MOB can be observed with nucleus stainings, such as DAPI or Nissl. The olfactory nerve (ON) which consists of axons of the olfactory sensory neurons in the olfactory epithelium, innervates into the MOB and

terminates in glomeruli in the glomerular layer (GL), the most outer bulbar layer. Glomeruli mainly consist of interneurons shaping the round structure of a glomerulus, ON axons, and apical dendrites of projection neurons. Major inhibitory neurons in the GL are periglomerular cells (PGCs) and short axon cells (SACs). Both are GABAergic and SACs are also known to express dopamine. Moreover, it is known that some of them receive direct excitatory inputs from the ON and others receive excitatory inputs from external tufted cells (eTCs) that are excitatory neurons located in the GL. PGCs form intraglomerular circuits, whereas SACs innervate neighboring glomeruli (Kiyokage et al., 2010). Juxtaglomerular interneurons, e.g., PGCs and SACs, inhibit excitatory neurons, such as eTCs and mitral cells (MCs) as well as each other (Liu et al., 2013; Liu et al., 2016; Shao et al., 2019). Thus, the GL is thought to be the first level of processing incoming olfactory signals. The most apical excitatory neurons in the MOB are eTCs. With their apical dendrites, they usually innervate a single glomerulus, where they receive excitatory inputs from the ON. As mentioned above, eTCs excite juxtaglomerular interneurons, but also excite projection neurons, such as tufted cells (TCs) and MCs via their tuft structure on apical dendrites. Those two subpopulations of bulbar projection neurons are defined by the location of their somata. TCs are located in the external plexiform layer (EPL), whereas MCs are located in the mitral cell layer (MCL). Both cell types innervate with their apical dendrites to glomeruli and lateral secondary dendrites through the EPL where they form reciprocal synapses with interneurons. Projection neurons send their axons to the olfactory cortex via the lateral olfactory tract. The granule cell layer is occupied mostly by GABAergic axonless interneurons, granule cells (GCs). They innervate with their dendrites to the EPL where dendrodendritic reciprocal synapses with secondary dendrites of projection neurons are formed. Since GCs are axonless, they inhibit projection neurons via dendrodendritic synapses. Accordingly, glutamate released from dendrites of projection neurons binds AMPA and NMDA receptors on GC dendrites resulting in GABA release from GC dendrites inhibiting projection neurons via GABA receptors on their dendrites (Nagayama et al., 2014).

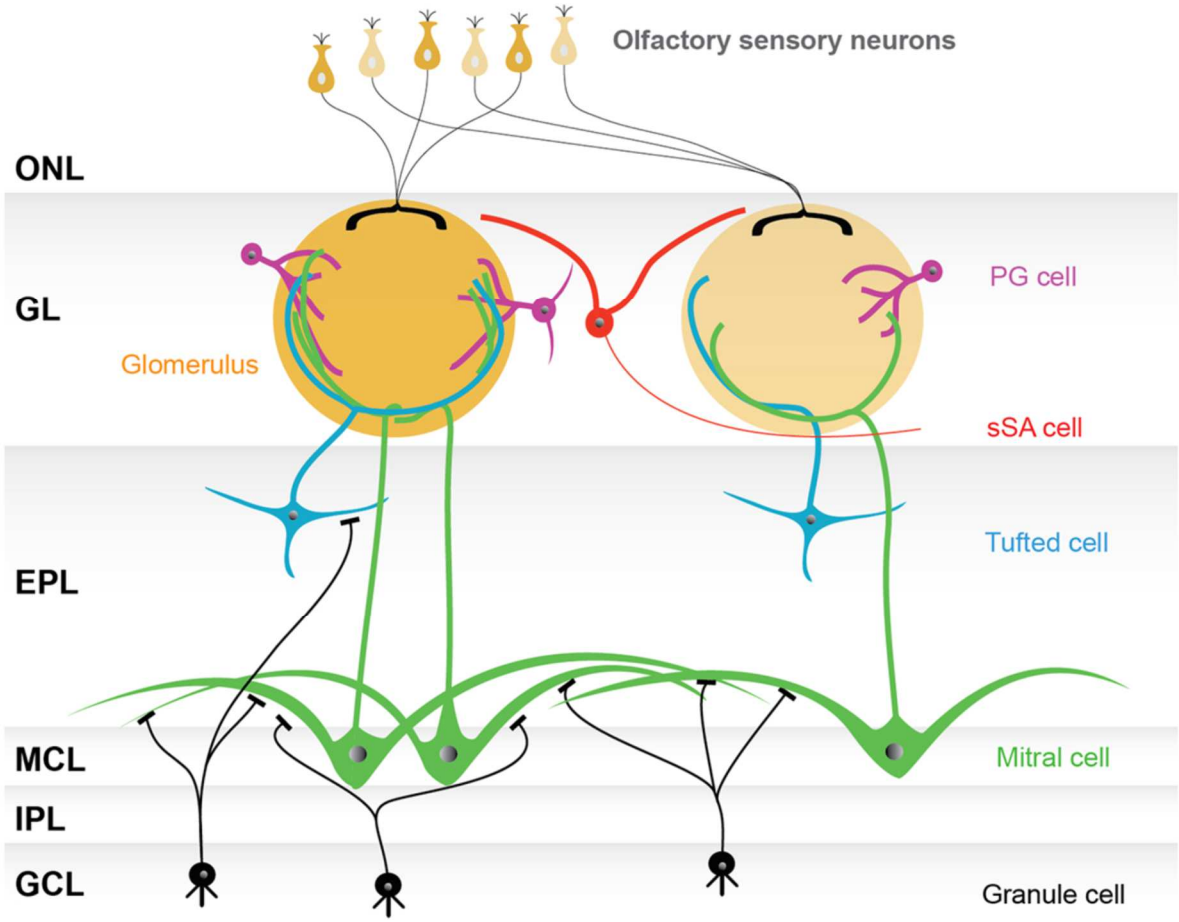

Fig. 1 **Overview of MOB anatomy**

ONL, olfactory nerve layer; GL, glomerular layer; EPL, external plexiform layer; MCL, mitral cell layer; IPL, internal plexiform layer; GCL, granule cells layer. Adapted from Nagayama et al. (2014).

1.2.3 The role of the MOB and the intrinsic neuropeptide system in social memory

It is thought that animals discriminate individuals via olfactory cues, individual olfactory signatures, during the social recognition/discrimination task. This was shown with the olfactory bulbectomy, which results in impairment of social memory (Dantzer et al., 1990). The vasopressin or oxytocin system in the MOB modulates social memory since it is shown that antagonists of vasopressin or oxytocin injected into the MOB impair social memory (Dluzen et al., 1998a; Tobin et al., 2010). Intriguingly, the impairment of the bulbar vasopressin system does not disrupt the recognition of simple odors. Thus, the vasopressin system is involved in social memory but not in simple odor perception (Tobin et al., 2010).

Not only the bulbar vasopressin effects on social discrimination, but also vasopressin expressing cells (VPCs) in the superficial EPL in the MOB were found (Fig. 2). They innervate with their apical dendrites to a single glomerulus having a dendritic tuft structure indicating that they receive direct inputs from the ON. In addition, they co-express vasopressin and glutamate, but not GABA. Thus, they are categorized as a subpopulation of eTCs (Tobin et al., 2010). Contrary to other excitatory projection cells, i.e., middle TCs and MCs, VPCs do not project their axons to most of olfactory cortices, i.e., the cortical amygdala, the piriform cortex, and the olfactory tubercle, although some projections into the anterior olfactory nucleus were found. Vasopressin receptors, both V1a and V1b receptors are expressed in various cell types in the MOB. *In-vivo* electrophysiological recordings revealed that vasopressin application reduces the firing frequency of MCs responding to odor stimulation in anesthetized rats (Tobin et al., 2010). However, the question remains what kind of stimuli excite VPCs to release vasopressin.

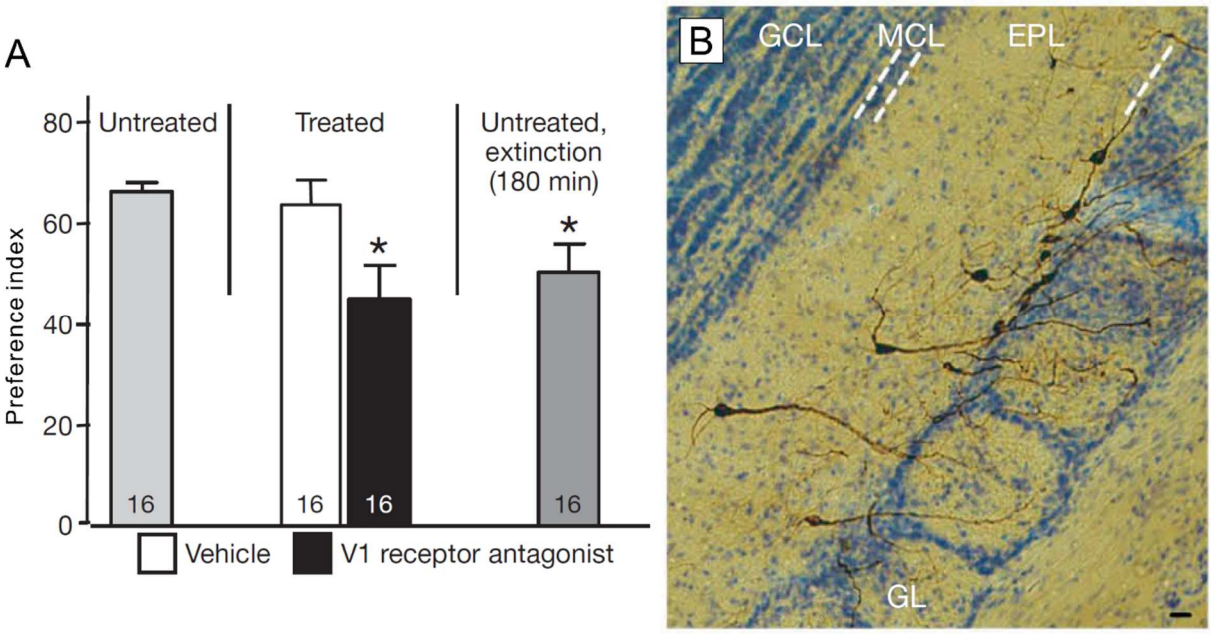

Fig. 2 **An intrinsic bulbar vasopressin system is involved in social discrimination**
(A) Preference index is the percentage of investigation time towards a novel stimulus rat over investigation time towards both, the known and a novel stimulus rat in the discrimination phase (inter-phase interval was 30 min for the untreated, Vehicle, and V1 receptor antagonist groups and 180 min for the untreated-extinction group). Bar charts represent mean ± SEM. *p<0.05 vs. Vehicle. (B) Representative picture of eGFP-expressing VPCs. GL, glomerular layer; EPL, external plexiform layer; MCL, mitral cell layer; GCL, granule cells layer. Scale bar, 20 µm. Adapted and modified from Tobin et al. (2010).

Wacker et al. (2011) addressed this question using transgenic vasopressin-eGFP rats with different types of stimulation, the mixture of non-social synthesized odorants, or a novel juvenile rat. Surprisingly, immunohistochemistry revealed that both stimulations barely lead to expression of c-Fos or Egr-1 in bulbar VPCs. I conducted similar experiments with exposures to a juvenile rat or urine from juvenile rats to explore VPC activity during social interaction using a different neural activity marker and discuss the results in chapter 3 (publication B).

In addition, indirect effects of oxytocin on GC activity and social memory via the anterior olfactory nucleus (AON) were shown (Oettl et al., 2016). In both the MOB and the AON, oxytocin receptors are expressed and the AON sends glutamatergic projections to the MOB (Vaccari et al., 1998; Matsutani and Yamamoto, 2008). Oettl et al. (2016) showed that on sagittal acute rat brain slices, the oxytocin receptor agonist, TGOT, applied onto the AON

increases the frequency of spontaneous excitatory postsynaptic currents (EPSCs) in GCs, although direct application of TGOT onto the MOB with a cut of projections between the MOB and the AON does not. Further, conditional oxytocin receptor KO in mouse AON impairs social memory (Oettl et al., 2016). Results suggest that the excitatory drive by oxytocin on GCs via the AON is involved in social memory.

1.3 Other social olfactory-related memory

As still only little is known in terms of the circuitry mechanisms of social memory in the rodent MOB, I intend to review studies on similar social olfactory-related memory, maternal memory in ewes, and the Bruce effect in mice. Although the sex of subject animals is female and their contexts can be more complex as parturition or mating is involved, lesion or inactivation of main or accessory olfactory systems impairs those social memory functions (Baldwin and Shillito, 1974; Kaba and Keverne, 1988), as it impairs social recognition/discrimination in rats (Dantzer et al., 1990). Thus, there should be notable mechanisms that can be shared between those social olfactory-related memories.

1.3.1 Lamb recognition in ewes

As described above, ewes recognize their own lambs to let them suckle and refuse lambs from others. This recognition is based on olfactory cues from lambs and it is functional already a day after birth (Tschanz, 1962). Interestingly, after artificial vaginocervical stimulation is performed, ewes accept also alien lambs as if they establish new memory indicating that vaginocervical inputs are involved in formation of lamb memory (Kendrick et al., 1991). Microdialysis revealed that the oxytocin level in the OB is elevated after birth or vaginocervical stimulation (Kendrick et al., 1988; Lévy et al., 1995). Moreover, the concentration of various other neurotransmitters in the OB is increased after parturition or vaginocervical stimulation, such as glutamate, GABA, dopamine, noradrenaline, and acetylcholine (Kendrick et al., 1988; Lévy et al., 1993). Indeed, oxytocin microinjection into

the OB of mothers mimicking release during the parturition enables them to establish new memory of other lambs (Kendrick et al., 1997b). Either microperfusion of a noradrenergic antagonist in the OB or the systemic injection of a muscarinic receptor antagonist during parturition increases acceptance of alien lambs (Lévy et al., 1990; Lévy et al., 1997). These results indicate that those neurotransmitter signals during the parturition are crucial for lamb recognition. Maternal behaviors are hypothesized to be modulated by altered activity in the MOB. Accordingly, *in-vivo* electrophysiological recordings after birth showed that more MCs are activated reacting to lamb odors than before birth, moreover, a part of them is more activated to odors of their own lamb than of alien lamb after birth (Kendrick et al., 1992). In addition to neurotransmitters, nitric oxide (NO) is released during parturition. Kendrick et al. (Kendrick et al., 1997a) demonstrated potential mechanisms of synaptic plasticity in the ewe OB responsible for lamb recognition (Fig. 3). When sheep give birth, information of both olfactory cues from a newborn lamb and vaginocervical stimulation reach the brain. Since the noradrenaline level is elevated through parturition as well, they proposed that noradrenaline is released reacting to vaginocervical stimulation and acts on β-noradrenergic receptors on GCs, inhibitory interneurons, reducing GABA release to MCs. Disinhibited glutamate release from MCs acts on NMDA receptors and/or AMPA receptors to induce NO release in MC-GC synapses. Moreover, NO is known to induce long-term potentiation (LTP) in the hippocampus (Zhuo et al., 1993). NO increases glutamate release that could induce LTP (Kendrick et al., 1997a). Finally, enhanced connectivity in lamb-odor stimulated MC-GC synapses would result in better odor representation which helps to recognize own-lamb odors.

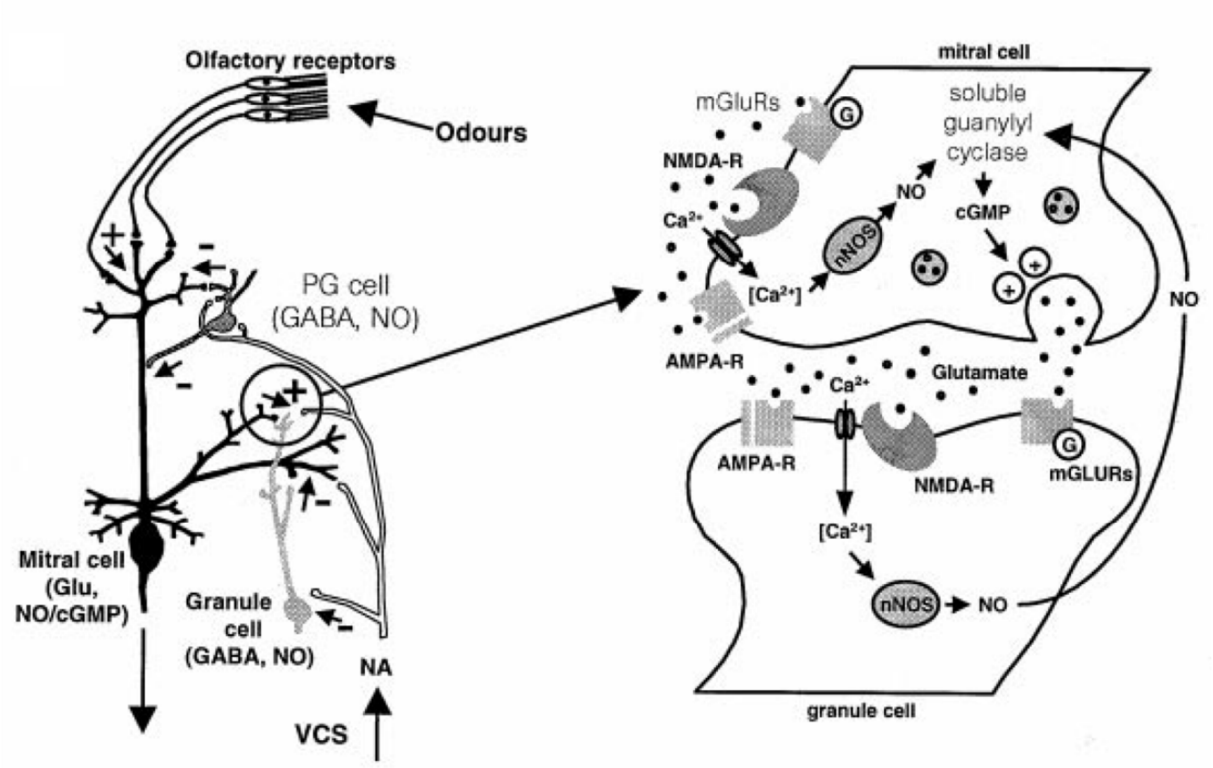

Fig. 3 **Schematic picture of neural mechanisms underlying lamb recognition**
The plus and minus signs represent excitatory and inhibitory effects, respectively. The right scheme shows the proposed molecular pathway influenced by NO. Glu, glutamate; nNOS, neural nitric oxide synthase. Adapted from Kendrick et al. (1997a)

1.3.2 The Bruce effect

Another example of social odor-related recognition is the Bruce effect. This pheromonal memory in female mice was introduced by Hilda M. Bruce in 1959 (see Fig. 4, Bruce, 1959). Memory of pheromonal patterns of their mating partner is formed in the female AOB within 5 hours after copulation (Kaba et al., 1989). Synaptic plasticity in MC-GC reciprocal synapses allows the AOB to transmit pheromonal information which is from a mating partner, to the medial amygdala less efficiently, due to stronger inhibition by GCs (Brennan et al., 1995; Matsuoka et al., 2004; Binns and Brennan, 2005). Whereas partner's signals are not transmitted efficiently further than the medial amygdala, pheromonal signals from other male strains reaching the medial amygdala finally stimulate dopaminergic neurons in the arcuate hypothalamic nucleus. Dopamine released there inhibits prolactin surges in the periphery

which is essential to maintain corpora lutea function in mice, resulting in a failure of embryo implantation, i.e., pregnancy block (Rosser et al., 1989; Matthews et al., 2013).

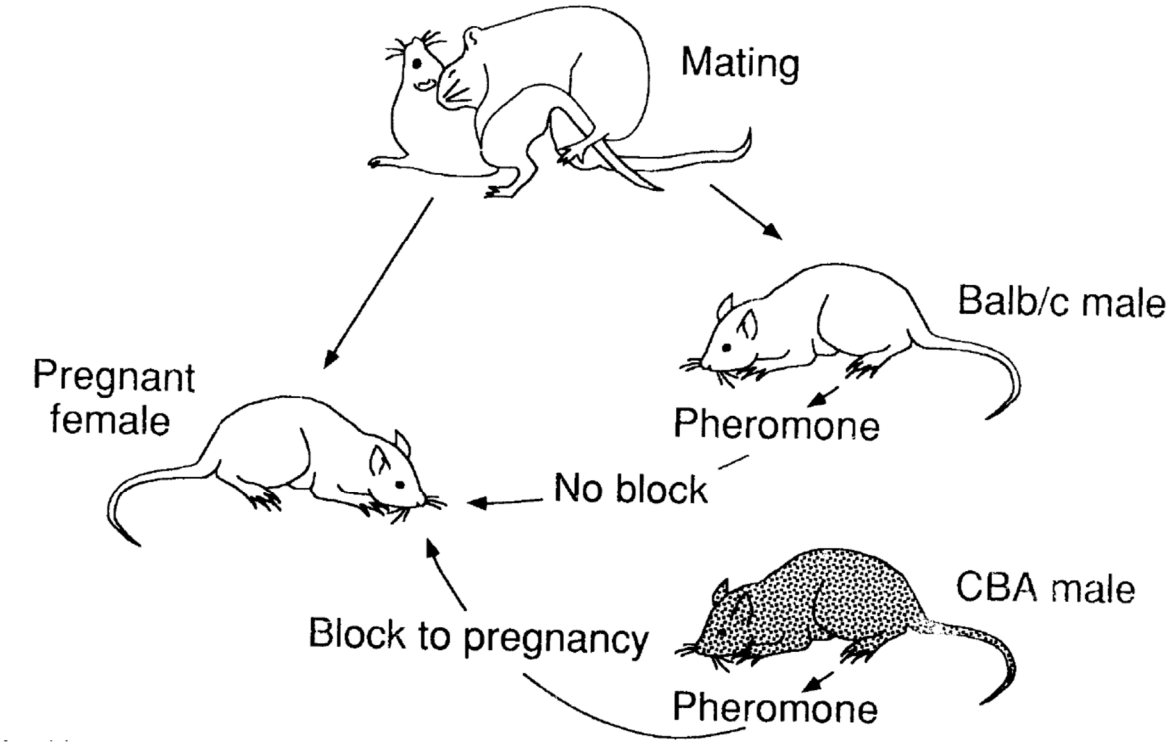

Fig. 4 **The Bruce effect**
Memory of pheromones from a mating partner is established following copulation. If Balb/c is the strain of the mating partner, pheromones from the same strain do not prevent pregnancy, however pheromones from other strains, e.g., CBA, block pregnancy. Adapted from Kaba et al. (1995).

The neural and molecular mechanisms of synaptic plasticity underlying the Bruce effect have been investigated as well. Like lamb recognition, this pheromonal memory is also hypothesized to be regulated by LTP in the MC-GC reciprocal synapses in the AOB. Indeed, 400 pulses of 20-Hz electrical antidromic stimulation of MCs is enough to induce facilitated field excitatory postsynaptic potentials (EPSPs) in presumable GCs (Fang et al., 2008). Electron microscopic observation supports this finding as more excitatory synapses are found after mating in MC-GC synapses (Matsuoka et al., 2004). Thus, more feedback inhibition from GCs onto MCs is indicated. Microdialysis revealed that after mating, the glutamate level is less elevated than only introduction of males without mating in the AOB.

Whereas, the noradrenaline level is elevated only in the mating group (Brennan et al., 1995). Furthermore, blockade of α-adrenergic receptors in the AOB or ablation of noradrenergic innervations by 6-hydroxydopamine impairs formation of pheromonal memory indicating involvement of noradrenaline (Rosser and Keverne, 1985; Kaba and Keverne, 1988). *In-vitro* electrophysiology demonstrated that bath-applied noradrenaline enables the facilitation of LTP within MC-GC reciprocal synapses using an antidromic subthreshold stimulation of MCs via α2 adrenergic receptors (Huang et al., 2018). Social behavior-related neuropeptides, such as vasopressin and oxytocin are also indicated to establish this pheromonal memory. Wersinger et al. (Wersinger et al., 2008) investigated them using transgenic mice, i.e., oxytocin KO, V1a receptor KO or V1b receptor KO mice. V1b receptor KO mice showed a low pregnancy block rate in both the familiar male exposure and unfamiliar male exposure group. However, V1a receptor KO mice showed a high pregnancy block rate only in the unfamiliar male exposure group as observed in wild-type mice. Results indicate the involvement of V1b receptors but not V1a receptors in pheromonal memory formation. In addition, oxytocin KO mice showed a high pregnancy block rate in both the familiar male exposure and unfamiliar male exposure group (Wersinger et al., 2008). Although KO of different genes results in variable consequences, results indicate that those neuropeptides play a role in establishing pheromonal memory. Further, oxytocin was shown to reinforce facilitation of LTP in MC-GC synapses *in-vitro*. Subthreshold stimulation of MCs can induce LTP within MC-GC synapses under oxytocin bath application (Fang et al., 2008). However, to my knowledge, effects of vasopressin on LTP facilitation in the AOB are still unknown.

1.4 Centrifugal neuromodulation in the olfactory bulb

The previous section demonstrated that not only classical neurotransmitters, e.g., glutamate, GABA, and intrinsic neuropeptides, but also centrifugal neuromodulators, e.g., noradrenaline and acetylcholine, are involved in memory formation. Indeed, the MOB receives dense

centrifugal projections of serotonin, noradrenaline, and acetylcholine (Fig. 5). In this section, I focus on the effects of centrifugal neuromodulators in the main olfactory system in rodents.

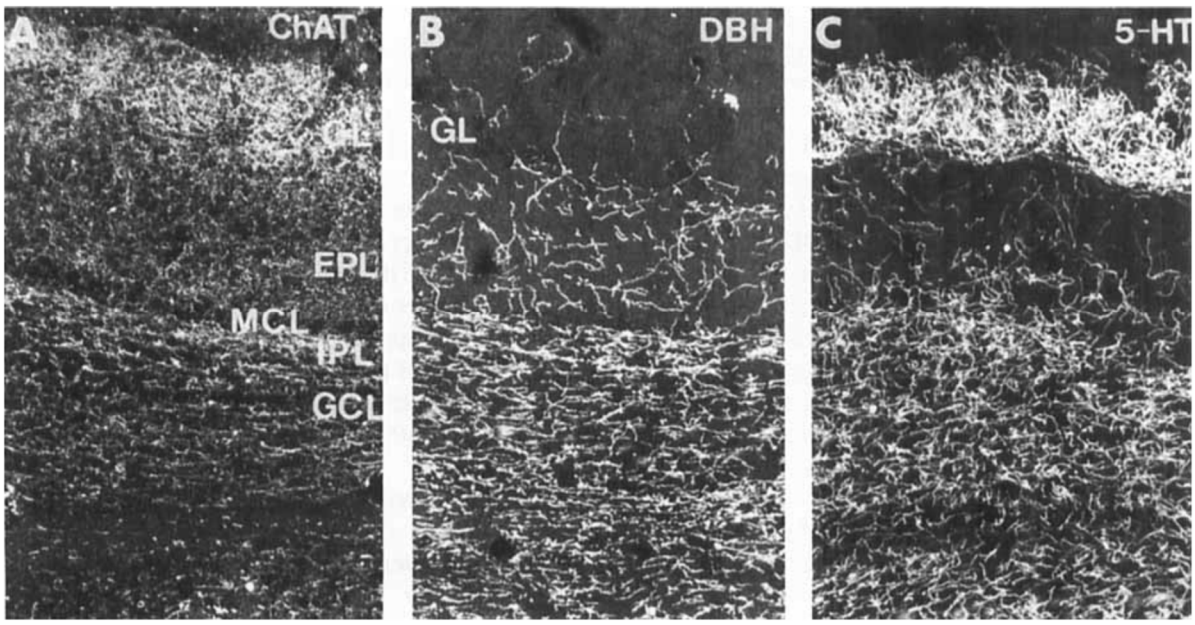

Fig. 5 **Centrifugal neuromodulatory projections in the MOB**
Immunohistochemistry pictures represent cholinergic (A), noradrenergic (B), and serotonergic (C) projections in the MOB. Projections were visualized using antibodies against ChAT (choline acetyl transferase, A), DBH (dopamine-B-hydroxylase, B), or serotonin (5-HT, C). Adapted from Shipley and Ennis (1996). GL, glomerular layer. EPL, external plexiform layer. MCL, mitral cell layer. IPL, internal plexiform layer. GCL, granule cell layer.

1.4.2 Serotonin

Bulbar serotonergic innervations originate from the raphe nucleus in the brain stem. The GL contains the most prominent serotonergic projections (McLean and Shipley, 1987). Several subtypes of serotonergic receptors are known in the OB, e.g., 5-HT_{2A} receptors in the GL and on MCs, and 5-HT_{2C} receptors in the GL (Yuan et al., 2003; Petzold et al., 2009; Brill et al., 2016). Via 5-HT_{2A} receptors, serotonin induces EPSCs and increases spontaneous firing frequency in eTCs and MCs (Liu et al., 2011; Brill et al., 2016). Serotonin excites SACs but not PGCs. SACs show depolarization in response to the application of serotonin, which is mediated by 5-HT_{2C} receptors. This excitation of SACs increases action potential-independent GABA release to eTCs, PGCs, and SACs themselves. In PGCs and SACs,

serotonin increases the frequency of both spontaneous EPSCs via 5-HT_{2A} receptors and spontaneous inhibitory post synaptic currents (IPSCs) via 5-HT_{2C} receptors (Brill et al., 2016). Serotonin is involved in sexual behavior and aggression in mammals. Serotonin tones down sexual behavior in both sexes (e.g., ejaculation or lordosis, Olivier et al., 2019). In aggression, it is likely that the serotonin activity should be finely tuned as both, high and low activity of tryptophan hydroxylase 2 which mediates serotonin synthesis, elevate aggression in mice (Tricklebank and Petrinovic, 2019). However, to my knowledge, relationships between serotonin effects on those social behavior and the OB function are not known yet. Olfactory-related behavioral effects of serotonin are shown in a paradigm in which preference to odor which was paired with an artificial brush stroke stimulus on neonatal rats is examined. As a control result, neonatal rats prefer odor which was paired with a stroke stimulus over non-paired odor. Depletion of serotonergic fibers in the OB impairs this preference (McLean et al., 1993) and serotonergic actions are mediated by 5-HT_2 receptors (McLean et al., 1996). These studies indicate that serotonin is involved in olfactory-related learning.

1.4.3 Noradrenaline

The locus coeruleus sends noradrenergic fibers to the OB, particularly in inner layers, such as the internal plexiform layer (IPL) and the granule cell layer (Mclean et al., 1989). Noradrenaline has inverted-U shape dose-dependent effects on MC inhibition via GC activity. Low concentration (<1 µM) decreases the frequency of spontaneous IPSCs in MCs and reduces spontaneous firing rates via hyperpolarization in GCs. This effect is shown to be mediated by activation of α2 receptors on GCs. Accordingly, action-potential independent IPSCs in MCs are reduced with selective activation of α2 receptors by simultaneous application of noradrenaline, α1, and β antagonists (Nai et al., 2009; Nai et al., 2010). However, intermediate concentrations (1-30 µM) show the opposite effects on both MCs and GCs. Thus, spontaneous IPSPs in MCs and spontaneous firing in GCs are increased with intermediate concentrations. This enhancement is mediated by α1 receptors or β receptors.

α1 receptors are presumably expressed on GCs since the frequency of action potential independent IPSCs in MCs is also enhanced by activation of α1 receptors. β receptors are likely expressed on MCs as the enhancement of the frequency of IPSCs in MCs by activation of β receptors is action-potential dependent (Nai et al., 2009; Nai et al., 2010). Interestingly, higher doses (>100 μM) show reduced enhancement of the spontaneous IPSC frequency in MCs than intermediate concentrations (Nai et al., 2009).

Noradrenaline is involved in social memory. Although pharmacological depletion of bulbar noradrenergic projections alone does not alter social discrimination, the depletion impairs prolongation of memory by VP or oxytocin injection in rats (Dluzen et al., 1998b). As mentioned above, noradrenaline is also known to modulate synaptic transmission in the MOB or the AOB to establish olfactory memory in sheep or mice, respectively, in reproductive contexts (Rosser and Keverne, 1985; Kaba and Keverne, 1988; Lévy et al., 1990; Huang et al., 2018). Moreover, olfactory learning in neonatal rats as shown above is also regulated by noradrenaline. Injection of the β-receptor agonist during odor presentation is sufficient to establish the preference towards that odor, even though no unconditioned stimulus, i.e., brush strokes on the rat body, was presented during acquisition. Like inverted-U shape dose-dependent effects shown *in-vitro*, 0, 1, 4 mg/kg doses (low and high doses) of the agonist do not establish but 2 mg/kg (intermediate doses) does establish the preference (Sullivan et al., 1991). Interestingly, activation of β receptors rescues impairment of the learning which is mediated by the depletion of serotonergic fibers in the OB (Langdon et al., 1997).

Olfactory perceptual learning in adult rodents has been investigated in terms of top-down neuromodulation in the OB. The principle of perceptual learning is that previous experiences of stimuli, e.g., odors, make the sensory acuity better. Accordingly, discrimination/recognition of similar odors, e.g., (+)-limonene and (-)-limonene, that subjects cannot differentiate without any treatments is assessed. Previous multiple-time exposures to those odors enable subject animals to discriminate/recognize them precisely (Mandairon et al., 2006b). As the

antagonist for α1 or β receptors applied systemically or directly into the OB during experiencing odors impairs the perceptual acquisition, it is considered to be modulated by noradrenaline (Veyrac et al., 2009; Vinera et al., 2015). The authors further described the involvement of the GC neurogenesis in noradrenergic actions on olfactory perceptual learning (Veyrac et al., 2009).

1.4.4. Acetylcholine

Since chapter 3 (publication B) will focus on cholinergic effects on VPCs, I give an introduction of acetylcholine in more detail.

Cholinergic fibers project to various brain regions, such as sensory cortices from the basal forebrain. The OB also receives dense cholinergic projections from the basal forebrain, the horizontal limb of the diagonal band of Broca (HDB) (Senut et al., 1989). The HDB projects not only cholinergic but also GABAergic innervations (Zaborszky et al., 1986), however here I will focus on the cholinergic action. Two subtypes of cholinergic receptors, nicotinic (nAChRs) and muscarinic receptors (mAChRs), are expressed in various bulbar cell types in various bulbar layers. The autoradiography using the antagonist and immunohistochemical analysis revealed that the α7 and β2 subunit nAChRs are found in the GL, EPL, MCL, and the IPL (Wamsley et al., 1984; Hill et al., 1993; del Toro et al., 1994). m2 mAChRs (m2AChRs) are expressed mainly in GABAergic cells (Crespo et al., 2000). Thus, no TCs and MCs are immunoreactive to m2AChRs. The majority of m2AChR immunoreactive cells were dopaminergic, SACs, in the GL. In the granule cell layer, although only a few GCs are m2AChR immunopositive, deep SACs that are known to inhibit GCs are m2R immunoreactive (Crespo et al., 2000). Importantly, nAChRs are generally excitatory cation-channel receptors, whereas mAChRs are G-protein coupled receptors, thus m1 mAChRs (m1AChRs) are excitatory and m2AChRs are inhibitory. Multiple-unit recordings in anesthetized rats showed that local application of acetylcholine (ACh) via electrode pipettes induce both, inhibitory and excitatory effects on the spontaneous activity in different layers. It

was further shown that the GL is more sensitive to ACh application than a deeper region, i.e., the MCL and the IPL, 73% and 55 % of cells are reactive to ACh, respectively (Ravel et al., 1990). Other *in-vivo* electrophysiological recordings from MCs combined with optogenetic activation of bulbar cholinergic fibers using transgenic mice showed that activation of cholinergic projections enhances spontaneous MC spiking and MC responses to either clean air inhalation or odorant inhalation (Rothermel et al., 2014; Bohm et al., 2020). In line with this observation, pair-pulse stimulation of either the ON or the lateral olfactory tract is modified by ACh. In the control condition, the amplitude of evoked field-potentials (eFPs) in the granule cell layer following the second pulse gets reduced, indicating decreased inputs onto GCs from MCs due to feed-back inhibition by GCs following the first pulse. ACh or carbachol abolishes this reduction in the second eFPs suggesting disinhibition of MCs mediated by mAChRs as atropine antagonizes their effects (Elaagouby et al., 1991). Moreover, administration of scopolamine, the mAChR antagonist, alone also reduces the amplitudes of eFPs with a single stimulation (Ravel et al., 1994). Thus, results indicate that muscarinic signaling disinhibits MCs. D'Souza and Vijayaraghavan (2012) further showed that specific nAChR activation by co-application of ACh and atropine suppresses the frequency of ON-evoked action potentials in MCs working as a high-pass filter so that only strong stimulation can elicit action potentials (D'Souza and Vijayaraghavan, 2012), which is contrary to muscarinic disinhibitory effects on MCs (Elaagouby et al., 1991; Ravel et al., 1994). Interestingly, Ca^{2+} activity in glomeruli during the odor presentation is modulated differently by electrical HDB stimulation according to the concentration of odors (Bendahmane et al., 2016). While reduction of the glomerular activity towards the high concentration of odors was observed, enhancement towards the low concentration presentation was observed following electrical HDB stimulation. Furthermore, application of agonists and antagonists demonstrated that mAChR signaling mediates enhancement and nAChR signaling is responsible for reduction of the odor-evoked glomerular activity (Bendahmane et al., 2016) which fits to the data described above. Thus, muscarinic signaling

disinhibits and nicotinic signaling inhibits MCs (Elaagouby et al., 1991; Ravel et al., 1994; D'Souza and Vijayaraghavan, 2012). Thus, the glomerular activity represents similar intensity throughout different concentrations, suggesting that neural representations in the OB can reflect the odor identity more precisely even if the concentration is different (Bendahmane et al., 2016).

Further, *in-vitro* results have dissected neural circuits mediating the ACh effects. As the apical region of the OB is highly sensitive to ACh (Ravel et al., 1990), juxtaglomerular cells might be promising candidates to be ACh targets. Indeed, ACh effects on individual cell types have been revealed. Application of ACh induces GABAergic inhibition in both excitatory and inhibitory juxtaglomerular cells. Puff-application of ACh onto the glomerulus evokes IPSCs and bath application of ACh increases spontaneous IPSCs in eTCs. Further, ACh glomerular puff-application decreases the amplitude of ON-evoked EPSCs in eTCs (Liu et al., 2015). In GABAergic cells, PGCs, and SACs, ACh or carbachol glomerular puff-application demonstrates direct inhibition, IPSP/Cs, and enhances spontaneous IPSCs. Results shown here are all mediated by mAChRs (Liu et al., 2015). More precisely, SACs are shown to be directly inhibited by m2AChRs (Pignatelli and Belluzzi, 2008). However, nAChR activation in the glomerulus inhibits ON-evoked responses in MCs as the amplitudes of ON-evoked EPSCs and frequency of ON-evoked action potentials are decreased (Spindle et al., 2018) and that inhibition is GABAergic (D'Souza and Vijayaraghavan, 2012).

The second ACh-reactive region is the MCL - the IPL (Ravel et al., 1990). Bath application of carbachol increases the frequency of action-potential dependent/independent IPSCs in MCs. Unlike what is observed in the GL, this increment is mediated by m1AChRs (Castillo et al., 1999). Increased frequencies of miniature IPSPs with carbachol application are not significantly different between in MCs with an intact apical dendrite and MCs with a cut apical dendrite implying that carbachol is unlikely to acts within the glomerulus, however rather acts on the dendrodendritic connection between MCs and GCs. The location of receptors seems to be on GCs, as antagonists of both AMPA and NMDA receptors have no effect on

carbachol action and no increment of action potential independent EPSCs by carbachol is observed in GCs (Ghatpande et al., 2006).

Manipulation of the cholinergic system by systemic pharmacology administration or gene KO modulates social memory. mAChR antagonist injection impairs social recognition in rats (Soffie and Lamberty, 1988) and m1AChR KO mice are unable to discriminate known and novel mice (Anagnostaras et al., 2003). Further, it is known that ACh is involved in non-social olfactory-related learning and odor recognition. Thus, local injection of scopolamine into the OB impairs olfactory fear conditioning. Moreover, optogenetic stimulation of bulbar cholinergic fibers during acquisition enhances fear reactions to the paired odor (Ross et al., 2019). Two ethyl-ester odors differing only one carbon chain are normally not distinguishable for rats. However, after one of them is paired with an electric shock, rats are able to differentiate them, indicating the involvement of ACh in perceptual learning (Fletcher and Wilson, 2002). This modification is via the mAChR signaling indicating that ACh enhances the ability to recognize/discriminate similar odors. Supporting this interpretation, microinjection of neostigmine, a choline esterase inhibitor into the OB itself is sufficient to enable rats to differentiate an odor only one carbon chain different from the habituated odor (Chaudhury et al., 2009). In addition, *in-vivo* electrophysiological recordings from MCs show that their responses are different towards two different odors with one carbon chain difference following neostigmine microinjection (Chaudhury et al., 2009). Similarly, in a habituation-dishabituation test, rats injected with both nicotinic and muscarinic antagonists show impaired odor recognition (Mandairon et al., 2006a). Since AChR antagonists injected rats show successfully decreasing investigation time through habituation sessions but not increasing towards a new odor contrary to control (Mandairon et al., 2006a), ACh may have a role in enabling rats to dishabituate odors. Ogg et al. (2018) demonstrated the dishabituation effects of ACh. Although glomerular Ca^{2+} activity declines through continuous odor presentation in the control condition, the activity gets increased again following electrical stimulation of the HDB in the middle of a continuous odor presentation.

Furthermore, the frequency of sniffing behavior to continuous odor application into a test chamber was analyzed. Consistent with the Ca^{2+} data, the frequency decreases through the continuous odor application in control and the HDB stimulation increases sniffing behavior again (Ogg et al., 2018). Intriguingly, multisensory modulation of ACh signaling was suggested, as dishabituation of sniffing behavior is mimicked with the presentation of a novel visual cue which is impaired by scopolamine. The glomerular Ca^{2+} activity dishabituation is also observed during novel visual stimulation (Ogg et al., 2018). These results suggest that cholinergic modulation of motivational salience to the same odor is regulated by novelty/attention and can be multisensory, as a novel visual context facilitates dishabituation.

1.5 Aims of this study

Although Tobin and colleagues found the subpopulation of TCs expressing vasopressin (2010), detailed characterization of bulbar VPCs, especially morphological or electrophysiological investigation has not been addressed yet. Therefore, the first aim of my thesis was to characterize the fundamental properties of bulbar VPCs. I visualized bulbar VPC neurites including dendrites and axons and examined as well as compared electrophysiological properties to other bulbar excitatory cells (chapter 2, publication A). Thus, I describe two morphological types of VPCs. In addition, I show the unique responses to ON stimulation, evoked IPSPs, in VPCs unlike evoked EPSPs in MCs. The second aim was to reveal how bulbar VPCs get activated. The bulbar vasopressin system was shown to be necessary for social discrimination but not for simple odor recognition (Tobin et al., 2010). This specificity might be regulated already at the level of VPC activation. I investigated bulbar VPC activity *in-vivo* in a context of social discrimination and also with *in-vitro* electrophysiology (publication B). Accordingly, the neural activity of VPCs during investigation on either water, rat urine, or a novel rat was examined using pERK as a neural activity marker. Furthermore, I investigated effects of centrifugal neuromodulators, i.e., serotonin, noradrenaline, and ACh, on ON-evoked responses in VPCs. Finally, the

involvement of ACh which showed the most prominent effects in electrophysiology and VP in social discrimination, was examined.

Chapter 2: Vasopressin cells in the rodent olfactory bulb resemble non-bursting superficial tufted cells and are primarily inhibited upon olfactory nerve stimulation

2.1 Abstract

The intrinsic vasopressin system of the olfactory bulb is involved in social odor processing and consists of glutamatergic vasopressin cells (VPCs) located at the medial border of the glomerular layer. To characterize VPCs in detail, we combined various electrophysiological, neuroanatomical and two-photon Ca2+ imaging techniques in acute bulb slices from juvenile transgenic rats with eGFP-labelled VPCs.

VPCs showed regular non-bursting firing patterns, and displayed slower membrane time constants and higher input resistances versus other glutamatergic tufted cell types. VPC axons spread deeply into the external plexiform and superficial granule cell layer. Axonal projections fell into two subclasses, with either denser local columnar collaterals or longer-ranging single projections running laterally within the internal plexiform layer and deeper within the granule cell layer. VPCs always featured lateral dendrites and a tortuous apical dendrite that innervated a single glomerulus with a homogenously branching tuft. These tufts lacked Ca^{2+} transients in response to single somatically-evoked action potentials and showed a moderate Ca^{2+} increase upon prolonged action potential trains.

Notably, electrical olfactory nerve stimulation did not result in synaptic excitation of VPCs, but triggered substantial $GABA_A$ receptor-mediated IPSPs that masked excitatory barrages with yet longer latency. Exogenous vasopressin application reduced those IPSPs, as well as olfactory-nerve evoked EPSPs recorded from external tufted cells.

In summary, VPCs can be classified as non-bursting, vertical superficial tufted cells. Moreover, our findings imply that sensory input alone cannot trigger excitation of VPCs, arguing for specific additional pathways for excitation or disinhibition in social contexts.

2.2 Significance statement

Efficient sensing of conspecific odor signatures is essential for most rodent social behavior. Although olfactory bulb vasopressin was shown to be a potent facilitator of social odor processing, little is known on the cellular substrate of the intrinsic vasopressin system. Here we provide a detailed characterization of the anatomical and electrophysiological properties of the bulbar vasopressin cells. While we also identify several targets of vasopressin action, we find that stimulation of the sensory inputs to the bulb results primarily in vasopressin cell inhibition, implying that excitation of the bulbar vasopressin system requires additional still unknown excitatory or dis-inhibitory inputs which might confer social specificity. These insights may complement the knowledge on vasopressinergic modulation of social stimuli in limbic brain structures.

2.3 Introduction

The neuropeptide vasopressin (VP) is primarily synthesized in neurons located within the supraoptic, paraventricular, and suprachiasmatic nuclei of the hypothalamus (Ludwig and Leng, 2006). These neurons release VP from their axonal projections to the neurohypophysis into the bloodstream to exert its peripheral physiological functions as a neurohormone, e.g., water retention in the kidney (Ondrasek, 2016). In the central nervous system, VP is known as a key modulator of social behavior and cognition in mammals, including rodents and humans (Meyer-Lindenberg et al., 2011; Lukas and Neumann, 2013; Lukas and de Jong, 2015). In this context, relevant VP release was shown to occur from somata and dendrites of the above mentioned VP cells (VPCs) in the hypothalamus as well as from hypothalamic and extra-hypothalamic fibers that target the components of the social behavior network throughout the mammalian brain, e.g. the lateral septum, the medial extended amygdala, the anterior and ventromedial hypothalamus, and the periaqueductal gray (Sterba, 1974; Buijs et al., 1983; Ondrasek, 2016). The extra-hypothalamic brain regions that also synthesize and release VP during social interactions are the bed nucleus of stria terminalis, the medial amygdala, and the olfactory bulb (OB), i.e., the first center of olfactory processing (de Vries and Buijs, 1983; Tobin et al., 2010; Lukas and de Jong, 2015).

Olfactory processing is an essential component of mammalian social communication, in rodents, sheep, and even humans (Porter et al., 1986; Brennan and Kendrick, 2006). Especially in rodents, the olfactory system is regarded as the main sensory pathway for mediating recognition and discrimination of individual con-specifics (Camats Perna and Engelmann, 2017). Several pharmacological studies suggest that endogenous VP release within the OB facilitates the discrimination of known and new individuals via their odor signatures (e.g., Dluzen et al., 1998a; Dluzen et al., 1998b; Tobin et al., 2010). The source of this VP release are bulbar VPCs, a subpopulation of glutamatergic tufted cells with lateral dendrites (Macrides and Schneider, 1982) (Hamilton, 2005 #1011, that resides at the border between the glomerular layer and the external plexiform layer (EPL) in both the accessory

OB (AOB) and the main OB {MOB, Tobin et al., 2010; Wacker et al., 2011). The presence of VPCs in both pathways for odorant detection (volatile/MOB and non-volatile/AOB) is in line with the view that volatile odor signals are especially important for the coding of individual body odor signatures (Brennan and Kendrick, 2006) and thus the AOB and MOB play complementary roles in processing social odor recognition (Baum and Kelliher, 2009; Stowers and Kuo, 2016).

As mentioned above, VP enhances social recognition of individuals on the level of the OB, but what could be the cellular mechanisms that are responsible for this facilitation of social odor processing? As a first step towards resolving these questions, here we provide a detailed investigation of basic electrophysiological and neuroanatomical properties of the OB VPCs, including their axonal projections. We also set out to identify synaptic inputs to VPCs, which turns out to be a challenging task since here we observe that they receive mostly inhibition upon stimulation of olfactory sensory axons. Moreover, we investigate the expression of VP in VPC axons and dendrites including their elaborate glomerular apical tuft, and test for effects of VP on glomerular synaptic signaling. To further explore potential mechanisms of dendritic release within a glomerulus, we also characterize the excitability of the apical dendritic tuft. Our results imply that bulbar VPCs are likely to be involved in a broad range of complex interactions both within glomeruli and deeper layers of the bulb.

2.4 Materials and Methods

2.4.1 Experimental animals

All experiments were carried out according to national and institutional guidelines, the rules laid down by the EC Council Directive (86/89/ECC) and German animal welfare. Wistar rats of either sex were either purchased from Charles River (Sulzfeld, Germany) or bred onsite in the animal facilities at the University of Regensburg. Heterozygous VP-eGFP Wistar rats (Ueta et al., 2005) of either sex that were used to identify VPCs in electrophysiological and imaging experiments were all bred at the University of Regensburg.

2.4.2 Slice preparation

Rats (postnatal day 11-21) were deeply anaesthetized with isoflurane and decapitated. Horizontal OB slices (300 µm) were cut in ice-cold carbogenized (O_2 [95 %], CO_2 [5 %]) artificial extracellular fluid (ACSF; [mM]: 125 NaCl, 26 $NaHCO_3$, 1.25 NaH_2PO_4, 20 Glucose, 2.5 KCl, 1 $MgCl_2$, and 2 $CaCl_2$) using a vibratome (Vibracut, Leica Biosystems, Germany) followed by incubation in carbogenized ACSF for 30 min at 36°C and then kept at room temperature (~21° C) until experimentation.

2.4.3 Electrophysiology

External tufted cells (eTC), mitral cells (MC), and middle tufted cells (mTC) were identified by their morphological appearance and their localization in the clearly defined glomerular layer, MC layer, and EPL, respectively (Halász 1990). VPCs were identified in OB slices from VP-eGFP rats excited with LED illumination (470 nm nominal wavelength, M470L2, Thorlabs Inc., Newton, NJ, USA) under a modified Zeiss Axioplan microscope (Carl Zeiss Microscopy GmbH, Jena, Germany). Epifluorescence was filtered by a longpass dichroic mirror (490 nm cutoff, DMLP490R, Thorlabs Inc., Newton, NJ, USA) and an emission filter (510 ± 21 nm, MF510-42, Thorlabs Inc., Newton, NJ, USA) and visualized with a digital camera (VisiCAM-

100, Visitron Systems, Puchheim, Germany). To perform somatic whole cell patch-clamp recordings cells were visualized by infrared gradient-contrast illumination via an IR filter (Hoya, Tokyo, Japan) and patched with pipettes sized 4-6 MΩ. Recordings were performed with an EPC-10 (HEKA, Lambrecht, Germany). Series resistances measured 10-30 MΩ. The intracellular solution contained [mM]: 130 K-methylsulfate, 10 HEPES, 4 $MgCl_2$, 4 Na_2ATP, 0.4 NaGTP, 10 NaPhosphocreatine, 2 ascorbate, at pH 7.2. The ACSF was gassed with carbogen and contained [mM]: 125 NaCl, 26 $NaHCO_3$, 1.25 NaH_2PO_4, 20 Glucose, 2.5 KCl, 1 $MgCl_2$ and 2 $CaCl_2$. Experiments were performed at room temperature (~ 21° C). The average resting potential of MCs/mTCs and eTCs/VPC was ranging from -60 to -75 mV and -55 to -60 mV, respectively, similar to previous data (Heyward et al., 2001; Hayar et al., 2004b; Tobin et al., 2010). Leaky cells with a holding current above ~ -30 pA were rejected. Experiments that showed a substantial drift in resting V_m were rejected.

Spontaneous activity (i.e., IPSPs in VPCs and bursts in eTCs) was recorded in current clamp mode at resting V_m. To characterize the firing pattern and passive properties of VPCs, eTCs and other tufted OB cell types, including membrane time constant (τ_m), input resistance (R_i), firing threshold, first/last spike amplitude ratio, first/last afterhyperpolarization (AHP) ratio, sag amplitude relative to the hyperpolarization level at the end of the current step, rebound amplitude, and coefficient of variance (CV) of the inter-spike interval (ISI), polarizing step pulses were applied via the patch pipette for 600 - 800 ms each. Firing pattern analysis was performed using Origin 2017 (OriginLab Corporation, Northampton, MA, USA).

2.4.4 Olfactory nerve (ON) stimulation

ON stimulation was performed with a custom-built four-channel-electrode (Chatterjee et al., 2016; Lukas et al., 2018). Briefly, the four electrodes consisted of teflon-coated silver wires (diameter uncoated 75 µm, coated 140 µm, item AG-3T, Science Products GmbH, Hofheim, Germany). The electrode was connected to a 4-channel stimulator (STG 1004, MultiChannel Systems, Reutlingen, Germany) that is controlled from a PC via an USB connection. In

current mode, the maximal stimulation strength per channel is 800 µA. The grounds from the stimulator channels were connected to a common wire and then to mass. The four-channel electrode was lowered on top of the acute brain slice under visual control using a manual manipulator (LBM-7, Scientifica, East Sussex, UK). During ON stimulation only the channel eliciting the best signal was used to stimulate the ON. The stimulation strength was adjusted via the stimulator's software (MC_Stimulus, V 2.1.5); the output of the stimulator was triggered via a TTL signal from the electrophysiology software (Patchmaster, HEKA, Lambrecht, Germany). Stimulation strengths sufficient to elicit MC, eTC and VPC responses were mostly in the range of 50 – 400 µA and 300 – 500 µA for 100 µs, respectively.

2.4.5 Pharmacology

The pharmacological agents used during electrophysiological experiments include 1(S),9(R)-(-)-Bicucullin methbromide (50 µM, Sigma-Aldrich Chemie GmbH, Munich, Germany), [Arg^8]-Vasopressin acetate salt (1 µM, Sigma-Aldrich Chemie GmbH, Munich, Germany), and the Manning Compound, a selective VP 1a/oxytocin receptor antagonist (10µM, $d(CH_2)_5[Tyr(Me)^2]AVP$, \Kruszynski, 1980 #2625}. The Manning compound was generously provided by Dr. Maurice Manning (University of Toledo, Toledo, OH, USA).

2.4.6 Ca^{2+} Imaging

Fluorescence was recorded by two-photon laser scanning microscopy on a Femto-2D microscope (Femtonics, Budapest, HU), equipped with a tunable, Verdi-pumped Ti:Sa laser (Chameleon Ultra I, Coherent, Glasgow, Scotland). The microscope was equipped with a 60x Nikon Fluor water-immersion objective (NA 1.0; Nikon Instruments, Melville, NY, USA), three detection channels (green fluorescence (epi and trans), red (epi) and infrared light (trans)) and controlled by MES v4.5.613 software (Femtonics, Budapest, Hungary).

VP-eGFP cells were identified in the green channel at an excitation wavelength of 950 nm. VPC bodies were patched in whole-cell mode with patch pipettes filled with regular

intracellular solution (see above). Alexa Fluor 549 (50 µM, Invitrogen, Carlsbad, CA, USA) and the Ca^{2+} indicator OGB-1 (100 µM, Invitrogen) were added for neurite visualization and calcium imaging. Fluorescence transients and image stacks were acquired at 800 nm laser excitation. Data were mostly collected from the medial surface of the OB.

Ca^{2+} imaging experiments were performed at room temperature (~21° C). The patched VPCs were held in current clamp mode near their resting potential of -55 mV. Again, leaky VPCs with a holding current beyond -30 pA were dismissed. A shift in baseline fluorescence F_0 of more than 15 % between the first and the last measurement of each region of interest (ROI) also led to a rejection of the experiment. Structures of interest were imaged in free line-scanning mode with a temporal resolution of ~ 1 ms. At a given dendritic location, several consecutive focal line-scans during somatically evoked single APs (by an injected current step of 1000 pA for 1 ms) or AP trains (20 stimuli at 50 Hz) were recorded (duration 1.5 s), averaged and smoothed. Dendritic Ca^{2+} transients were analyzed in terms of $\Delta F/F$ relative to the resting fluorescence F_0 (Egger et al., 2003). For extracting the distance of the Ca^{2+} measurements from the soma and the tuft origin and performing correlation analysis MES 4.5 (Femtonics, Budapest, Hungary) and SigmaPlot 13.0 (Systat Software GmbH, Erkrath, Germany) were used, respectively.

After sufficient filling of the dendritic tree (for at least 15 min), stacks of scans of the entire cell were recorded at 1 µm z-resolution. Each scan included 3 images, recorded in the red (Alexa 594) and green (OGB-1) fluorescent channel and at the same time in the trans-infrared channel of the microscope, to gather information on both the dendritic tree and glomerular structure. The xy-resolution was 900x900 pixels with a pixel width of 0.197 µm. All tufts fit within one scanning window and were fully sampled. In some instances, we noted upon reconstruction that cells had been incompletely scanned, mostly because the stack's z-coordinate was not set deeply enough. These neurons were not used for morphological analyses.

2.4.7 Histology

To chemically label dendritic and axonal processes of VPCs for later investigation by light microscopy and to verify the lack of lateral dendrites of eTCs, in some of the electrophysiological experiments biocytin (5 mg/ml) was added to the intracellular solution. Slices were post-fixed overnight at 4°C in 4% paraformaldehyde. Afterwards, slices were stored up to 2 weeks at 4°C in 0.1 M PB (80 mM Na_2HPO_4, 20 mM NaH_2PO_4, pH 7.4) until further processing.

Staining was performed according to the protocol proposed by Marx et al. (2012). Briefly, slices were washed in PB (6-8 x 10 min). Then endogenous peroxidase activity was quenched via incubating slices for 45 min in 3% H_2O_2 (in PB). Again, the slices were washed for approx. 3 times in PB until no more bubbles were visible. Slices were incubated in ABC Solution (VECTASTAIN Elite ABC-Peroxidase Kit, Vector Labs, Burlingame, Ca, USA: Solution A [1 %], Solution B [1 %]; Triton-X [0.01 %] in 0.1 M PB) in the dark for 60 min at RT and then overnight at 4 °C, followed by several washing steps in the dark (3x10 min in PB, then 3x in 0.05 M TrisHCl [pH 7.6]). Before starting the peroxidase reaction slices were incubated in DAB solution (3,3'-diaminobenzidine [0.02 %], $CoCl_2$ [0.002 %], NH_4NiSO_4 [0.004 %], in TrisHCl [pH 7.4]). To start the peroxidase reaction we added 3 % H_2O_2 to the DAB solution (approx. 60 sec, until staining was sufficiently strong), the reaction was then stopped in 0.1 M PB, and the slices were washed finally in 0.1 M PB (6-8x10min). Subsequently the slices were mounted on objective slides using Moviol as mounting medium (6g Glycerol, 2.4g Moviol 4-88, 12ml 200mM TrisHCl [pH 8.5], 6ml H_2O).

Additionally, in-vitro slices containing biocytin-filled eGFP VP cells were post-fixed as described above and prepared for fluorescent double-labelling. Briefly, free-floating slices were washed in PBST (0.3 % Triton-X; 3 x 10 min) and incubated for 60 min in PBST containing 5 % NGS (Normal Goat Serum S-1000; Vector Laboratories, Burlingame, CA, USA). Sections were incubated with the diluted primary VP-neurophysin antibody (1:100, PS41, kindly provided by Dr. Harold Gainer, NIH, Bethesda, USA Ben-Barak et al., 1985;

Bader et al., 2012) for 48 h at 4°C. After three rinses for 10 min in PBST, the bound primary antibodies were visualized using goat anti-mouse antibodies conjugated to CF633 (1:1000; Biotium, Fremont, CA, USA) diluted in PBST/5 % NGS for 2 h at room temperature. Following washing in PBST (3 x 10 min) slices were finally incubated in streptavidin conjugated to CF488A (1:400; Biotium, Fremont, CA, USA) for 1 h at room temperature followed by incubation overnight at 4°C and 1 h at room temperature. Following final washing steps (PBST; 3 x 10 min) the slices were mounted in objective slides using DAPI Fluoromount-G (SouthernBiotech, Birmingham, AL, USA).

Both biocytin-DAB stains of dendritic and axonal structures of VPCs as well as fluorescent double-labelling were imaged on an inverted confocal laser scanning microscope (Leica TCS SP8, Leica Microsystems, Wetzlar, Germany). Digital images were processed (Merging and Z-projections) using the Leica Application Suite X (Leica) and Fiji (Schindelin et al., 2012). The detailed morphology of the lateral dendrites and axonal structures of VP cells was reconstructed and analyzed with the Fiji plugin Simple Neurite Tracer (Longair et al., 2011) from the z-stack. Although in light microscopy thin spineless dendritic branches of juxtaglomerular cells can be mistaken for axons and vice versa, especially within the glomerular layer and superficial external plexiform layer (Kiyokage et al., 2010), classification of dendrites and axons was achieved based on the observation that all deeper projections into the mitral cell layer (MCL) clearly resemble axons in their appearance and all diverge from one single process extending directly from the soma or a thick dendritic neurite near the soma. From this analysis the number of branch points and the average branch length of dendritic and axonal arborizations were extracted. Further, the projection area of the dendritic/axonal structures in the glomerular/external plexiform layer (GL/EPL) as well as in the mitral cell/granule cell layer (GCL) was determined by measuring the area of the smallest obtuse polygon that inscribes these structures in a z-projection of the reconstructed VPC. The reconstructed VPCs were classified as type I or type II depending on how many times their projections cross the MCL from the EPL (type 1: multiple times; type 2: one time).

Collaterals crossing back from the GCL to the EPL were not counted. Cells with axons that did not cross the MCL at all were dismissed as these axons clearly were truncated due to slicing.

2.4.8 Reconstruction and analysis of apical tufts and glomerular shape

Reconstruction and analysis of dendritic tuft-like structures and glomeruli was performed as previously described in detail in Bywalez et al. (2016). Briefly, the detailed morphology of the apical tuft of VPCs and MCs was reconstructed with the Fiji plugin Simple Neurite Tracer (Longair et al., 2011) from the fluorescence z-stack scans of the Ca^{2+} imaging experiment. The glomerular contours were reconstructed from the trans-infrared image stacks with the ImageJ plugin TrakEM2 (Cardona et al., 2012). The glomerular arborization patterns of reconstructed dendritic tufts were analyzed by custom-written software based on IGOR Pro 5.0 (Wavemetrics, Lake Oswego, OR, USA, Bywalez et al., 2016). The aligned representations were used to determine the density and fraction of branch points within shells of the glomerulus. For analyzing the relation between the apical tuft of a VPCs and its surrounding glomerulus, five shell volumes were calculated based on the real glomerular shape via shrinking of the reconstructed glomerular surface by steps of one fifth of the radius from the center of mass of the glomerulus. The density of branch points within a shell was determined by dividing the number of branch points by the volume of the glomerular shell they are located in. The fraction of branch points was determined by normalization of the branch point number in a certain shell to the total number of branch points in the whole tuft. To better illustrate these data, we put them into the context of other well-known glomerular dendritic structures by including a data set from rat MC apical dendritic tufts and their surrounding glomeruli. MCs had been filled with Alexa Fluor 594 (50 µM; wild-type rats, P12 - P16).

2.4.9 Statistical analysis

Statistics was performed using SPSS 22.0 (IBM, NY, USA) and G*Power 3.1.9.2 (Franz Faul, University of Kiel, Kiel, Germany). Significance was accepted at $p < 0.05$. For details see statistical table (Table 1).

Table 1 **Statistical Table**

	Data structure	Type of test	Power (Calculated for α=0.05)
a	Normal distribution	T-test for independent variables (cell type [independent])	1.00 (sag) 1.00 (rebound)
b	Normal distribution	ANOVA (cell type [independent]) followed by a post-hoc comparison using Bonferroni correction	1.00 (τ_m) 1.00 (R_i) 0.993 (threshold) 0.999 (CV of ISI) 1.00 (spike ratio) 1.00 (AHP ratio) 0.993 (AP FWHM) 1.00 (AP AHP)
c	Normal distribution	T-test for independent variables (cell type [independent])	0.515
d	Normal distribution	2 x (2) mixed model ANOVA (cell type [between subject] x neurite type [within-subject]) followed by a post-hoc comparison using Bonferroni correction.	0.795 (cell type)
e	Normal distribution	2 x (3) mixed model ANOVA (cell type [between subject] x layer [within-subject]) followed by a post-hoc comparison using Bonferroni correction.	0.795 (cell type)
f	Normal distribution	2 x (2) mixed model ANOVA (cell type [between subject] x neurite type [within-subject]) followed by a post-hoc comparison using Bonferroni correction.	1.00 (neurites) 0.611 (cell type) 0.526 (interaction)
g	Normal distribution	2 x (3) mixed model ANOVA (cell type [between subject] x layer [within-subject]) followed by a post-hoc comparison using Bonferroni correction.	0.884 (layer)
h	Normal distribution	T-test for independent variables (cell type [independent])	0.994 (τ_m)
i	Normal distribution	2 × (5) mixed model analysis of variance (ANOVA) (cell type [between subject] × shell segment [within-subject]) followed by a post-hoc comparison using Bonferroni correction.	0.820 (cell type)
j	Normal	2 × (5) mixed model analysis of variance (ANOVA) (cell type	0.058 (cell type)

	distribution	[between subject] × shell segment [within-subject]) followed by a post-hoc comparison using Bonferroni correction.	
k	Normal distribution	Linear Regression ($\Delta F/F_0$ [dependent], distance [independent])	0.927 (dendrite) 0.121 (tuft)
l	Normal distribution	Analysis of covariance (ANCOVA) (cell type [response variable], distance from soma [covariate])	1.00 (AP) 1.00 (50 Hz)
m	Normal distribution	T-test for dependent variables (treatment [dependent])	1.00
n	Normal distribution	2 × (8) mixed model ANOVA (treatment [between subject] × time [within-subject]) followed by a post-hoc comparison using Bonferroni correction	0.935 (treatment) 0.610 (time) 0.945 (interaction)
o	Normal Distribution	2 × (8) mixed model ANOVA (treatment [between subject] × time [within-subject]) followed by a post-hoc comparison using Bonferroni correction	0.999 (treatment) 0.971 (time) 1.00 (interaction)
p	Normal distribution	Repeated measures ANOVA (treatment [dependent])	0.996 (treatment)

2.5 Results

2.5.1 Electrophysiological properties of vasopressin cells (VPC)

To characterize the electrophysiological properties of VPCs and to investigate potential differences from other large glutamatergic bulbar neurons, we systematically performed current clamp *in-vitro* recordings from eGFP-labeled VPCs and other tufted glutamatergic cells in the olfactory bulb (OB), i.e., mitral (MC), middle tufted (mTCs), and external tufted cells (eTC), that were identified based on the location and size of their somata. The identity of eTCs was further verified by biocytin-DAB staining to confirm the lack of lateral dendrites (Fig. 6A+B).

Whole cell current clamp recordings at resting V_m sometimes revealed spontaneous IPSP activity in VPCs (Fig. 6A+C; 16 of 37 cells from 26 rats). Only 1 of the 37 VPCs showed small spontaneous EPSPs, whereas bursting activity was never observed. In contrast, eTC recordings always contained spontaneous EPSPs and often also the characteristic spontaneous action potential (AP) bursts (10 of 18 cells from 12 rats, Hayar et al., 2004a) or low threshold spikes (LTS; 4 of 18 cells, Fig. 6B+C).

In both VPCs (n=23 from 23 rats) and eTCs (n=17 from 12 rats) application of strongly hyperpolarizing current steps (-90 to -100 pA) resulted in the expression of a sag (Fig. 6D+E), followed by a small rebound depolarization in VPCs or bursting (LTS+spikes) in eTCs. In 9 out of 23 VPCs the rebound depolarization resulted in rebound spiking (Fig. 6D). Both sag amplitude ($t_{(38)}$=6.35, $p<0.001$) and rebound depolarization ($t_{(38)}$=-12.2, $p<0.001)_a$ of VPCs (n=23) were significantly smaller than the sag amplitude and the LTS component of eTCs (n=17).

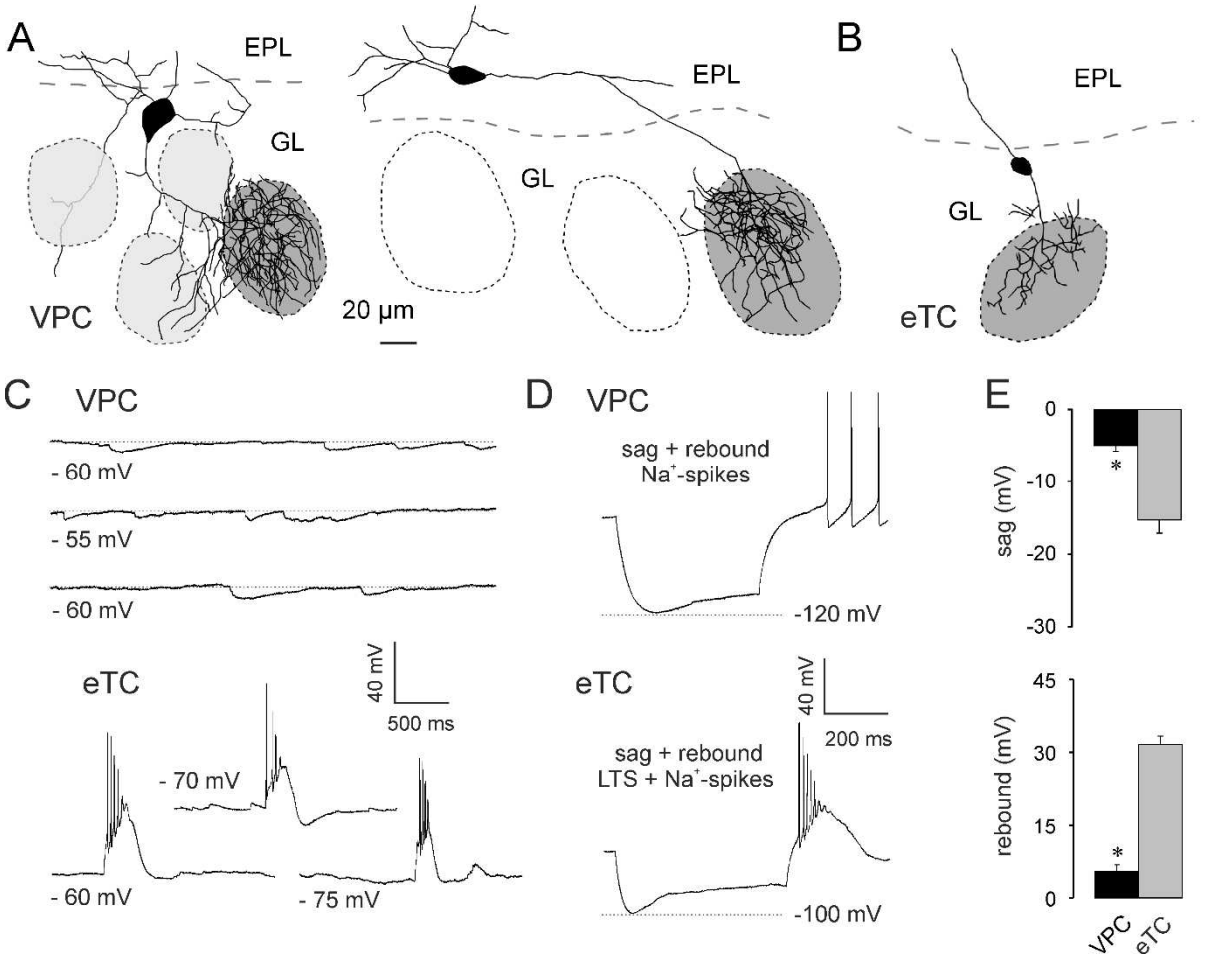

Fig. 6 (A) Two representative VPC reconstructions. The dark grey shading indicates the glomerulus innervated by the dendritic tuft of the respective VPC. VPCs bear several lateral dendrites that either run below the GL or lie above or underneath other glomeruli (light grey shading). (B) Representative reconstruction of an eTC. (C) Representative spontaneaous IPSPs and bursts of 3 different VPCs and eTCs, respectively. (D) Representative responses to somatically applied current steps (-90 to -100 pA; 800 ms) to VPCs and eTCs. (E) Cumulative comparison of the sag (upper panel) and the rebound depolarization/LTS (lower panel) of VPCs (n=23) and eTCs (n=17). * $p < 0.001$ vs. eTC. T-test for independent variables. Data are means ± SEM.

Application of depolarizing current steps (80 to 120 pA) to VPCs in whole cell patch clamp recordings resulted in regular, non-bursting firing patterns with a slight adaption in spike amplitude (n=24 from 20 rats) that were similar to the regular, non-bursting MC firing patterns (n=25 from 23 rats), but clearly distinguishable from the irregular patterns of mTCs and bursting eTCs (n=18+18 from 10+12 rats; Fig. 7A). The regularity of the VPC firing pattern showed in its coefficient of variance of the inter-spike-interval (CV of ISI), since the VPCs' CV of ISI was comparable to that of MCs but significantly lower than that of irregularly firing

mTCs ($F_{(3,51)}$=11.4, p<0.001; n=55; Fig. 7B)$_b$. Note that already small depolarizing current injections (20 pA) were able to induce continuous firing in VPCs (n=31 from 30 rats; Fig. 7A), in contrast to the adaption observed at higher current injections (see above). The lack of bursting in VPCs was reflected in their significantly higher last/first spike amplitude ratio and afterhyperpolarization (AHP) amplitude ratio compared to those of bursting eTCs (spike ratio: $F_{(3,57)}$=64.7, p<0.001; n=61; AHP ratio: $F_{(3,57)}$=14.4, p<0.001; n=61; Fig. 7B)$_b$.

Current pulse application (1000 pA, 1 ms) resulted in APs in VPCs that were similar in amplitude to the other cell types tested (Fig. 7C). However, VPC APs were significantly broader (full width at half maximum (FWHM): VPC, 1.7 ± 0.06 ms; MC, 1.5 ± 0.05 ms; mTC, 1.3 ± 0.5 ms, eTC, 1.5 ± 0.07ms; $F_{(3,81)}$=8.72, p<0.001, n=85). VPC AHPs were similar to those of mTCs and MCs and clearly different from the afterdepolarization observed in eTCs (VPC, -6.5 ± 0.79 mV; MC, -7.0 ± 0.50 mV; mTC, -5.9 ± 0.72 mV, eTC, 7.7 ± 1.2 mV; $F_{(3,73)}$=71.8, p<0.001, n=77)$_b$.

Hyperpolarizing current steps (-20 to -10 pA) elicited slowly hyperpolarizing voltage responses from VPCs, compared to the faster hyperpolarization in MCs and mTCs or the very fast hyperpolarization in eTCs (Fig. 7A). Accordingly, the membrane time constant (τ_m) of VPCs was more than 2 times higher than that of MCs, mTCs and eTCs ($F_{(3,81)}$=37.9, p<0.001; n=85; Fig. 7B)$_b$. Besides the high τ_m, the input resistance (R_i) in VPCs was also more than 2 times higher than the R_i of the analyzed MCs, mTCs and eTCs ($F_{(3,81)}$=27.1, p<0.001; n=85; Fig. 7B)$_b$. Regarding the spiking threshold VPCs did not differ from MCs and eTCs. However, their spiking threshold was significantly higher than that of mTCs ($F_{(3,74)}$=8.77, p<0.001; n=78; Fig. 7B)$_b$. In summary, although VPCs showed a slow τ_m they were still as excitable as the other TCs since their high R_i compensates for the sluggish polarization.

In conclusion, the electrophysiological properties of VPCs, especially the lack of bursting, suggests an overlap of VPCs with the population of external tufted cells with lateral dendrites described by Antal et al. (2006).

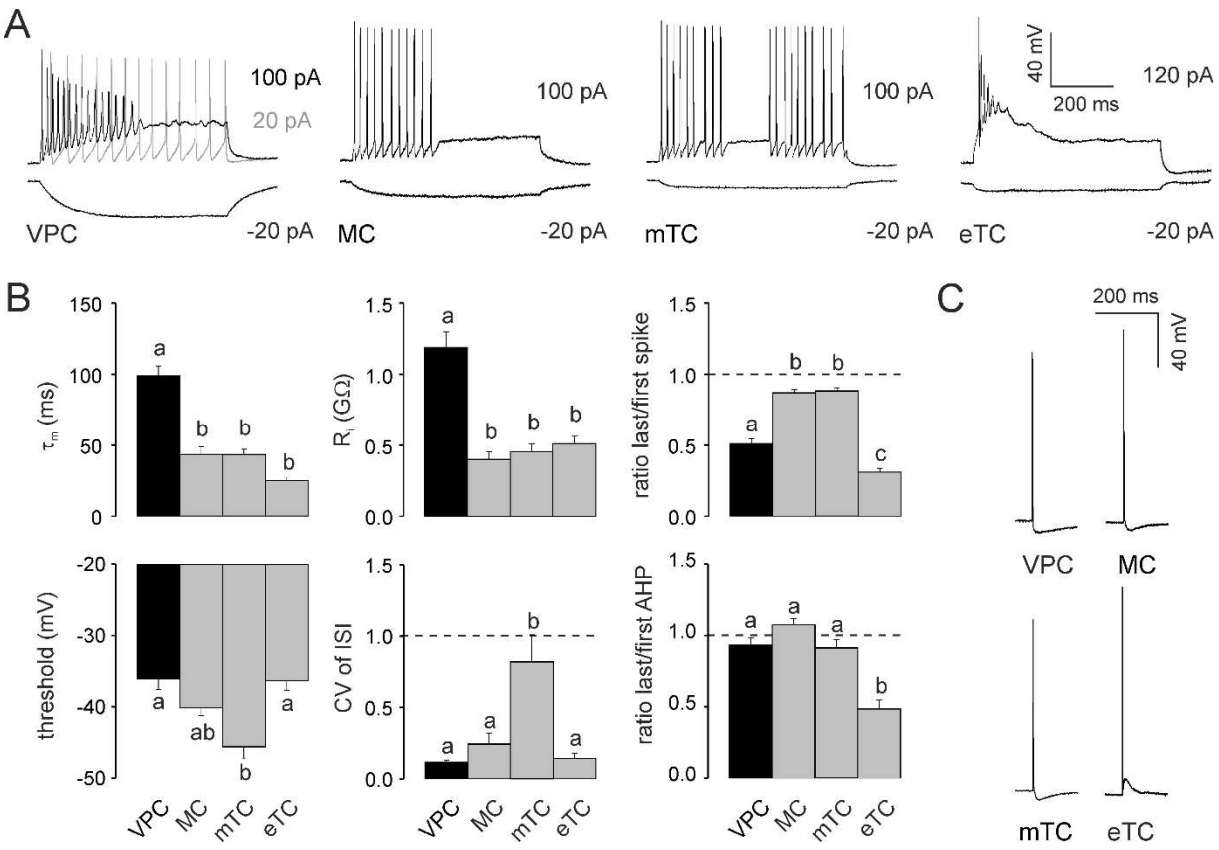

Fig. 7 (A) Representative responses to somatically applied current steps (600 - 800 ms) to VP cells (VPC), mitral cells (MC), middle tufted cells (mTC), and external tufted cells (eTC) at their corresponding resting potential (-55 mV, -70 mV, -70 mV, and -60 mV). (B) Cumulative comparison of the membrane time constant (τ_m, n=24/25/18/18), input resistance (R_i, n=24/25/18/18), firing threshold (n=24/23/18/18), coefficient of variance of the inter-stimulus-interval (CV of ISI, n=22/13/13/7), last/first spike amplitude ratio (n=24/13/13/11), and last/first afterhyperpolarization (AHP, n=24/13/13/11) amplitude ratio measured from corresponding current step responses (see A). (C) Representative action potentials evoked by somatic current injection (1000 pA, 1 ms). Arabic letters above columns illustrate if means are statistically different (e.g. a vs. b vs. c) or not (e.g. a vs. a vs. ab). One-way ANOVA followed by post-hoc comparison using Bonferroni correction. Data are means ± SEM.

2.5.2 Subcellular VP expression in VPCs

The local presence of VP protein is a prerequisite for local VP release. In hypothalamic VPCs VP is known to be expressed within and released from their soma, dendrites and axon (Pow and Morris, 1989). In order to investigate the actual expression of VP in the different sub-structures of OB VPCs, we double-stained streptavidin-fluorophore-enhanced biocytin-filled eGFP-labelled VPCs for VP/neurophysin. Unfortunately, the fluorescent labelling for VP/neurophysin could not be visualized in all thin axonal structures or the thin ramifications of the apical tuft (Fig. 8A+B). However, the double-staining clearly demonstrated that VP/neurophysin is expressed in the lateral dendrites and the origins of axonal structures (Fig. 8A2+B1+B2) as well as in the proximal thick branches of the apical tuft (Fig. 8A1) and the soma. Thus, all compartments of VPCs are potential release sites. In the following we examine the different morphological compartments more closely.

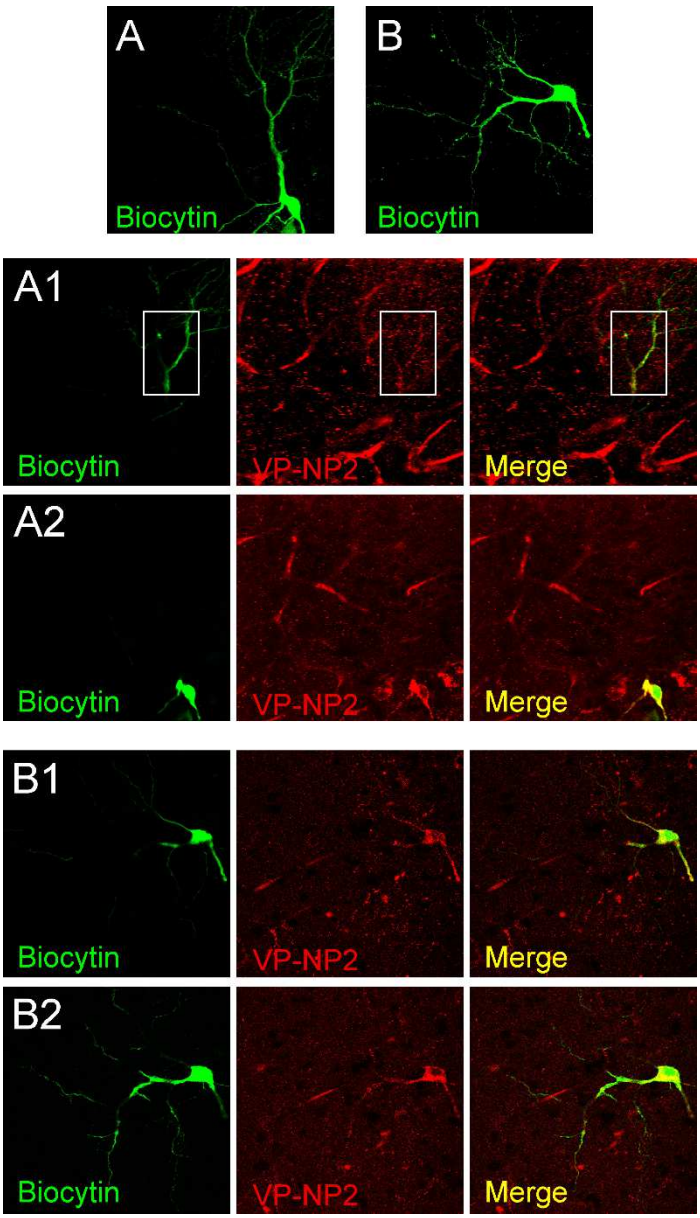

Fig. 8 (A+B) Average z-projections of eGFP-VPCs labelled with biocytin (visualized with streptavidin-conjugated CF488A) and corresponding staining of VP-Neurophysin 2 (VP-NP2, CF633)

2.5.3 Morphology of lateral dendrites and axons

VP-binding VP and oxytocin receptors have been localized in the glomerular, external plexiform, MC and superficial granule cell layer (GL, EPL, MCL, GCL) of the OB (Ostrowski et al., 1994; Vaccari et al., 1998; Tobin et al., 2010). However, it is unknown so far whether neurites of VPCs are sufficiently proximal to all these receptor locations to release VP onto them. Since fluorescent dyes often cannot properly visualize thin neuronal processes, in particular axons (e.g., Bywalez et al., 2016), we filled VPCs with biocytin and in a first step reconstructed the lateral dendrites and axons before focusing on the prominent apical tuft.

We found that in VPCs an average of 3.7 ± 0.5 (n=19 from 18 rats) lateral dendritic branches originated from their somata. All these cells had at least one (n=1) or more lateral dendrites.

The detailed dendritic and axonal reconstructions indicated the existence of two 2 subtypes of VPCs depending on whether their axon innervates the MCL via multiple projections (type 1) or via one main collateral (type 2, Fig. 9A), since the number of crossings into the MCL was bi-modally distributed (n=19, Fig. 9, insert). There was no significant difference in soma size or in the distribution of the somata across the GL and EPL between the two types (table 2). Although type 1 had significantly less lateral dendrites than type 2 ($t_{(17)}$=-2.41, p=0.028; table 2)$_c$, the projection areas of the dendritic and axonal structures did not differ between the two types (table 2). Also, there were no differences between the two projection types in the number of dendritic branch points or average dendritic branch length (table 2), but they were significantly different concerning the distribution of their axons below the GL. Type 1 showed a significantly higher number of axonal branch points (post-hoc: p=0.003; cell type effect: $F_{(1,17)}$=8.73; p=0.009; n=11/8 from 18 rats; table 2)$_d$. When comparing the axonal branch points of the two types with regard to their distribution within the layers of the OB, type 1 had a significantly higher number of axon branch points in the GL and EPL than type 2 (post-hoc: p<0.001; table 2; cell type effect: $F_{(1,17)}$=8.73; p=0.009; n=11/8 from 18 rats, table 2)$_e$. In contrast, the average axonal branch length of type 1 was significantly lower than that of type 2 (post-hoc: p=0.022, cell type effect: $F_{(1,17)}$=5.66; p=0.029; n=11/8 from 18 rats; table 2)$_f$.

Interestingly, the two projection types also differed with respect to an electrophysiological parameter, their membrane time constant (τ_m): type 1 cells had a significantly faster τ_m than type 2 cells ($t_{(16)}$=-3.09, p=0.007; n=11/7 from 18 rats; table 2)$_h$. The R_i, spiking threshold, spike amplitude, spike ratio, and AHP ratio were not different between the two morphological groups (table 2).

A comprehensive analysis of the axonal morphology including also non-reconstructed VPCs revealed a much higher overall prevalence of type 1 (n=63) compared to type 2 (n=10).

In summary, type 1 more densely (more branch points) innervates the superficial layers with its axon and features multiple but short local projections (shorter branch length) to the deeper layers, i.e., MCL and superficial GCL. Type 1 axonal projections are thus more prominent directly medial to the home glomerulus, probably interacting with the respective glomerular column (Willhite et al., 2006). Conversely, type 2 has a more sparse overall axonal innervation (less branch points) in total but has wider-ranging projections (longer branch length), especially below the MCL reaching either deeper into the GCL or alongside the internal plexiform layer to more distant targets (Fig. 9).

Since the biocytin-DAB staining that was used for the axon visualization relies on post-fixation and extensive post-hoc histochemical treatment the reconstructions suffer from tissue shrinkage, especially in the z-direction of the slice (Egger et al., 2007). This effect complicates the reconstruction of the very dense structure of the apical dendrite/tuft of VPCs. Thus, we reconstructed the tufts of eGFP-labelled VPCs filled with fluorescent dye from unfixed slices along with their “home glomeruli” as described previously for juxtaglomerular neuron types (Bywalez et al., 2016).

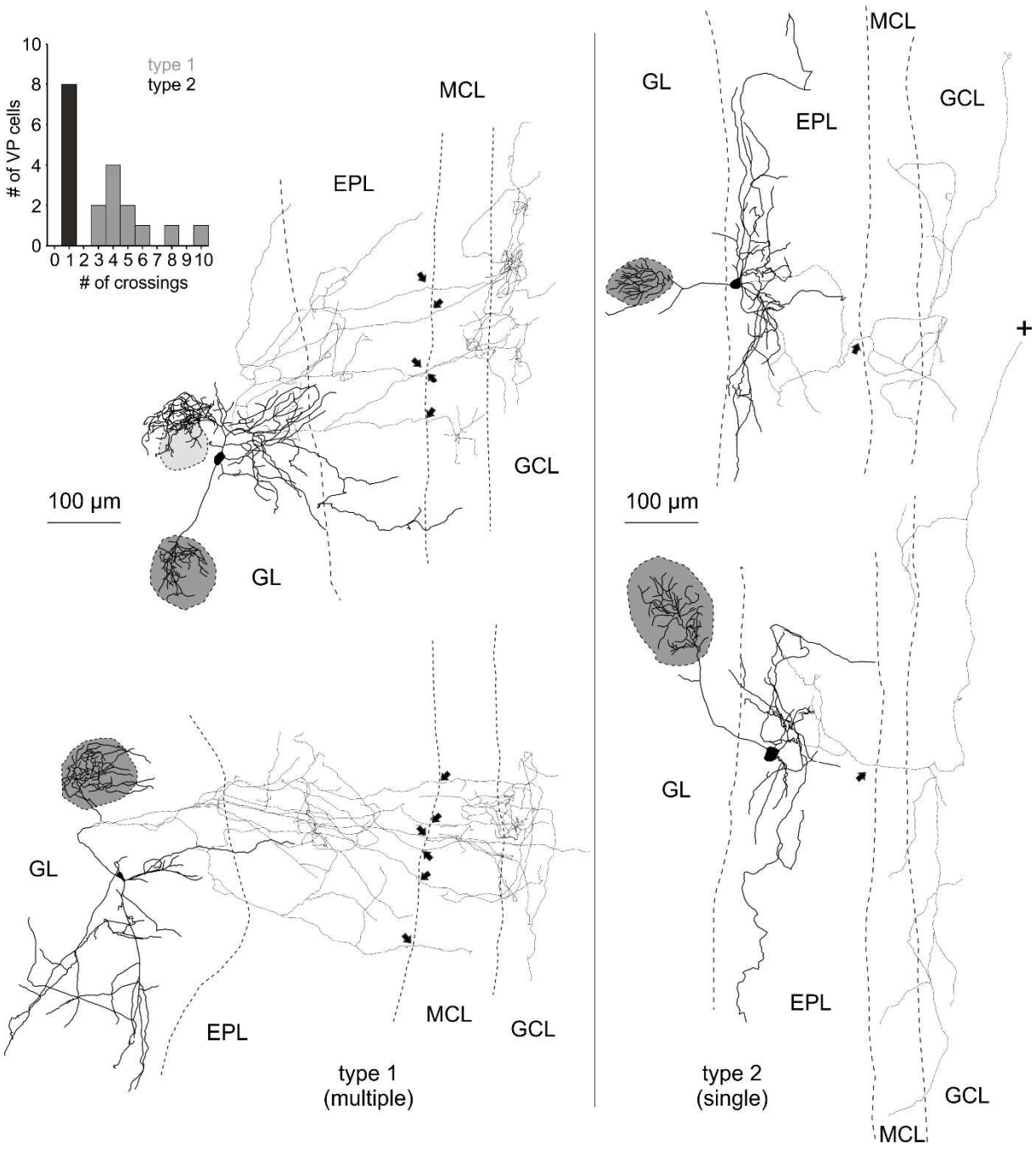

Fig. 9 (A) Reconstructions of eGFP-VPCs labelled with biocytin. Two representative examples of type 1 (multiple innervations of MCL, left panel) and type 2 cells (single top-down innervation of MCL, right panel). EPL, external plexiform layer; GCL, granule cell layer; GL, glomerular layer; MCL, mitral cell layer. +: truncation of axonal projection. Arrows: site of axonal MCL crossing from EPL into GCL. The dark grey shading indicates the glomerulus innervated by the dendritic tuft of the respective VPC. Light grey shading indicates that dendrites lie above or below respective glomerulus. The VPC in the upper left panel displays a conspicuous dendritic ramification that does not enter the adjacent glomerulus. Similar structures were found in 4 out of 35 reconstructed cells. Insert: number of crossings vs. number of cells.

Table 2 **Electrophysiological and morphological properties of type 1 and type 2 VPCs.**

	Type 1 (n=11)			Type 2 (n=8)		
Pre-selection parameter						
Crossings MCL	5 ± 0.7			1		
Neurites	Dendrites	Axon		Dendrites	Axon	
Layers	GL + EPL	GL + EPL	MCL + GCL	GL + EPL	GL + EPL	MCL + GCL
Branchpoints[d,e]	32 ± 5.5	23 ± 2.4*	17 ± 6.0	28 ± 4.4	4.1 ± 1.0#	6.6 ± 2.7#
	32 ± 5.5	40 ± 6.8*		28 ± 4.4	11 ± 3.1	
Branch length	40 ± 3.4	63 ± 5.4#	68 ± 8.8	46 ± 5.3	81 ± 11#	117 ± 29#
(µm)[f,g]	40 ± 3.4	62 ± 5.9*#		46 ± 5.3	93 ± 12#	
Area neurites	0.05 ± 0.01	0.5 ± 0.3		0.05 ± 0.01	0.1 ± 0.04	
(mm²)						
Area soma (µm²)	146 ± 25			182 ± 26		
Location Soma	8 x GL vs. 3 x EPL			2 x GL vs. 6 x EPL		
Lateral dendrites[c]	3 ± 0.4*			5 ± 0.3		
$\tau_{(m)}$ (ms)[h]	65 ± 6.9*			96 ± 6.3		
R_i (MΩ)	530 ± 78.2			927 ± 204		
Threshold (mV)	-50 ± 1.7			-48 ± 1.2		
AP amplitude (mV)	76 ± 2.1			67 ± 5.6		
Last/first spike ratio	0.73 ± 0.04			0.66 ± 0.08		
Last/first AHP ratio	1.1 ± 0.04			0.88 ± 0.11		

Mixed model ANOVA followed by a post-hoc comparison *d,e,f,g* using Bonferroni correction or t-test for independent samples *c,h*; * p<0.05 vs. Type 2; # p<0.05 vs. Dendrites; Data are means ± SEM

2.5.4 Morphology of the apical tuft

Using 2-photon microscopy z-projections of fluorophore-filled VPCs, we were able to reconstruct and characterize the branching patterns of the glomerular innervation by the apical dendrite/tuft of VPCs and compared them to MCs. In contrast to the rather straight apical dendrites of MCs and mTCs, VPCs' apical dendrites (length 109.1 ± 13.3 µm, n=13 from 10 rats) often take a tortuous route around neighboring glomeruli to innervate one single glomerulus with a tuft-like structure (Fig. 6A+10A). All VPC tufts showed a uniform, widespread innervation of their "home glomerulus" (Fig. 6A+10A). The neighboring glomeruli are not innervated, since also lateral VPC dendrites were not found to enter them (Fig. 6A+10A). To quantify the glomerular innervation pattern of the apical dendritic tuft, we measured the density of branch points and fraction of total branch points within shell segments of the respective glomerulus in VPCs (n=13 from 10 rats) and MCs (n=8 from 8 rats, see methods and Bywalez et al., 2016). VPCs had a significantly lower branch point density ($F_{(1,19)}$=9.20, p=0.07)$_i$ but a similar branch point distribution across their glomerular shells ($F_{(1,19)}$=0.080, p=0.780)$_j$ compared to MCs (Fig. 10B). Thus, similar to MCs, VPC tufts would be in a position to both receive inputs and provide output throughout the whole glomerulus - in contrast to classical eTCs that fan out in only part of the glomerulus (Fig. 6B, Pinching and Powell, 1971).

This dense innervation of its 'home glomerulus' by the apical tuft, along with the subcellular VP expression (Fig. 8) and the presence of VP-receptive VP and oxytocin receptors throughout the glomerular layer (Vaccari et al., 1998; Manning et al., 2008; Tobin et al., 2010) implies a functional role of the VPC tuft as a potential site of release for VP.

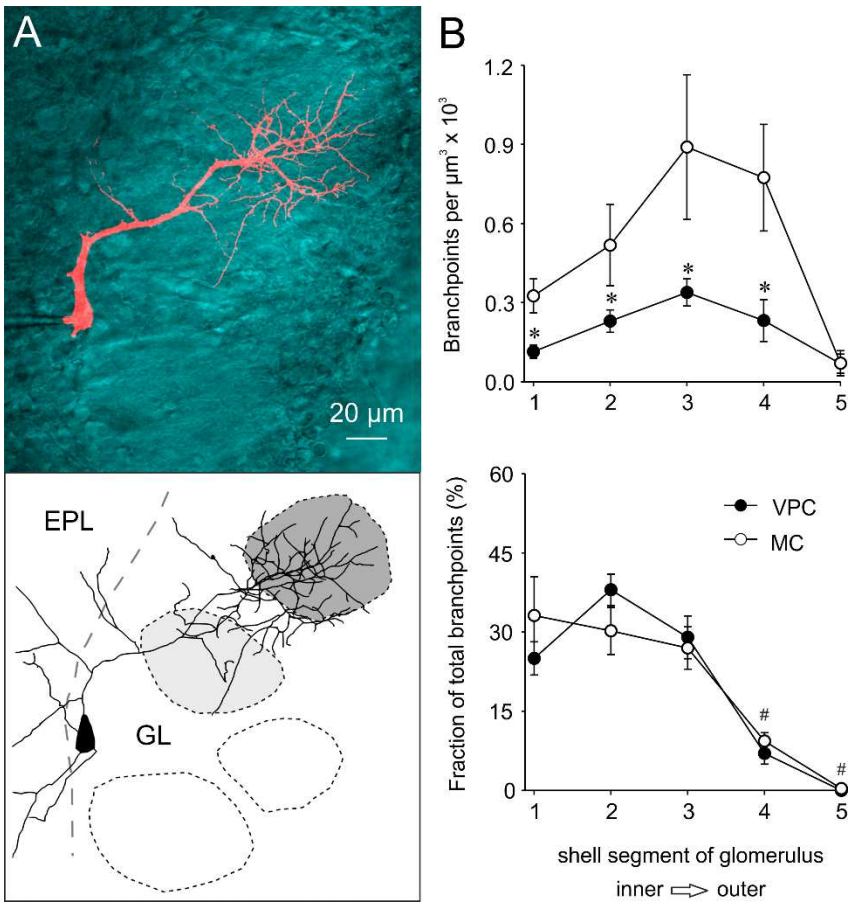

Fig. 10 (A) Maximal z-projection of a VPC filled with Alexa-594 and overlaid with the single z-plane of the trans-infrared channel that showed the maximal extent of the innervated glomerulus. Bottom panel: Reconstruction of cell above. The dark grey shading indicates the glomerulus innervated by the dendritic tuft of the respective VPC. The other glomeruli have no contact with the VPC (white) or lie above or underneath the dendrites of the VPC (light grey shading). Imaging was performed in acute slices (300 µm) using 2-photon laser scanning microscopy. (B) Density of branch points and fraction of total branch points within shell segments of the respective glomerulus in VPCs (n=13) and MCs (n=8). Statistical comparisons indicate a lower branch point density but similar branch point distribution in VPCs compared to MCs.

$p<0.05$ vs. respective MC; # $p<0.05$ vs. segment 1+2; Mixed model ANOVA followed by post-hoc test with Bonferroni correction.

EPL, external plexiform layer; GL, glomerular layer; MC, mitral cell; VPC, vasopressin cell.

2.5.5 Tuft excitability as established by backpropagating action potentials

Neurons in the OB that are capable of dendritic release usually feature strong AP backpropagation from the soma which is accompanied by substantial dendritic Ca^{2+} entry. Such Ca^{2+} signals were observed in apical dendrites of granule cells (GCs) and lateral dendrites, apical dendrites and tufts of MCs (Xiong and Chen, 2002; Debarbieux et al., 2003; Egger et al., 2003). Therefore we hypothesized that VPCs' tufts would be similarly excitable. We imaged Ca^{2+} signals in response to backpropagating somatically evoked single APs (sAPs) and trains (20 APs at 50 Hz) within the apical dendrite and tuft. Surprisingly, we consistently observed very small or no dendritic Ca^{2+} transients in response to sAPs (tuft $\Delta F/F$ amplitude: 3.9 ± 0.8 %, n=38 measurements in 11 cells from 9 rats; soma/apical dendrite below tuft $\Delta F/F$: 2.7 ± 0.4 %, n=42 measurements/11 cells from 9 rats; Fig. 11B). Trains caused a moderate rise in $\Delta F/F$ (tuft: mean amplitude 56 ± 3.0 %, n=38 measurements/11 cells; soma/dendrite: 46 ± 3.6 %; Fig. 11B), which demonstrates that voltage-gated Ca^{2+} channels are indeed present in the tuft. These $\Delta F/F$ responses to trains significantly increased along the apical dendrite ($R=0.475$, $R^2=0.225$, $p=0.001$, n=42 measurements/11 cells)$_k$, but only until the main branch point of the glomerular tuft ($R=-0.128$, $R^2=0.016$, $p=0.445$, n=38 measurements/11 cells)$_k$.

To control for the small size of sAP-mediated Ca^{2+} signals in VPCs (n=11 from 9 rats) we compared these data to a corresponding data set of MCs (n=13 from 10 rats) recorded with the same technique (Egger and Stroh, 2009). In these cells, single APs as well as prolonged trains produced substantial, significantly higher Ca^{2+} signals than in VPCs (sAP: $F_{(1,125)}=1035$; $p<0.001$; n=128 measurements/24 cells; 50 Hz: $F_{(1,107)} = 268$; $p < 0.001$; n=110 measurements/24 cells; Fig. 11C)$_l$.

In conclusion, in terms of Ca^{2+} entry VPC tufts appear much less responsive to propagating APs than MC tufts. Therefore, single APs are highly unlikely to admit an amount of Ca^{2+} sufficient for VP release from the dendrite. However, this observation does not exclude the possibility that synaptic inputs e.g., from the ON can provide local synaptic excitation and

thus substantial local Ca^{2+} entry (as known for MC tufts, e.g., Zhou et al., 2006) that could trigger VP release from VPCs in a local reciprocal manner.

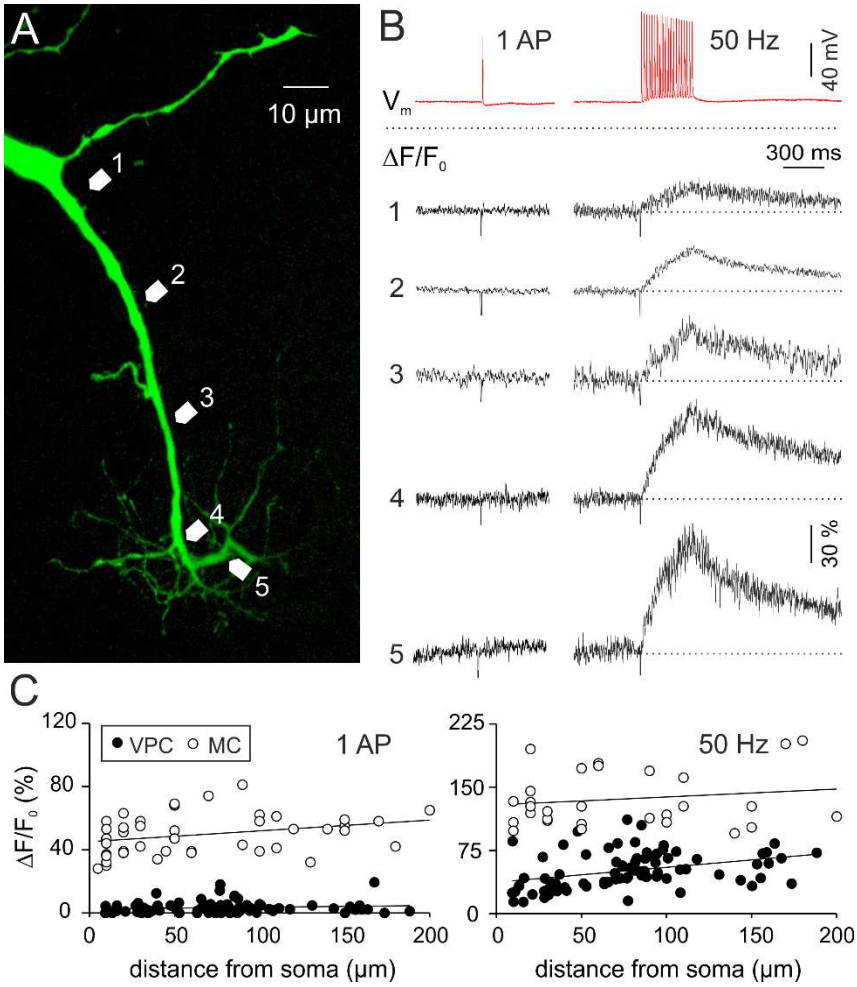

Fig. 11 (A) Two-photon scan of a representative VPC filled with the Ca^{2+}-sensitive dye OGB-1. Numbered arrows in the scan correspond to the locations of the numbered averaged (n=4) ΔF/F transients shown in (B), in response to a single somatically-evoked action potential (1000 pA, 1 ms) or a 50 Hz train (20 APs, 50 Hz, 400 ms). (C) ΔF/F of apical dendrites and tufts versus distance from soma in VPCs (n=11) and MCs (n=13).
MC, mitral cell; VPC, vasopressin cell

2.5.6 Olfactory nerve-mediated inputs to VPCs

Tufted glutamatergic MCs, mTCs, and eTCs receive mono- and/or di-synaptic excitation from the ON onto their apical dendritic tufts (Heyward et al., 2001; Hayar et al., 2004b; Burton and Urban, 2014). Therefore, we expected that ON activation would also excite VPCs. We performed whole cell recordings from VPCs and electrically stimulated the ON axons anterior to the glomeruli above the soma of the recorded VPC. Surprisingly, single ON stimulation did not result in direct excitation, but induced IPSPs (n=97 VPCs from 77 rats; Fig. 12B). The observed IPSPs had a mean amplitude of -10.7 ± 0.6 mV (n=11 from 10 rats). Their mean latency of more than 10 ms after ON stimulation (12.6 ± 0.8 ms) indicates a polysynaptic pathway of inhibition. ON-evoked VPC IPSPs had slow kinetics (rise time: 35 ± 3 ms, decay in terms of half duration: 254 ± 30 ms) compared to the kinetics of spontaneous IPSPs in MCs recorded under similar conditions (risetime: 12 ± 7 ms, half duration: 40 ± 15 ms, Egger and Stroh, 2009).

Stronger ON stimulation with trains of current pulses (20 x at 50 Hz), did also not result in an excitatory postsynaptic response (Fig. 12C, n=3 from 3 rats). For additional confirmation of the unexpected finding of predominantly inhibitory responses we recorded ON-evoked EPSPs from MCs located proximal to a VPC that responded with IPSPs to stimulation at the same site (n=4 from 4 rats; Fig. 12D). Therefore, it is highly unlikely that the observed IPSPs are artefacts of our stimulation technique (e.g., wrong positioning or insufficient stimulation strength) or due to other systemic parameters (ACSF, intracellular solution, etc.).

To investigate if these VPC responses are indeed GABAergic, VPCs were current-clamped from -55 mV to -95 mV. Responses to ON stimulation then became depolarizing, arguably due to the reversal of Cl^--currents through GABA receptors (Fig. 12B; n=7 from 6 rats). Next, the $GABA_A$ receptor antagonist bicuculline completely blocked IPSPs recorded at -55 mV ($t_{(7)}$=-5.48, $p<0.001$; n=8 from 8 rats)$_m$ and unmasked barrages of putative EPSPs (Fig. 12E). These barrages had an amplitude of 6.9 ± 1.8 mV and even longer onset latencies (46.1 ± 27.5 ms) indicating a polysynaptic nature also for these inputs.

A detailed analysis of all our VPC recordings with both ON stimulation and recovered morphology revealed that 69 of the 70 VPCs (from 58 rats) that responded with IPSPs still had an intact apical tuft, whereas 11 of the 15 VPCs (from 12 rats) without or a massively cut tuft did not show any ON-evoked IPSPs. Thus, candidate inhibitory inputs should be restricted to juxtaglomerular interneurons that innervate glomeruli, e.g., periglomerular cells or 'short-axon' cells. As to the excitatory barrages, 15 out the 15 VPCs without apical tuft showed either small IPSPs with no late depolarization (n=4 from 12 rats) or no signal at all (n=11 from 12 rats) upon ON stimulation, indicating that the postsynaptic origin of this excitatory signal, like the inhibitory one, is most likely located in the apical tuft. Thus, we propose that the postsynaptic origins of both IPSP and EPSP barrage are located within the "home glomerulus", i.e., on the VPC tuft.

These findings imply that ON inputs alone are unlikely to excite VPCs and thus cannot invoke glomerular VP release by themselves. Nevertheless, many cells in the glomerular layer express VP-receptive VP and oxytocin receptors (Vaccari et al., 1998; Manning et al., 2008; Tobin et al., 2010), the dendritic tuft is excitable (Ca^{2+} entry) by somatic depolarization, and VP is expressed in apical and lateral dendrites of VPCs (Fig. 8, de Vries and Buijs, 1983). Thus, even though at this point we do not know the origin of physiologically relevant excitatory stimuli that could result in glomerular VP signaling, we next investigated whether VP can indeed affect glomerular synaptic processing.

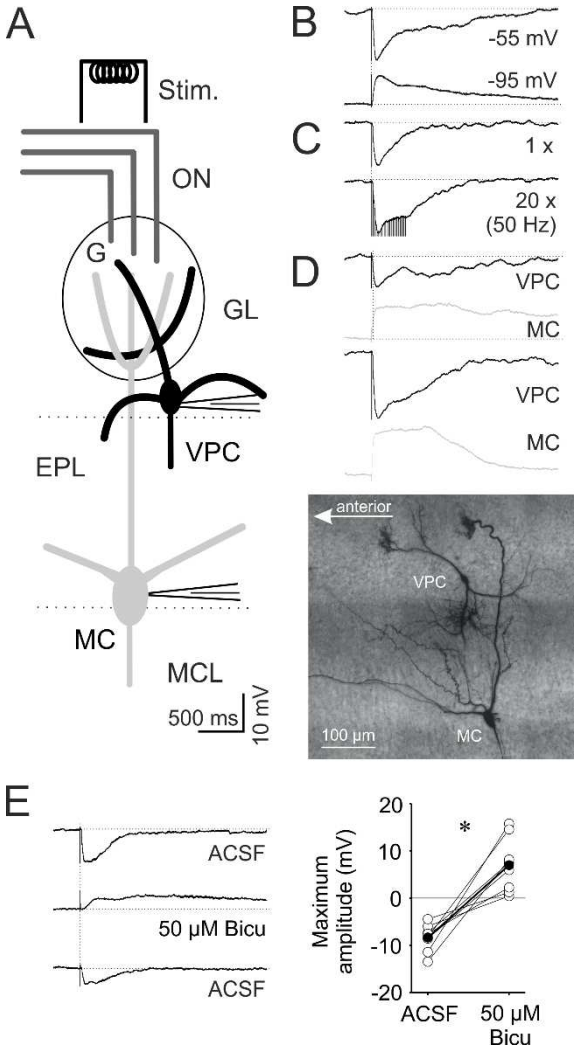

Fig. 12 (A) Schematic drawing of experimental setup. Whole-cell patch clamp recordings in 300 µm in-vitro slices of responses to electrical olfactory nerve stimulation (ON, 400 µA, 100 µs, 30s intervals). (B) Representative averaged (10 traces) ON-evoked IPSPs recorded from a VPC at resting potential of -55 mV (total n=97) and hyperpolarized to -95 mV (total n=7). (C) Representative averaged (10 traces) ON-evoked IPSPs stimulated one time and 20 times at 50 Hz recorded from a VPC at resting potential of -55 mV (n=3). (D) Representative averaged PSPs from two pairs of VPCs and MCs sequentially stimulated, but at the same location within the same slice (Image: maximal z-projection of a representative pair of a VPC and MC from this experiment visualized by subsequent biocytin-DAB staining). (E) Bath application of 50 µM bicuculline (competetive $GABA_A$ receptor antagonist). Left panel: Representative averaged (10 traces) ON-evoked PSPs recorded from a VPC. Right panel: cumulative presentation of bicuculline effect on PSP amplitudes (n=8). Empty dots represent single measurements, whereas filled dots represent means.

* $p<0.05$ vs. ACSF. T-test for dependent variables. Amplitudes of stimulus artifacts were truncated.

ACSF, artificial cerebrospinal fluid; Bicu, bicuculline; EPL, external plexiform layer; G, glomerulus; GL, glomerular layer; MC, mitral cell; MCL, mitral cell layer; ON, olfactory nerve; VPC, VP cell.

2.5.7 Effects of VP on glomerular layer tufted cells (eTCs and VPCs)

If VP application had an effect on synaptic glomerular signaling, such observations could provide additional indirect evidence for a role of endogenous release of VP in glomerular processing. The fact that the dendritic compartment of eTCs consists solely of an apical tuft within one glomerulus (and no lateral dendrites, Fig. 6B, Hayar et al., 2005) makes them utilizable as glomerular VP sensors.

To activate synaptic glomerular processing, we again used ON-stimulation, and recorded from individual eTCs. As expected, eTCs responded with EPSPs (Hayar et al., 2004b), further confirming our finding of ON-evoked IPSPs in VPCs. Application of 1 µM of VP *in vitro* slightly but significantly reduced ON-evoked EPSP amplitudes to 85 ± 2.8 % of baseline (interaction effect: $F_{(9,117)}$=4.94, p=0.002; n=15 from 12 rats; see Fig. 13B). This finding supports the hypothesis that endogenously released VP could exert these direct or indirect effects preferentially within the eTC's home glomerulus and thus originate from a VPC tuft in the same glomerulus.

Further, we were interested whether ON stimulation as such is capable of causing VP release. However, application of a selective VP antagonist (10 µM, Manning compound) did not modulate the amplitude of ON-evoked EPSPs in eTCs and was also significantly different from the effect of the VP application (amplitude 99 ± 3.2 % of baseline; n=15 from 12 rats, interaction effect: $F_{(9,117)}$=4.94, p=0.002; see Fig. 13B)$_n$. This finding implies that ON activity is unlikely to induce endogenous glomerular VP release, in line with our previous finding of predominantly inhibitory ON-action on VPCs (Fig. 12). Moreover, the experiment may serve as a control against run-down of eTC EPSPs in response to extended repeated ON stimulation.

Further, to elucidate whether VPCs are capable of autocrine self-excitation like VPCs in the hypothalamus (Sabatier et al., 1997), we investigated the effects of exogenous VP on ON-evoked IPSPs in VPCs. Application of 1 µM of VP *in vitro* reduced the evoked IPSP amplitude to 69 ± 3.9 % of baseline (n=12 from 12 rats, interaction effect: $F_{(7,70)}$=10.3,

$p<0.001$; see Fig. 13C)$_o$ compared to further ACSF application. This reduction of ON-evoked VPC inhibition might serve to increase the probability for VPC excitation and thus release via other pathways. Finally, during recordings of ON-evoked excitatory EPSP barrages from VPCs in the presence of the GABAergic blocker bicuculline (50 µM, see also Fig. 12E), bath application of 1 µM VP could not further increase the amplitude of the excitatory signal (n=6, $F_{(2,10)}=32.0$, $p=0.002$; Fig. 13D)$_p$. This indicates that VP acts on the transmission of GABAergic interneurons, but rather not on excitatory inputs to VPCs, like eTCs, mTCs, MCs, and ON, as otherwise the isolated EPSP barrages would have been also modulated by VP.

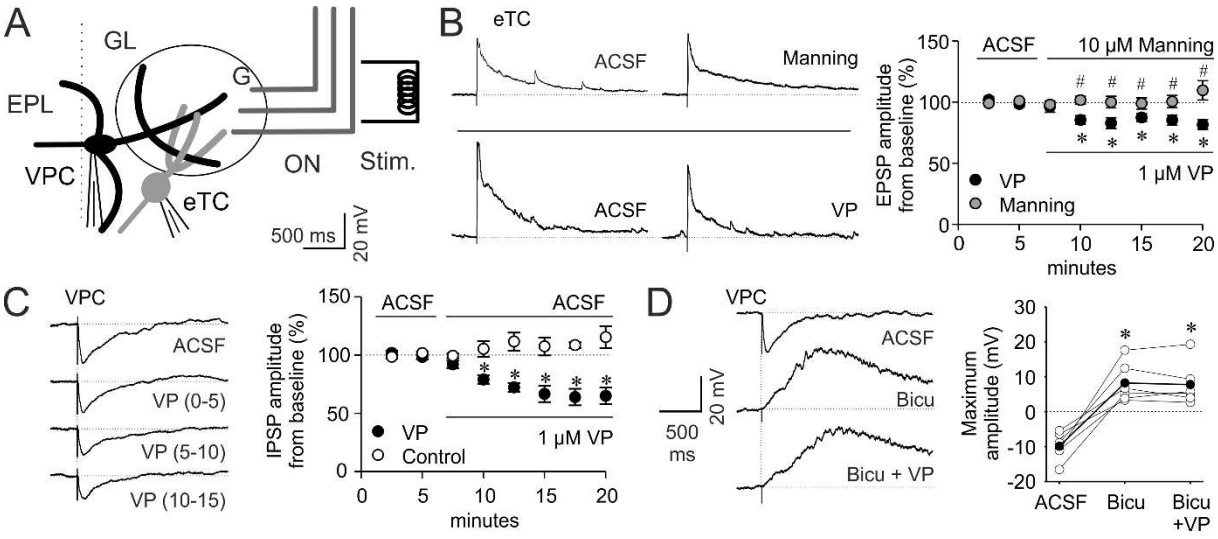

Fig. 13 (A) Schematic drawing of experimental setup. Whole-cell patch clamp recordings from VPCs or eTCs of responses to electrical olfactory nerve stimulation (ON, 20-400 µA, 100 µs, 30s intervals). Bath application of 1 µM VP or 10 µM of a VP receptor antagonist (Manning compound). (B) Left panel: Representative averaged (10 traces) ON-evoked EPSPs recorded from an eTC. Right panel: Cumulative averaged (5 traces) presentation of VP/Manning compound effect on EPSP Amplitudes (n=8/7). (C) Representative averaged (10 traces) ON-evoked PSPs recorded from a VPC and cumulative averaged (5 traces) presentation of 1µM VP effect on IPSP Amplitudes (n=6, numbers in brackets represent time bins in minutes after VP). (D) Bath application of 50 µM bicuculline (competitive $GABA_A$ receptor antagonist) and 1 µM VP. Left panel: Representative averaged (10 traces) ON-evoked IPSPs recorded from a VPC. Right panel: Cumulative presentation of bicuculline/VP effect on PSP amplitudes (n=6). Empty dots represent single measurements, whereas filled dots represent means. Data points are means ± SEM. * $p<0.05$ vs corresponding ACSF. # $p>0.999$ vs. ACSF. T-test for dependent variable (D).

2.6 Discussion

2.6.1 Vasopressin cells as superficial tufted cells

Our detailed investigation revealed that VPCs feature several unique electrophysiological and anatomical properties that differentiate them from other glutamatergic tufted cell types in the OB. In the initial study by Tobin et al. (2010) VPCs were considered as classical eTCs, based on the observation of bursting firing patterns and spontaneous bursts that characterize classical eTCs without lateral dendrites (Hayar et al., 2004b). In our study VPCs always featured non-bursting, regular firing patterns and lateral dendrites. Notably, classical eTCs have been described to reside in the GL (Hayar et al., 2004b), whereas TCs located at the border between EPL and GL including the superficial part of the EPL – as observed here for VPCs - are often referred to as superficial tufted cells (sTCs, Hamilton et al., 2005; Nagayama et al., 2014; Tavakoli et al., 2018). Just like sTCs, VPCs bear several lateral dendrites that spread in the EPL and an apical dendrite that takes a tortuous route through the GL before entering its 'home glomerulus' and forming a tuft. By comparison, classical eTCs feature a tuft that originates almost directly from the soma, and lack lateral dendrites. Also, the VPC apical tuft branching pattern inside the glomerulus shows a uniform, widespread innervation very similar to that of MCs, but clearly different from the fan-like, more restricted tuft described for classical eTCs (Pinching and Powell, 1971; Hayar et al., 2004b).

Although, sTCs were described with both, bursting and non-bursting firing properties (Liu and Shipley, 1994; Kiyokage et al., 2010; Nagayama et al., 2014), according to Antal et al. (2006) the absence of bursting in juxtaglomerular TCs strongly predicts the presence of lateral dendrites, as found for all our VPCs. Conversely, in our sample of classical eTCs without lateral dendrites we were always able to reproduce bursting firing patterns and observed spontaneous bursts in more than half of the cells. Therefore, the observed lack of bursting in VPCs seems not to be related to our recording conditions. VPCs showed sags during long

hyperpolarizing current injections (to -100 to -120 mV), which are smaller in amplitude compared to sags recorded from our sample of eTCs at comparable hyperpolarization. These sags are typically mediated via hyperpolarization-activated currents (I_h). Varieties of I_h channels were shown to be expressed in all subtypes of juxtaglomerular TCs, including eTCs and sTCs, with a higher prevalence for HCN4 in sTCs (Holderith et al., 2003; Fried et al., 2010). However, in our hands VPCs lack L-/T-type Ca^{2+} channel mediated low-threshold spikes (LTS) during firing, a prerequisite for intrinsic spontaneous activity in bursting eTCs (Liu and Shipley, 2008) that we also recorded from eTCs during spontaneous bursts or the rebound phase following hyperpolarizing current steps. Additionally, the presence of LTSs is reflected in the very low last/first AHP ratio in the firing patterns of eTCs compared to the other cell types in our analysis, including VPCs. It should be mentioned, however, that the discrepancy between the Tobin paper and our study with respect to the occurrence of bursts might be related to the young age of the rats in our data set, since conductances relevant for bursting could be developmentally regulated (e.g., Kanyshkova et al., 2009). Then again, rats in the Antal et al. study (2006) were older than in ours, presumably overlapping with the Tobin study. Further in line with Antal et al. (2006), another criterion to classify VPCs as non-bursting sTCs rather than eTCs is their slow membrane time constant (τ_m) since we found VPCs to display a twofold slower τ_m than MCs and mTCs and even fourfold slower than eTCs.

Thus, the results from both neuroanatomical and electrophysiological characterizations suggest that VPCs correspond to the sTC subtype of TCs or a non-bursting subclass thereof. Interestingly, a recent study by Tavakoli et al. (2018) used cluster analysis of randomly patched juxtaglomerular cells in mice based on dendritic morphology and electrophysiological properties and identifies a previously unknown cluster E of “vertical superficial tufted cells”. Cluster E likely overlaps with VPCs since these cells feature a similar dendritic/axonal morphology, large somata (98.9 µm²), and similarly high $\tau_{(m)}$ (40.7 ± 20.1 ms) as well as $R_{(i)}$ (0.65 ± 0.31 GΩ), and a low CV of ISI (0.17 ± 0.10). Tavakoli et al. (2018)

also noted the similarity of cluster E with the type 2/sTCs described by Antal et al. (2006), whereas they propose VPCs to be part of their cluster G („horizontal superficial tufted cells", see their table 5). Based on our observations listed above and their characteristic vertical orientation of lateral dendrites and axons, we rather expect VPCs to be identical to cluster E or at least a subpopulation thereof. Intriguingly, Tavakoli et al. (2018) could not find synaptically connected pairs between other juxtaglomerular neurons and cluster E cells, which might be related to the tortuous apical dendrite and the overall low local excitatory connectivity observed here.

While nothing is known on synaptic inputs and other network interactions of cluster E sTCs so far (Tavakoli et al., 2018), sTCs in general have been suggested to integrate feedback information of interneurons in the GL and EPL and even of GABAergic network inputs from superficial GC dendrites via both their pronounced dendritic tuft and lateral dendrites, whereas classical eTCs are obviously limited to input from the GL (Macrides and Schneider, 1982; Antal et al., 2006). Additionally, the strong dendritic innervation of the GL was suggested to imply that sTCs might be optimized to receive excitatory sensory signals (Antal et al., 2006), either via direct ON input or mediated via eTCs (De Saint Jan et al., 2009). However, this scenario is rather unlikely to hold for VPCs since under our recording conditions electrical ON stimulation primarily caused strong inhibition of VPCs, which occurred mostly via their tuft, while the lateral dendrites were not found to receive ON-mediated inputs.

2.6.2 Possible origins of excitatory inputs to VP cells: sensory vs. centrifugal

Since the glomerular synaptic connectivity of VPCs was not known and endogenous VP release is supposed to happen during presentation of volatile social odors (Lévy et al., 1995), we initially presumed that like classical eTCs, VPCs might receive excitation from the ON (Hayar et al., 2004b). As stated above, to our knowledge it has not been investigated before whether vertical sTCs (cluster E) receive excitation directly from the ON and/or via eTCs,

while horizontal sTCs were observed to receive inputs from classical eTCs (cluster G, Tavakoli et al., 2018). In our study ON stimulation does not result in immediate excitation but predominantly causes $GABA_A$ receptor-mediated polysynaptic inhibition of VPCs as determined by the glutamatergic nature of ON transmitter release and the long latency (~10 ms). Thus these inputs to VPCs might be generated either disynaptically via direct ON-excitation of GABAergic interneurons or via the ON → eTC → periglomerular cell circuit, like most GABAergic inhibition in the GL (Fig. 14, Aungst et al., 2003; Hayar et al., 2005). Finally, we also found that 50 Hz stimulation of the ON could not reverse VPC inhibition.

Although our findings imply that direct monosynaptic excitation of dendritic tufts of VPCs via the ON is unlikely to exist, the pharmacological blockade of the ON-evoked IPSPs unmasked barrages of depolarizing potentials that occurred with a yet longer latency than the IPSPs. Since tuftless VPCs never showed any excitatory responses to ON stimulation, these barrages may reflect excitatory local glomerular network reverberations between eTCs and projection neurons, i.e., MCs and mTCs (Fig. 14, De Saint Jan et al., 2009). Similar barrages upon ON stimulation have been observed previously in MCs (“long-lasting depolarizations”, Aroniadou-Anderjaska et al., 1999; Carlson et al., 2000). This hypothesis is also supported by the very long and highly variable barrage onset latency (Nicoll, 1971). Still, it remains to be clarified whether these excitatory inputs to VPCs are originating from MC/mTCs and/or eTCs and/or else.

Thus in order to excite VPCs, inputs are required that either inhibit the GABAergic origin of the ON-evoked inhibition (i.e., disinhibition) and/or deliver enough direct excitation to outweigh the inhibition. These additional inputs could restrict bulbar VP release to occasions when social odors are processed. For example, the detection of pheromones in the AOB could provide the required specificity for social stimuli via local excitatory inputs to the main OB (Vargas-Barroso et al., 2016). Another candidate region for social-specific inputs is the anterior olfactory nucleus (AON) that provides numerous glutamatergic centrifugal afferents to the OB (Markopoulos et al., 2012; Rothermel and Wachowiak, 2014) and receives

projections from the hypothalamus, that enhance input from the AON to OB granule cells during social interactions, resulting in an improved signal-to-noise ratio of olfactory input processing (Oettl et al., 2016). A similar social interaction-driven excitation of VPCs via AON projections to the GL seems plausible (Luskin and Price, 1983). Finally, the perception of other, non-olfactory sensory social cues (visual, auditory, tactile) could act as top-down social go-signal (Fig. 9). The most prominent modulatory centrifugal inputs that could mediate such signals include noradrenergic fibers from the locus coeruleus, cholinergic fibers from the horizontal limb of the diagonal band of Broca and serotonergic fibers from the dorsal raphe nucleus (Matsutani and Yamamoto, 2008), since all three neuromodulatory systems were shown to be involved in facilitating social odor discrimination (Lévy et al., 1995; Dluzen et al., 1998b; Cavalcante et al., 2017).

2.6.3 Mechanisms of dendritic VP release in OB vs. hypothalamic VPCs

Although so far, the mechanisms for suprathreshold VPC excitation and thus subsequent release of VP are not yet known, several of our findings and previous observations suggest that VPCs are able to release VP within the cellular network of the OB from both dendrites and axons:

1) The observed VP immunoreactivity in soma, dendrites, and axons indicates that these structures are potential release sites. Unfortunately, due to the low immunofluorescence of VP-neurophysin we could not prove that VP is present also within the finer branches of the neurites. Yet, early histological studies by De Vries et al. (1985) describe “scattered elongated” VP-immunoreactive fibers in the EPL of the rat OB. Since we observed that VPC axons are widely spread throughout the EPL, we would like to suggest that all VPC substructures express VP.
2) The presence of VP-receptive VP- and oxytocin receptors (Manning et al., 2012) throughout all layers of the OB (Vaccari et al., 1998; Tobin et al., 2010) indicates that

several components of the OB cellular network are able to detect endogenous VP release.

3) The observation of effects of exogenous VP application on ON-induced synaptic inputs to 2 OB cell types with glomerular dendritic tufts (sTCs/VPCs and eTCs), indicates a functional relevance of VP signaling in olfactory processing. This notion is strongly supported by earlier findings demonstrating that blockade of endogenous VP receptors via intrabulbar infusion of a selective VP receptor antagonist reduces MC excitation as well as social odor discrimination abilities *in-vivo* (Tobin et al., 2010).
4) The occurrence of moderate Ca^{2+} entry into VPC apical tufts following somatic AP trains indicates the presence of voltage-gated Ca^{2+} channels (VGCCs) that could contribute to triggering VP release.
5) The threshold for AP generation in VPCs is similar to other TCs, like MCs and eTCs. Further, VPCs fire APs upon both small positive current injections and the rebound following hyperpolarization. Thus, given an adequate excitatory stimulus is present, VPCs should be sufficiently excitable to sustain AP trains that might be required for both dendritic and axonal release of VP.

Although the exact release mechanisms of VP from OB VPCs remain to be elucidated in future studies, a comparison of our findings with the release mechanisms of hypothalamic VPCs may also yield insights into this matter in bulbar VPCs. Hypothalamic VPCs release VP from axon terminals in the periphery, but also centrally from their dendrites and the surface of their soma (Pow and Morris, 1989). With respect to dendritic/somatic release mechanisms in general, MCs, granule cells and other dendritically-releasing neurons in the OB and elsewhere dispose of an effective dendritic AP backpropagation mediated by active dendritic conductances such as voltage-gated Na^+ and Ca^{2+} channels (Stuart et al., 1997; Egger et al., 2003; Zhou et al., 2006). However, in VPCs we observed no Ca^{2+} entry upon single backpropagating APs and only moderate intracellular Ca^{2+} transients in response to prolonged AP trains. These observations possibly indicate that substantial Ca^{2+} entry into

VPC apical tufts sufficient for release cannot be achieved via somatic AP firing alone. In line with that idea, in hypothalamic VPCs antidromic axonal electrical stimulation (50 Hz for 3 s) is not enough to induce somato-dendritic VP release (Ludwig et al., 2005), although dendritic Ca^{2+} spike propagation via VGCCs is possible during long-lasting current application (>400 ms, Bains and Ferguson, 1999). In hypothalamic VPCs dendritic release can be transiently uncoupled from peripheral axonal release in the neural lobe of the pituitary (Ludwig et al., 1994). Accordingly, Bains et al. (Bains and Ferguson, 1999) suggest that dendritic VGCCs (L, N, and T-type according to Sabatier et al., 1997) are located in some distance from the soma. Intriguingly, while the somata of OB VPCs are mostly located very superficially in the EPL, they always keep a certain distance from the glomerulus containing the tuft (100 µm), resulting in a longer apical dendrite below the tuft compared to the almost inexistent apical dendrite of classical eTCs (Pinching and Powell, 1971). Thus, the long VPC apical dendrite with its poor backpropagation may allow for a certain degree of functional compartmentalization, i.e., uncoupling between the tuft and the soma, which was also proposed as explanation for the long primary dendrites of MCs and TCs (Chen et al., 2002; Migliore et al., 2005). One possibility to induce somato-dendritic VP release in the hypothalamus is the application of VP itself (Ludwig et al., 1994). In line with that finding our experiments demonstrate that exogenous VP reduces ON-induced VPC inhibition. However, a direct excitatory effect of VP on VPCs is not supported by our results. Another known trigger for dendritic vesicle release in hypothalamic VPCs is postsynaptic Ca^{2+} influx via NMDA receptors (De Kock et al., 2004), accordingly photolysis of caged-NMDA efficiently evokes dendritic VP release (Son et al., 2013). It is tempting to speculate that similar mechanisms also exist in the OB.

In this case a strong excitatory synaptic input to the apical dendrite would be required to enable VP release, thus the question remains where such synaptic inputs might originate from if not the ON?

2.6.4 Possible targets of axonal VPC output and implications for social odor processing

Provided that during social odor sensing *in vivo* there are adequate inputs to activate the OB VP system, what would be the targets of axonal VP release in the OB? The more common morphological VPC type 1 densely innervates the EPL with numerous short branches that feature multiple but localized projections to the MCL and superficial GCL, possibly within a distinct functional modular column determined by its "home glomerulus" (Willhite et al., 2006). The second, less numerous type 2 also innervates the EPL but has long-ranging projections below the MCL reaching either medially into the GCL or along the internal plexiform layer. Projection patterns similar to that of VPC type 2 shown here were described for cholecystokinin (CCK) immunoreactive sTCs in the OB (Liu and Shipley, 1994; Ma et al., 2013). As CCK immunoreactivity is found in most subtypes of sTCs (Fried et al., 2010), type 2 VPCs in the OB may be a subpopulation of CCK cells. Interestingly, CCK cells were shown to be part of the intrabulbar association system, since axonal projections of CCK cells synapse onto GCs and MCs of the isofunctional glomerulus that receives inputs from the same olfactory receptor. This association results in a positive feedback circuit for amplifying glomerular outputs of the same stimulus (Liu and Shipley, 1994; Ma et al., 2013). If the type 2 VPCs were also part of the intrabulbar association system (which we could not demonstrate in acute slices), this would be an efficient way to globally amplify relevant social signals and thereby sharpen the profile of an individual social odor signature.

In the hippocampus, a brain region that relies on endogenous VP release to facilitate social odor discrimination in rodents, VP signaling generally increases GABAergic inhibition (Cilz et al., 2019). The dense axonal and dendritic innervation of type 1 and type 2 VPCs in the GL, EPL, and GCL would enable these processes to release VP onto GABAergic periglomerular cell and GC somata and their presynaptic dendrites. As VP receptors were shown to be expressed in both, GL and GCL (Vaccari et al., 1998) and application of VP inhibited eTC EPSPs *in-vitro* as well as MC activity *in-vivo* (Tobin et al., 2010), it is conceivable that VP-

induced increased synaptic inhibition improves the discrimination of very similar odors, as known for non-social binary odor mixtures (Abraham et al., 2010). Indeed, an highly sensitive discrimination of social odors may be desirable since gas chromatography has revealed that the volatile component of individuals' body odors contains largely overlapping sets of odor molecules and thus the individual identity is mainly coded via the relative composition of shared volatile components (Singer et al., 1997; Schaefer et al., 2002).

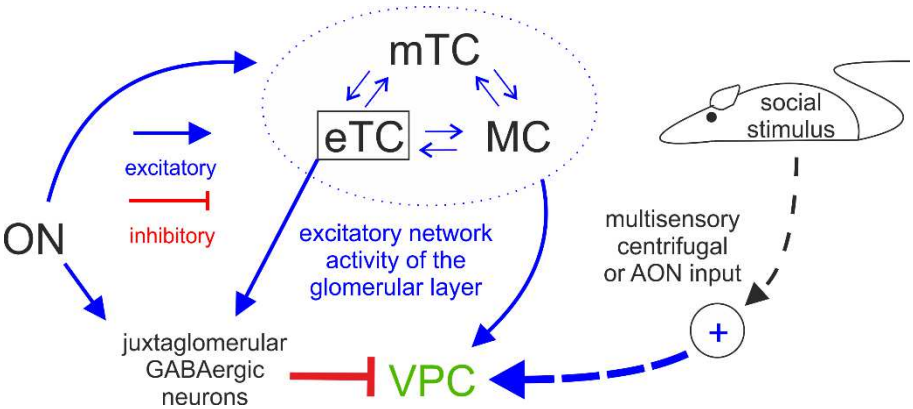

Fig. 14 **Graphic summary of detected inputs to olfactory bulb vasopressin cells (VPC)**
Blue arrows represent excitatory inputs indicated by this study and from literature. Red lines represent inhibitory inputs indicated by this study. The strength of the lines indicates the strength of the input. The cells within the dashed blue circle indicate the excitatory network within the same home glomerulus. Arrows labeled with question marks indicate speculative excitatory inputs to VPCs.
AON, accessory olfactory bulb; eTC, external tufted cell; MC, mitral cell; mTC; middle tufted cell; ON, olfactory nerve; VPC, vasopressin cell.

2.7 Summary

VPCs are non-bursting sTCs that feature a subtype that seems to be predestined for involvement in local 'glomerular'/columnar processing and one subtype that has the potential to be involved in more 'global', long-range intra-bulbar network processing. Further, VPCs receive indirect excitatory and inhibitory inputs via the ON that are dominated by GABAergic signaling. Since we observed that ON-inputs could not directly excite VPCs, the activation of the bulbar VP system possibly relies on additional direct or indirect modulatory inputs from within the olfactory system or upstream, multi-sensory pathways that are triggered by social

stimuli. As to the output of VPCs, previous studies and our preliminary results indicate that VP is rather involved in increasing the inhibitory signaling in the OB.

Chapter 3: Top-down acetylcholine signaling via olfactory bulb vasopressin cells contributes to social discrimination in rats

3.1 Abstract

Social discrimination in rats requires activation of the intrinsic bulbar vasopressin system, but it is unclear how this system comes into operation, as olfactory nerve stimulation primarily inhibits bulbar vasopressin cells (VPCs). Here we show that stimulation with a conspecific can activate bulbar VPCs, indicating that VPC activation depends on more than olfactory cues during social interaction. A series of *in-vitro* electrophysiology, pharmacology and immunohistochemistry experiments implies that acetylcholine probably originating from centrifugal projections can enable olfactory nerve-evoked action potentials in VPCs. Finally, cholinergic activation of the vasopressin system contributes to vasopressin-dependent social discrimination, since recognition of a known rat was blocked by bulbar infusion of the muscarinic acetylcholine receptor antagonist atropine and rescued by additional bulbar application of vasopressin. Thus, our results implicate that top-down cholinergic modulation of bulbar VPC activity is involved in social discrimination in rats.

3.2 Introduction

Many mammals use olfactory cues as a fundamental communication tool, for the recognition and discrimination of individual conspecifics. A prominent example for a behavioral reaction that depends on olfaction-based discrimination of individuals is that ewes recognize the body odor of their own offspring and as a result, deny strange lambs to suckle (Baldwin and Shillito, 1974). Moreover, in prairie voles, the olfaction-based recognition of their mating partners enables them to establish monogamous pairbonds (Williams et al., 1992). Rats and mice, the most common mammalian laboratory animals, also discriminate individual conspecifics via their odor signatures. This discrimination can then lead to various essential behavioral reactions (Matsuo et al., 2015). To quantify the ability of rats to recognize individuals, so-called social discrimination tests are used (Engelmann et al., 2011). Briefly, rats are exposed to a conspecific (sampling phase). After a short time of separation, rats are exposed to both, the same and a novel conspecific (discrimination phase). If the rats recognize the known conspecific, they investigate it less compared to the novel conspecific (Engelmann et al., 2011).

The peptidergic neuromodulator vasopressin (VP), an important mediator of various social behaviors in the mammalian brain (Lukas and Neumann, 2013), is a major player in facilitating social discrimination. For example, microinjection of VP into the OB enhances social discrimination (Dluzen et al., 1998a). Further, Tobin et al. (2010) demonstrated the existence of an intrinsic bulbar VP system, consisting of VP-expressing cells (VPCs), and an impairment of social discrimination by the blockade of bulbar V1a receptors.

Recently, we classified these bulbar VPCs as non-bursting superficial tufted cells, featuring an apical dendritic tuft within a glomerulus, lateral dendrites along the top part of the EPL and extended axonal ramifications, mostly within the entire EPL (Lukas et al., 2019). The dense apical tuft implies that VPCs receive excitatory inputs from the olfactory nerve (ON) just like other bulbar cells with glomerular tufts such as mitral cells (MCs, Halász 1990), e.g., during sampling of a conspecific's body odors. Intriguingly, we found that electric ON stimulation

elicits primarily inhibitory postsynaptic potentials (IPSPs) as recorded at the soma. This dominant GABAergic input masks a delayed barrage of excitatory postsynaptic potentials (EPSPs). Therefore, if ON activation inhibits VPCs and thus cannot trigger VP release, it is unclear how intrinsic VP neurotransmission is at all possible during social discrimination. We hypothesize that to fully excite VPCs and allow VP release, non-ON inputs are required that either inhibit the GABAergic origin of the ON-evoked inhibition and/or deliver enough direct excitation to VPCs to outweigh the inhibition.

During social interaction, rats sample not only olfactory cues including urinary cues, but also other sensory cues, like vocalizations or touch (Bobrov et al., 2014). Also, the sheer presence of a novel stimulus in their known environment may contribute to changes in their physiological and behavioral state. Thus, we suggest that states of arousal, attention, and/or the perception of non-olfactory cues during social interaction may be required for olfactory activation of bulbar VPCs. For the integration of such additional inputs into bulbar neurotransmission, top-down modulation is the most likely option. The most prominent modulatory centrifugal inputs to the OB are noradrenergic, serotonergic, and cholinergic fibers (Shipley et al., 1985; McLean and Shipley, 1987; Ojima et al., 1988). Those neuromodulatory systems were shown to be involved in changes of internal states (Acquas et al., 1996; Popova and Amstislavskaya, 2002; Purvis et al., 2018), but more interestingly, they are also facilitators of social discrimination behavior, acting either directly in the OB or in other brain regions (Dluzen et al., 1998b; Prado et al., 2006; Cavalcante et al., 2017). Thus, we propose them as candidate activators of the bulbar VP system.

This notion leads to the following questions: (1) Are bulbar VPCs indeed activated during social interactions (although they are predominantly inhibited by activated olfactory afferents)? (2) Can any of the candidate centrifugal neuromodulators increase excitation of bulbar VPCs? (3) If so, is centrifugal modulation of bulbar VPCs involved in VP-dependent social discrimination? We approach these questions by investigating neuronal activity and synaptic mechanisms *in-vitro* as well as applying behavioral pharmacology *in-vivo*.

3.3 Methods

3.3.1 Animals

All experiments were conducted according to national and institutional guidelines for the care and use of laboratory animals, the rules laid down by the EC Council Directive (86/89/ECC) and German animal welfare. The study protocol was approved by the Government of Unterfranken (RUF-55.2.2-2532-2-539 and RUF-55.2.2-2532-2-1291). Wistar rats of either sex were purchased from Charles River Laboratories (Sulzfeld, Germany) or bred onsite in the animal facilities at the University of Regensburg. Heterozygous VP-eGFP Wistar rats (Ueta et al., 2005) of either sex were bred at the University of Regensburg. The light in the rooms was set to an automatic 12 h-cycle (lights on 07:00-19:00).

3.3.2 *In-vivo* social stimuli exposure experiment

3.3.2.1 Stimuli exposure

Three cohorts of male VP-eGFP rats (5-6 weeks) were single-housed at least 3 hours before the experiment for habituation to the new environment. Stimuli used were water, juvenile rat urine (collected and mixed from at least 3 juvenile males, stimulus rats) and juvenile rats (3-4 weeks, male non-cage mates). Water and urine (both 50 µl) were applied on filter papers (2 cm x 3 cm). The different stimuli were gently introduced in the cage and the rats could explore freely. A stimulus exposure lasts 4 min in which the behavior of the rats was video-taped for confirmation of proper stimulus sampling. Rats that did not directly sniff at the filter paper containing water or urine as well as rats that did not perform proper social investigation (sniffing anogenital and head region, for details see Video analysis: Social investigation) were excluded from the experiment. Immediately after the exposure, rats were deeply anesthetized for transcardiac perfusion and fixation of the brain.

3.3.2.2 Transcardiac perfusion

Rats were deeply anesthetized with an i.p. injection of ketamine-xylazine (100 mg/kg and 10 mg/kg, respectively). The abdomen and the diaphragm were incised to expose the thoracic cavity. After opening the mediastinum, a needle was inserted into the left ventricle. Following incision of the right atrium, 0.1 M PBS pH 7.4 was perfused for 4 min with a speed of 9.5 mL/min by a pump (GZ-07528-30, Cole-Parmer, Wertheim, Germany) followed by 4 % PFA-PBS for 4 min. Rats were decapitated and the whole brains were extracted. Brains were post-fixed in 4 % PFA-PBS overnight at 4 °C and stored in 30 % sucrose-0.1 M PB at 4 °C for at least 2 days then kept at 4 °C until slicing.

3.3.2.3. Immunohistochemistry

Brains were sliced with a cryostat (CM3050 S, LEICA, Wetzlar, Germany) at approx. -20 °C, then stored in cryoprotectant solution (0.1 M phosphate buffer, 500 mL; Ethylene Glycol, 300 mL; Sucrose, 300 g; Polyvinyl-pyrrolidone, 10 g) at -20 °C until staining. The OB was cut horizontally with a thickness of 30 µm. On average, six slices from one bulb of each experimental rat were used for staining. The HDB (Figure 24-28 (1.08 - 0.60 mm from the Bregma) in the rat brain atlas (Paxinos and Watson, 2009)) was cut coronally with a thickness of 30 µm. Three slices of each experimental rat were used for staining.

All immunohistochemistry procedures were performed in 12 well plates (Corning Incorporated, Corning, NY, USA) with the free-floating method. Slices were washed three times with 0.3 % Triton-X100 in PBS (PBST) for 10 minutes. Then slices were incubated in methanol for 10 minutes at -20 °C. After washing with PBST for 10 minutes, incubation with 0.1 M Glycine in PBS was performed for 20 minutes at room temperature, followed by washing with PBST for 10 minutes. Slices were incubated with the blocking solution for one hour at room temperature. The blocking solution contained 0.2 % of cold water fish skin gelatin (AURION, Wegeningen, Netherlands) and 0.01 % of NaN3 in normal donkey serum (NB-23-00183-1, NeoBiotech, Nanterre, France). Incubation with primary antibodies (see

Antibodies) diluted in the blocking solution was carried out for 72 hours at 4 °C. After washing three times with PBST for 10 minutes, secondary antibodies diluted in the blocking solution were added and incubated for two hours at room temperature, followed by washing three times with PBST for 10 minutes. From the incubation in secondary antibodies on, every procedure was performed in the dark to avoid bleaching fluorescence. For choline acetyltransferase (ChAT) staining, the protocol was modified. Additional blocking by incubation with avidin and biotin (both 0.001% in PB, Sigma-Aldrich, Darmstadt, Germany) for 30 min and a 10 min wash with PBST in between were carried out before incubation with the blocking solution. Moreover, after the last washing with PBST, incubation in streptavidin conjugated with CF488 (1:400 in PBST, #29034, Biotium, Fremont, CA, USA) for two hours at room temperature was carried out. After staining itself, slices were washed three times with PBST for 10 min. Slices were mounted on objective slides (Thermo Fisher Scientific, Waltham, MA, USA) using DAPI fluoro mount-G (Southern Biotech, Birmingham, AL, USA).

3.3.2.4 Antibodies

Primary antibodies were goat anti-GFP (1:1000, #600-101-215S, Rockland, Limerick, PA, USA), Rabbit anti-P-p44/42 MAPK (1:1000, #9101S, Cell Signaling Technology, Frankfurt am Main, Germany), Sheep Anti-Choline Acetyltransferase (1:125, ab18736, Abcam, Berlin, Germany). Secondary antibodies were Donkey anti-Goat IgG conjugated with CF488 (for GFP, 1:1000, #20016-1, Biotium), Donkey anti-Rabbit IgG conjugated with CF594 (for pERK, 1:1000 for the OB and 1:500 for the HDB, #20152, Biotium), biotinylated Donkey anti-Sheep IgG (for ChAT, 1:250, #20191-1, Biotium). All antibodies were diluted in the blocking solution. All purchased antibodies were validated for target and species specificity as indicated in the data sheets of the respective companies' websites.

3.3.2.5 Fluorescent Microscopy

Fluorescent images of the stained slices were obtained using a DM6 B microscope (LEICA) and the software, LAS X (LEICA). DAPI, CF488 and CF633 were stimulated with an exposure time of 300 ms, 300 ms and 500 ms, respectively. Tile-stitching and z-stack of pictures were performed by LAS X. After taking pictures, those were processed by 3D deconvolution or the Lightning & Thunder process (LAS X) to improve the contrast. Pictures were converted to .tif files using Fiji (ImageJ, downloaded from https://imagej.net/Fiji/Downloads) and contrast was adjusted to the same levels in every picture. Z-stack pictures from approx. 5-6 different z-positions per bulb or rats were used for analysis.

3.3.2.6 Cell counting

Immunoreactive cells were counted manually using the multi-point tool or cell counter plug-in in Fiji. 4-6 OB slices and 2 HDB slices were analyzed. Double positive cells were identified by comparing two color channels. The position of counted cells was saved as .roi files or .xml files. The number of cells was averaged per experimental rat and bulb. The counting was done in 4-6 non-overlapping sections of one olfactory bulb of a respective rat. The total number of positive cells was averaged over the number of counted sections, to account for variance in cell distribution and number of sections analyzed. In the OB double-labelled cells were counted, if the typical soma shape was visible without a staining of the nucleus area in the GFP-channel (green) and could be identified with the same outline in the pERK channel (magenta, see example in Fig. 15A). In the HDB double-labelled cells were counted, if the typical soma shape was visible in the pERK-channel (magenta) and could be identified with the same outline in the ChAT-channel (green, see example in Fig. 19A). For control the localization of the nucleus was double-checked in the DAPI channel (blue).

All the data was analyzed by an observer blinded with respect to stimulation groups.

3.3.3 Electrophysiology

3.3.3.1 Slice preparation

11-18 day-old juvenile VP-eGFP rats were used for *in vitro* electrophysiology experiments. The rats were deeply anesthetized with isoflurane and quickly decapitated. Horizontal and sagittal slices (300 µm) were cut in ice-cold carbogenized ACSF (artificial cerebrospinal fluid; mM: 125 NaCl, 26 NaHCO3, 1.25 NaH2PO4, 20 glucose, 2.5 KCl, 1 MgCl2, and 2 CaCl2) using a vibratome (VT 1200, LEICA) and afterwards incubated in ACSF at 36 °C for 45 min. Until experiments, the slices were kept at room temperature (approx. 21°C) in ACSF.

3.3.3.2 Electrophysiology

Brain slices were placed in a recording chamber on the microscope's stage perfused with carbogenized ASCF circulated by a perfusion pump (ISM 850, Cole-Parmer). GFP-labeled vasopressin cells (VPCs) were identified with LED illumination (470 nm) under a modified Zeiss Axioplan microscope (Carl Zeiss Microscopy, Oberkochen, Germany). Epifluorescence was filtered by a long-pass dichroic mirror (490 nm cutoff) and an emission filter (510 ± 21 nm) and visualized with a digital camera (VisiCAM-100, Visitron Systems, Puchheim, Germany). To perform whole-cell patch-clamp recordings, cells were visualized by infrared gradient-contrast illumination via IR filter (Hoya, Tokyo, Japan). Glass pipettes for recordings were pulled by a pipette puller (Narishige, Tokyo, Japan) sized 4-6 MΩ and filled with intracellular solution (in mM: 130 K-methylsulfate, 10 HEPES, 4 MgCl2, 4 Na2ATP, 0.4 NaGTP, 10 Na Phosphocreatine, 2 ascorbate, pH 7.2). Recordings were performed with the current-clamp configuration using an EPC-10 (HEKA, Lambrecht, Germany) digital oscilloscope. Series resistance was measured 10-30 MΩ. The average resting membrane potential was -50 to -60 mV. Experiments were only started in case the patched cells had a holding current below ~ -50 pA and no drastic drift in the resting membrane potential. Experiments were performed at room temperature (approx. 21°C).

In experiments with AOB stimulation, sagittal slices including the accessory olfactory bulb (AOB) were used. VPCs for these experiments were identified in the posterior-dorsal area of the MOB (Supplementary Fig. 2C) since intact projections of AOB mitral/tufted cells to this area in sagittal slices were demonstrated using antidromic electrical stimulation previously (Vargas-Barroso et al., 2016). Glass pipettes, intracellular solution and settings of oscilloscope were same as experiments with horizontal slices.

3.3.3.3 Electrical extracellular stimulation

Olfactory nerve (ON) stimulation was performed with a glass pipette stimulation electrode sized around 2 MΩ. Glass pipettes were filled with ACSF. The electrode was connected to an external stimulator (STG 1004, Multi-Channel Systems, Reutlingen, Germany) controlled by a PC. The stimulation strength was adjusted with the stimulator's software (MC_Stimulus, V 2.1.5) and stimulation was triggered by the amplifier software (Patchmaster v2x73.5, HEKA). Stimulation pipettes were gently placed in the ON layer anterior to a cell to patch using a manual manipulator (LBM-7, Scientifica, East Sussex, UK) under optical control with the microscope. The stimulation strength was 50-400 µA for 100 µs. The stimulation was triggered every 30 s to avoid desensitization of the neural networks.

AOB stimulation was performed with a glass pipette stimulation electrode; the stimulator and the software were the same as for MOB ON stimulation. Stimulation pipettes were gently placed in the vomeronasal nerve layer or in the EPL/mitral cell layer in the AOB using a manual manipulator (LBM-7, Scientifica, East Sussex, UK) under optical control with the microscope. The stimulation strength was 50-500 µA for 100 µs.

3.3.3.4 Ca^{2+} Imaging

Fluorescence was recorded by two-photon laser scanning microscopy on a Femto-2D microscope (Femtonics, Budapest, Hungary), equipped with a tunable, Verdi-pumped Ti:Sa laser (Chameleon Ultra I, Coherent, Glasgow, Scotland). The microscope was equipped with

a 60x Nikon Fluor water-immersion objective (NA 1.0; Nikon Instruments, Melville, NY, USA), three detection channels (green fluorescence (epi and trans), red (epi) and infrared light (trans)) and controlled by MES v4.5.613 software (Femtonics).

VP-eGFP cells were identified in the green channel at an excitation wavelength of 950 nm. VPC bodies were patched in the whole-cell mode with patch pipettes filled with regular intracellular solution (see Electrophysiology), Alexa Fluor 549 (50 µM, Invitrogen) and the Ca^{2+} indicator OGB-1 (100 µM, Invitrogen, Thermo Fisher Scientific) were added for neurite visualization and Ca^{2+} imaging. Fluorescence transients and image stacks were acquired at 800 nm laser excitation. Data were mostly collected from the medial surface of the OB. Ca^{2+} imaging experiments were performed at room temperature (approx. 21° C). The patched VPCs were held in the current clamp mode near their resting potential of -55 mV. Structures of interest were imaged in free line-scanning mode with a temporal resolution of approx. 1 ms.

3.3.3.5 Experimental design and data analysis

All drugs (see Pharmacology) diluted in ASCF were bath-applied via the perfusion system. Recordings under pharmacology were performed at least 5 min after the onset of administration to ensure that the drugs reached the recorded cell. Two average traces from 3-5 recordings in each condition were analyzed. The data was averaged per condition. The amplitudes of PSPs were measured using Origin 2018b (Origin Lab Corporation, Northampton, MA, USA). The amplitudes of IPSPs following pharmacology were normalized to the amplitudes during the ACSF condition (100 %). The amplitudes of EPSPs following bicuculline application with pharmacology were normalized to the amplitudes during the bicuculline condition (100%). APs, EPSPs, IPSPs in experiments with ACh application were defined as: APs, the existence of AP (s) after ON stimulation; EPSPs, observation of depolarization with amplitudes of >1.5 mV; IPSPs, the absence of APs and EPSPs. In some experiments with ACh, current (40, 60, 80, 100 pA, 600 ms) was injected via the recording

electrode into the cell to test if ACh application alters the intrinsic excitability in VPCs. Spiking rates of AP trains were calculated as the number of spikes divided by the duration of AP trains. Latency of the first spike was measured as the duration between the current injection onset and the peak of the first spike.

In some experiments, simultaneous to the electrophysiological recordings, intracellular Ca^{2+} transients were measured at the tuft and at the apical dendrite directly apical to the soma (see Ca^{2+} Imaging) following ON stimulation. Three consecutive focal line-scans were performed during ON stimulation (see Olfactory nerve stimulation). To confirm that the cell was correctly filled with Ca^{2+}-dye, VPCs were also stimulated with somatic 50 Hz trains (20 APs) via the patch pipette which was shown to reliably trigger Ca^{2+} Influx in case ON stimulation did not result in Ca^{2+} signals near the soma during olfactory nerve stimulation (Lukas et al., 2019). The three line scans per pharmacological condition were averaged for analysis. Dendritic Ca^{2+} transients were analyzed in terms of $\Delta F/F$ relative to the resting fluorescence F_0 (Egger et al., 2003). The time course of pharmacology and analysis were the same as for electrophysiological data mentioned above.

All the data was analyzed by an observer blinded with respect to pharmacology.

3.3.3.6 Pharmacology

All pharmacological agents used were diluted in ACSF for bath application: serotonin hydrochloride (20 µM, Sigma-Aldrich), DL-Norepinephrine hydrochloride (20 µM, Sigma-Aldrich), acetylcholine chloride (100 µM, Sigma-Aldrich), mecamylamine hydrochloride (20 µM, Sigma-Aldrich), atropine (10 µM, Sigma-Aldrich), (-)-Nicotine, Ditartrate (100 µM, Merck KGaA, Darmstadt, Germany), (+)-Muscarine chloride (1µM, Sigma-Aldrich), 1(S),9(R)-(-)-bicuculline methyl bromide (50 µM, Sigma-Aldrich).

The doses used were chosen based on minimal doses reported to elicit *in-vitro* effects (Castillo et al., 1999; Li et al., 2001; Pignatelli and Belluzzi, 2008; Liu et al., 2011; Sun et al., 2013; Zimnik et al., 2013; Liu et al., 2015; Lukas et al., 2019).

3.3.4 Behavioral Pharmacology

3.3.4.1 Cannula implantation

Three cohorts of 5-6 week-old male Wistar rats were group-housed until surgery. To allow local injection of pharmacological solutions in the OB without anesthesia, we bilaterally implanted guide cannulae (23 G, Injecta GmbH, Klingenthal, Germany) in the rat OB. Before surgery, all surgical instruments were autoclaved at 121 °C for 20 min. The rats were anesthetized by isoflurane using a TEC 3 isoflurane vaporizer (Eickemeyer, Tuttlingen, Germany). The concentration of isoflurane was maintained between 2-3 %. The rats were fixed on a stereotaxic frame (TSE, Bad Homburg Germany/Kopf, Tujunga, CA, USA) using ear bars. To prevent hypothermia, the rats were kept warm using a warming pad (ThermoLux, Witte + Sutor, Murrhardt, Germany). Analgetics (buprenorphine, 0.1 mg/kg s.c., Bayer, Beline, Germany) and antibiotics (enrofloxacin, 10 mg/kg s.c., Bayer) were injected before surgery. After shaving the head and disinfection of the operation site with 70 % ethanol, we incised the scalp and the supporting tissue on the skull. Injection of lidocaine hydrochloride (2 %, around 100 µL, bela-pharm, Vechta, Germany) under the scalp was operated if needed. Two stainless steel jeweler's screws were inserted into the skull using a surgical drill (NM 3000, NOUVAG, Goldach, Switzerland). One on the left anterior to bregma and the other one on the right posterior to bregma to secure dental cement fixation. Holes for guide cannulae were made by a drill, followed by placement of cannulae 7 mm anterior and 1.2 mm lateral relative to bregma as well as 1 mm ventral from the surface of the skull where 2 mm above the injection coordinates. Thus, the coordinates for injection were 3 mm ventral to the surface of the skull (Paxinos and Watson, 2009). Cannulae and the two screws were fixed together by the dental cement (Kallocryl, Speiko-Dr. Speier GmbH, Muenster, Germany). Once the cement dried, the connection between the cement and the scalp was disinfected by iodine solution and cannulae were blocked by insertion of stainless steel stylets (25 G, BD, Heidelberg, Germany) to prevent dust entering the cannulae that could result in infection or

blockage. The rats were removed from the frame and placed in fresh cages for recovering from anesthesia under observation until they are awake. The rats were weighed prior to surgery and on the next day to see if they recovered properly after surgery. Their health condition and behavior were checked for at least five days. After surgery, they were single-housed until experiments to prevent damage to the guide cannulae. Meanwhile, the rats were handled and habituated to the removal and insertion of stylets every day until experiments. Stylets were cleaned with 70 % ethanol every time they were removed from the guide cannula.

3.3.4.2 Social discrimination with pharmacology

We combined the social discrimination paradigm (Engelmann et al., 2011) and microinjection of pharmacology into the OB. The social discrimination paradigm consists of a sampling phase and a discrimination phase. Experiments were performed in the afternoon. In the sampling phase (4 min), one stimulus rat was gently introduced into the cage of the experimental rats. Then the stimulus rat was removed from the cage and the experimental rat stayed in the cage alone for an inter-exposure interval of 30 min. In the discrimination phase (4 min), two stimulus rats, one is the same as during the sampling phase and the other one is a novel stimulus rat, were gently introduced into the cage. During both phases, the behavior of the experimental rat was video-taped from above through a transparent plastic plate for post-hoc analysis. Stimuli were 3-4 week-old group-housed male rats that were single-housed only in between the social exposures of the behavioral experiments to prevent mixing of body odors. They were marked with a red or black pen of the same brand (Edding, Ahrensburg, Germany) to allow visual differentiation by the observers. Pharmacological agents diluted in ACSF include atropine (1 µg in 1 µL) and [Arg8]-vasopressin acetate salt (1 ng in 1 µL, Sigma-Aldrich). 40 min before the sampling phase, either ACSF or atropine was injected into both OB hemispheres (1 µL each). 10 min before the sampling phase, either ACSF or VP was injected into both OB hemispheres (1 µL each).

All injections were carried out with microinjection syringes (Hamilton, Bonaduz, Switzerland) connected to a self-made injection system which consists of plastic tubes and 10 mm-long 30 G needles (2 mm longer than the guide cannulae). After every injection (1 µL), the injection systems rested in place for 1 min to allow the injected solution to diffuse fully in the tissue. The doses used were chosen based on minimal does reported to elicit behavioral effects (Dluzen et al., 1998a; Saboory et al., 2014). No anatomical outliers in stereotaxic cannula implantation had to be excluded from behavioral analysis (Fig. 20C). However, one animal from the control group was removed, as it showed a high amount of unspecific sexual/mounting behavior towards the stimulus animals throughout the sampling as well as the discrimination phase.

To confirm that neither atropine nor VP microinjection into the OB induced unspecific behavioral effects, we demonstrated that these manipulations did not interfere with non-social investigatory/play behavior and habituation (towards amyl acetate (Sigma-Aldrich)/ (-)-carvone (Sigma-Aldrich) presented in a teaball or a juvenile rat). The play behavior was measured during the sampling phase of the social discrimination experiment. The non-social investigatory behavior in a separate experiment on the next day. Experimental rats and treatments were the same as in the social discrimination experiment.

3.3.4.3 Confirmation of injection sites

Immediately after the last experiments, the rats were killed with CO_2. Then 1 µl of blue ink was injected with an injection system via the guide cannulae into both OBs followed by decapitation. The OB was extracted and quickly frozen in isobutanol on dry ice and stored at -20 °C until use. Correct placement of Injection was identified on 40 µm cryostat sagittal sections stained with cresyl violet (Fig. 19C). No anatomical outliers in stereotaxic cannula implantation had to be excluded from behavioral analysis.

3.3.4.4 Video analysis: Social investigation

The analysis was done by an observer blind to the pharmacological treatment using JWatcher (downloaded from https://www.jwatcher.ucla.edu/). Thereby the duration of investigation of the stimulus rats by the experimental rats was measured. Investigation was defined as sniffing the anogenital or neck region of stimulus rats including obvious nose movements (sniffing). Aggressive behavior (e.g., aggressive grooming), only staying next to the stimulus rats, and rough and tumble play were not considered investigation (Fig. 19B, Engelmann et al., 2011). One animal from the control group was removed, as it showed high amounts of unspecific sexual/mounting behavior towards the stimulus animals throughout the sampling as well as the discrimination phase.

3.3.4.5 Statistics and reproducibility

Statistics were performed with SPSS (ver. 26, IBM, Armonk, NY, USA) and G*Power (ver. 3.1.9.2, Franz Faul, University of Kiel). All statistical analysis performed was two-sided and significance was accepted at $p<0.05$. Type of statistic was determined using the Kolmogorov-Smirnov test for normal distribution in SPSS. Effect sizes for parametric statistics (Cohen's *d, dz*, *f*) were determined using SPSS and G*Power. Effect sizes for non-parametric statistics were calculated from z-scores (Pearson's $r = |z|/\sqrt{n}$) (Rosenthal et al., 1994). Sample sizes were either based on prior studies or an a priori power analysis. Power and sample sizes (for $\alpha=0.05$) were determined using G*Power.

All Ns indicate biological replication, that is, data from different samples (different cells or different animals). To better illustrate replication in acute *in-vitro* slice experiments it is also clearly indicated in the results section from how many different animals the measurements originate from.

For complete details concerning type of statistic (parametric or non-parametric), type of test, test statistics (F, t, W, U, z-score), degrees of freedom, p-value, effect size, and achieved power of every statistical analysis performed in the result section see table 3. Figure

identifiers and lower case arabic letters in the table represent affiliation to the statistical data represented in the figures and the text, respectively.

3.4 Results

3.4.1 Social interaction activates bulbar VPCs

As we recently demonstrated *in-vitro* (Lukas et al., 2019) that ON stimulation alone primarily inhibits VPCs, we infer that bottom-up olfactory nerve input is unlikely to excite VPCs. On the other hand, during social discrimination VPCs should be strongly excited as VP neurotransmission was shown to be essential for this behavior (Tobin et al., 2010). To test this hypothesis, male juvenile VP-eGFP rats (Ueta et al., 2005) were exposed to either, water (control) or one of two stimuli that are commonly used in social discrimination paradigms, i.e., rat urine or a novel juvenile rat (Engelmann et al., 2011). We then compared the neuronal activity of bulbar VPCs between these different types of stimulation as reflected in phosphorylated extracellular signal-regulated kinase (pERK) induction in eGFP-labeled VPCs (Fig. 15A). The average section size of the main OB (MOB, water 4.48 ± 0.4 mm^2, urine 4.58 ± 0.3 mm^2, rat 4.85 ± 0.3 mm^2) and average number of $eGFP^+$ VPCs per section (water 81 ± 5 VPCs, urine 79 ± 5 VPCs, rat 85 ± 3 VPCs) were not different across animal groups (section size; p=0.723, ANOVA. $eGFP^+$ VPCs, Supplementary Fig. 15A; p=0.670, ANOVA, water n=10 rats, urine n=9, rat n=10)$_a$. While there is a substantial background of $pERK^+$ VPCs *in-vivo* (see discussion), indeed, the exposure to a rat resulted in significantly higher fractions of $pERK^+$ VPCs than the exposure to water. However, rat exposure did not differ significantly from urine exposure (Fig. 15C+D; p=0.038, ANOVA, rat vs. water p=0.011, rat vs. urine p=0.197, water vs. urine p=0.195)$_b$. These findings indicate (1) that bulbar VPCs are indeed excitable *in-vivo* and (2) that during social interaction additional yet unknown factors enable increased activation of VPCs.

The number of $pERK^+$ MCs was increased following the exposure to a rat compared to water or urine (Fig. 15B+E; p=0.042, ANOVA, rat vs. water p=0.025, rat vs. urine p=0.034, water vs. urine p=0.949)$_c$.

In addition, we analyzed activation of VPCs and mitral/tufted cells (M/TCs) in the accessory olfactory bulb (AOB), as the MOB and the AOB are both related to social discrimination in rats (Bluthe and Dantzer, 1993). The average number of eGFP$^+$ VPCs per section were not different across animal groups (Supplementary Fig. 1C; p=0.539, ANOVA, n=9 rats per group)$_d$. However, pERK$^+$ VPCs were rarely observed (Supplementary Fig. 1D; water 2.1 ± 0.7 % (0.4 ± 0.1 VPCs), urine 2.4 ± 0.8 % (0.5 ± 0.1 VPCs), rat 3.4 ± 0.8 % (1.0 ± 0.2 VPCs)) and the fraction of pERK$^+$ VPCs was similar between the different groups (Supplementary Fig. 1D; p=0.485, ANOVA, n=9 rats per group)$_e$. Thus, AOB VPCs are unlikely to play an important role in facilitating social discrimination compared to MOB VPCs. The number of activated AOB M/TCs was not different between groups (Supplementary Fig. 1F; p=0.164, ANOVA)$_f$.

Taken together, an increased activation of VPCs was found following social interaction, and MOB VPCs showed more prominent activation than AOB VPCs. Thus, social interaction is likely to involve additional inputs (beyond olfactory nerve input) that enable/unlock VPC activation via modulation.

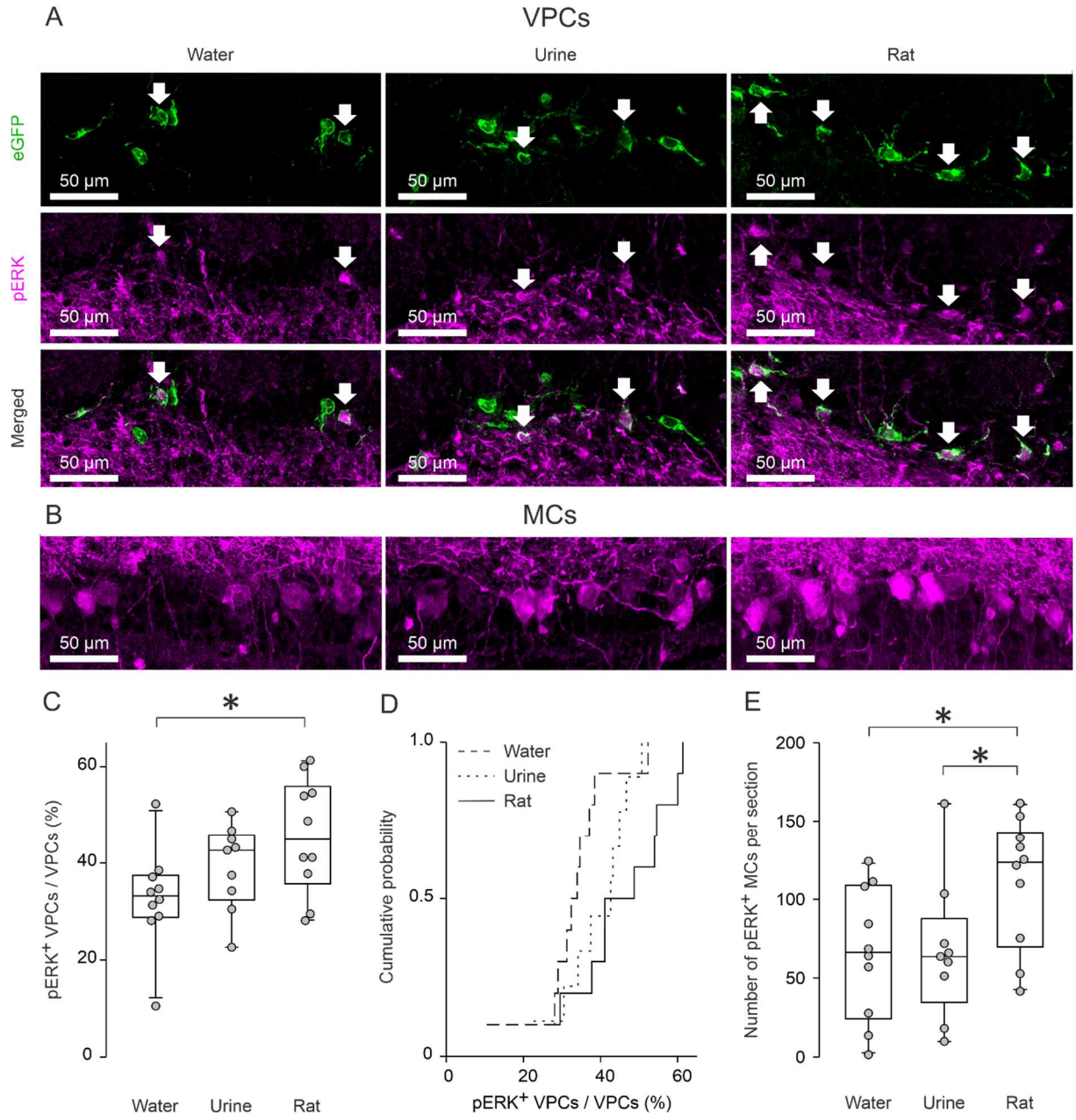

Fig. 15 **Social interaction activates bulbar VPCs**

Representative average z-projections of the olfactory bulb that were immune-stained for eGFP (green, CF488) and pERK (magenta, CF 594). Scale bar, 50 µm valid for all images in the same panel. VPCs following water, urine, or rat stimulation. Arrows indicate cells that are double-labeled for eGFP and pERK (A). $pERK^+$ MCs (B). (C) Averaged fraction of $pERK^+$ VPCs of all VPCs in different stimulation groups (%). One-way ANOVA, LSD for single comparison, *p<0.05 rat vs. water. (D) Cumulative probability of averaged fraction $pERK^+$ VPCs of all VPCs in different stimulation groups (%). (E) Averaged number of $pERK^+$ MCs per section in different stimulation groups. One-way ANOVA, LSD for single comparison, *p<0.05 rat vs. water and rat vs. urine. Data are presented as box-plots including first, median, and third quartiles with whiskers representing the range of data points and distribution of single data points. n=10 rats (water), n=9 rats (urine), n=10 rats (rat).

3.4.2 Cholinergic modulation triggers excitatory responses and action potentials during ON stimulation of VPCs

The OB, especially the glomerular layer (GL) and the external plexiform layer (EPL) where VPCs are located, receives many centrifugal projections that release neuromodulators. These projections originate from various brain areas (Shipley et al., 1985; McLean and Shipley, 1987; Ojima et al., 1988). The receptors of these neuromodulators are expressed in the entire MOB (Le Jeune et al., 1995; Yuan et al., 2003). We hypothesized that such centrifugal neuromodulatory inputs to the MOB could mediate the increased VPC activity that we observed during social interaction. Thus, we performed whole-cell patch-clamp recordings from VPCs and stimulated the ON (Lukas et al., 2019) while bath-applying neuromodulators (Fig. 16A).

Serotonin (5-HT, 20 µM) decreased the amplitudes of ON-evoked IPSPs to 69.7 ± 10.1 % of control (Fig. 16B+C; p=0.012, n=8 from 8 rats)$_g$. Noradrenaline (NA, 20 µM) reduced IPSP amplitudes to 62.9 ± 9.5 % of control (Fig. 16D+E; p=0.011, n=9 from 8 rats)$_h$. Thus, 5-HT and NA modulation can reduce ON-evoked inhibition of VPCs but are unlikely to enable activation of VPCs as observed during social interaction (Fig. 15).

In contrast, wash-in of ACh (100 µM) switched inhibitory to excitatory responses in the majority of VPCs: 65 % of VPCs fired action potentials (APs, 13 out of 20 cells from 19 rats), 10 % of VPCs responded with EPSPs to ON stimulation. The rest all showed decreased inhibition (Fig. 16F+G; p<0.001 for net response amplitude change towards positive/less negative values)$_i$. Accordingly, the distribution of response amplitudes in the presence of ACh was significantly different from control (Fig. 16H; p<0.001)$_j$, as well as different from the 5-HT or NA condition (Fig. 16I; ACh vs. 5-HT p=0.003, ACh vs. NA p=0.002, 5-HT vs. NA p=1.0)$_k$. These excitatory ACh effects were not due to an increased intrinsic excitability of VPCs since ACh did not alter VPC AP spike frequencies during prolonged somatic current injections (Supplementary Fig. 2A+B; Treatment p=0.417, Current intensity p<0.001, Treatment*Current intensity p=0.528, n=10 from 9 rats)$_l$. Moreover, an increased latency of

the first spike was observed for lower current injection levels, indicating rather reduced excitability during ACh treatment (Supplementary Fig. 2A+C; Treatment $p=0.080$, Current intensity $p<0.001$, Treatment*Current intensity $p=0.015$, ACh vs. ACSF (40 pA) $p=0.029)_m$.

Rat AOB M/TCs send axons to the dorsal MOB (Vargas-Barroso et al., 2016), and it was shown that pheromonal AOB inputs are involved in social discrimination (Bluthe and Dantzer, 1993; Noack et al., 2010). To investigate whether AOB inputs can elicit excitation in MOB VPCs, we electrically stimulated the AOB during whole-cell patch-clamp recordings from MOB VPCs. Acute *in-vitro* slices for these experiments were prepared at a cutting angle that should preserve the respective projections (Supplementary Fig. 2D, Vargas-Barroso et al., 2016). However, no VPC showed any responses (Supplementary Fig. 2E; $n=21$), suggesting that modulation of MOB VPCs via AOB inputs is unlikely.

Taken together, we have identified ACh as a strong candidate neuromodulator that can unlock VPC APs and thus enable axonal VP release in the MOB.

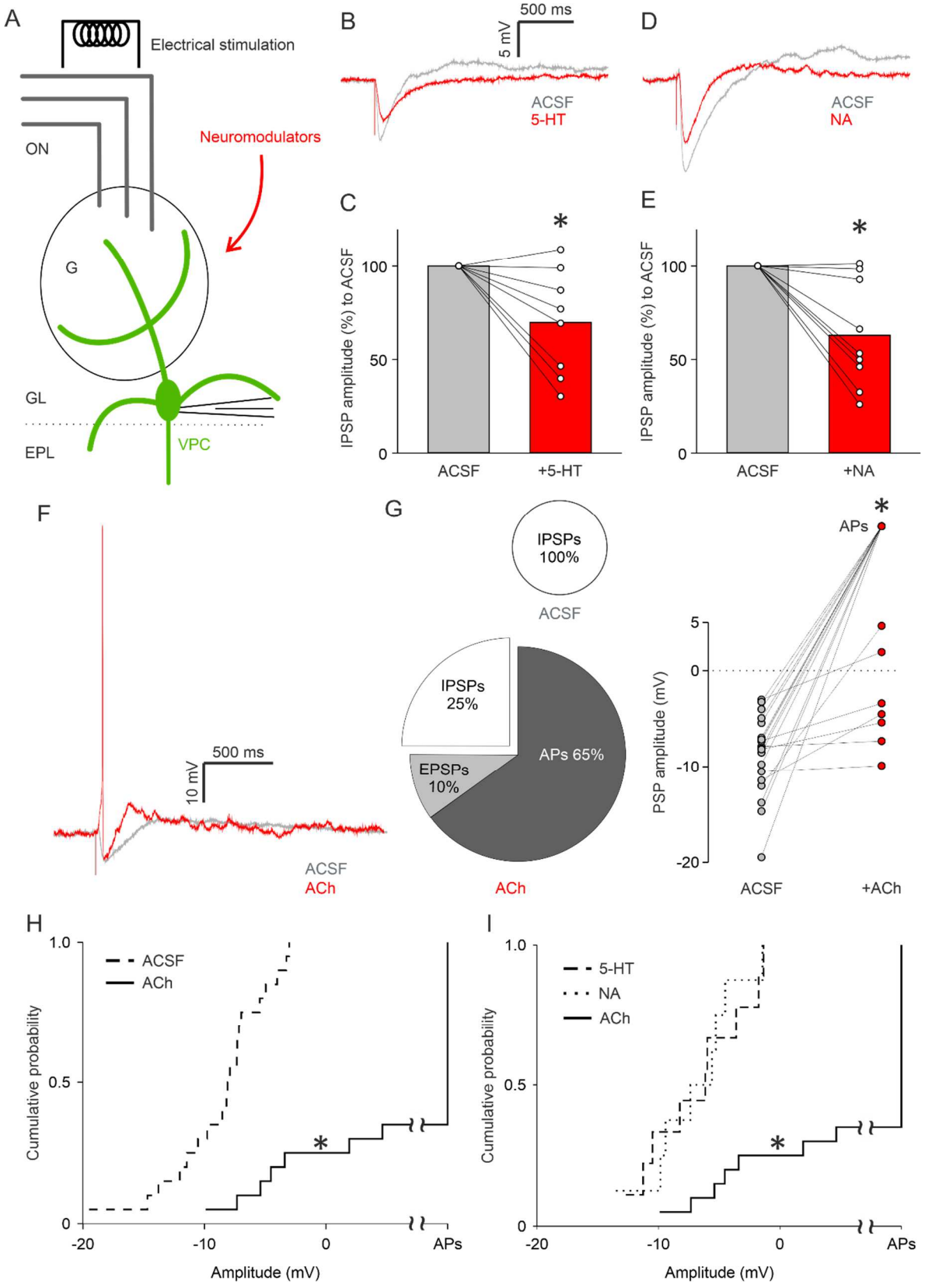

Fig. 16 **Cholinergic modulation triggers excitatory responses and action potentials during ON stimulation of VPCs**

(legend continued on next page)

(A) Schematic drawing of the experimental setup. Whole-cell patch-clamp recordings in 300 µm *in-vitro* slices of response from VPCs to electrical ON stimulation (50 µA, 100 µs, 30 s intervals) (B) Representative averaged traces of responses following ON stimulation in the ACSF condition (artificial cerebrospinal fluid, grey) and during bath application of 5-HT (serotonin 20 µM, red). (C) Cumulative analysis of normalized IPSP amplitudes of evoked IPSPs to the ACSF control condition during bath application of 5-HT (n=8 cells). Data are presented as means including distribution of single data points. Lines between data points represent related measurements. Related-Samples Wilcoxon Signed Rank Test, *p<0.05. (D) Representative averaged traces of responses following ON stimulation in the ACSF condition (artificial cerebrospinal fluid, grey) and during bath application of NA (noradrenaline 20 µM, red). (E) Cumulative analysis of normalized IPSP amplitudes of evoked IPSPs to the ACSF control condition during bath application of NA (n=9 cells). Data are presented as means including distribution of single data points. Lines between data points represent related measurements. Related-Samples Wilcoxon Signed Rank Test, *p<0.05. (F) Representative averaged traces of responses to ON stimulation in the ACSF condition (grey) and a single trace during bath application of ACh showing APs (acetylcholine, red). (G) Pie-chart represents the proportion of VPCs showing either APs, EPSPs or IPSPs in the ACSF and ACh condition. Dot-plots represent cumulative analysis of amplitudes of PSPs or APs (set as 100 mV) in the ACSF and ACh condition. Related-Samples Wilcoxon Signed Rank Test, *p<0.05. n=20 cells. (H+I) Cumulative probability of evoked PSP amplitudes in the ACSF, 5-HT, NA, or ACh condition (n=20/8/9/20 cells). The amplitudes of APs were set as 100 mV. Kruskal-Wallis test for variation comparison, Bonferroni post-hoc, *p<0.05 ACh vs. ACSF, 5-HT, NA.

ON, olfactory nerve. G, glomerulus. GL, glomerular layer. EPL, external plexiform layer. VPC, vasopressin cell

3.4.3 ACh modulates both ON-evoked inhibition and excitation but does not increase Ca^{2+} influx into the apical dendrite

For further dissection of the cellular underpinnings of these ACh effects, we quantified the amplitude changes of evoked IPSPs in VPCs that did not turn into APs or EPSPs in ACh (5 out of 20 cells, Fig. 16G). In these 5 cells, ACh decreased the amplitudes of evoked IPSPs to 67.8 ± 11.3 % of control (Fig. 17A+B; p=0.043, n=5 from 5 rats)$_n$. This observation indicates that ACh, like 5-HT and NA, also reduces inhibition of VPCs. We also examined the effect of ACh on the isolated excitatory components of ON-driven inputs in VPCs. After the detection of evoked IPSPs in ACSF, bicuculline, a GABA-A receptor antagonist, was applied to unmask evoked EPSPs (Lukas et al., 2019), followed by ACh administration. Half of VPCs occasionally showed evoked APs under ACh application (Fig. 17D; 3 out of 6 cells from 5 rats). We averaged all subthreshold traces and found that ACh application increased the amplitudes of evoked EPSPs to 204.4 ± 39.8 % from bicuculline alone (Fig. 17D; p=0.043, n=5 from 5 rats)$_o$. This increase in EPSP amplitudes indicates that ACh enhances ON-

evoked excitation to activate VPCs, on top of reducing inhibition, possibly via acting on both excitatory and inhibitory glomerular neurons (Shipley and Ennis, 1996; Liu et al., 2015). In addition, we analyzed the onset of ON-evoked APs in VPCs triggered by ACh modulation from Fig. 16 (8.6 ± 0.7 ms; n=12 from 12 rats, corresponding to Fig. 16G) and compared them to the onset of evoked EPSPs in bicuculline alone, which was significantly slower (32.8 ± 12.1 ms; n=6 from 5 rats, corresponding to Fig. 17C; $p=0.002)_p$, further supporting the idea of additional excitation by ACh.

Since VPCs innervate glomeruli via apical dendritic tufts (Lukas et al., 2019) which are known to receive sensory excitation in bulbar principal neurons, the mitral and tufted cells (Halász 1990), ACh-mediated excitation might act on processing within VPC tufts. To investigate subcellular processing in VPCs, we simultaneously performed whole-cell patch-clamp recordings of PSPs from the soma and two-photon Ca^{2+} imaging in the tufts and near the soma during ON stimulation (100 µM OGB-1, Fig. 17E+F). In the control condition, a single ON stimulation was able to elicit Ca^{2+} influx in the tufts but not in the proximal apical dendrite near the soma of VPCs (Fig. 17F+G; tuft vs. soma p=0.002, n=8 from 8 rats)$_q$. However, upon ACh wash-in, although APs and EPSPs were recorded at the soma, ACh did not further increase Ca^{2+} influx neither in the tufts nor the soma (treatment $p=0.203)_q$. This observation implies that Ca^{2+} influx at the soma is not responsible for the unlocking of somatic APs. Since 50 Hz-AP trains can elicit Ca^{2+} signals also close to the soma in the proximal apical dendrites, the lack of such signals in response to single APs in the presence of ACh is not a technical artefact but probably due to a very low density of voltage-gated Ca^{2+} channels in these compartments, as known from hypothalamic VPCs (Fig. 17G, ON/soma vs. 50Hz/soma p=0.014, n=8 from 8 rats, Bains and Ferguson, 1999)$_r$. Moreover, in the imaging experiments (with 100 µM OGB-1 in the internal solution) there was no difference in the effect of ACh on the increase of evoked PSPs compared to the previous electrophysiological experiments (Supplementary Fig. 3, p=0.456; n=9 vs. 11)$_s$ and therefore this effect is independent of the potential buffering of postsynaptic Ca^{2+} by the Ca^{2+} indicator. In

conclusion, Ca^{2+} influx into the tuft or proximal apical dendrite appears to be neither required for, nor modified by the ACh-mediated modulatory effects on ON-evoked postsynaptic PSPs.

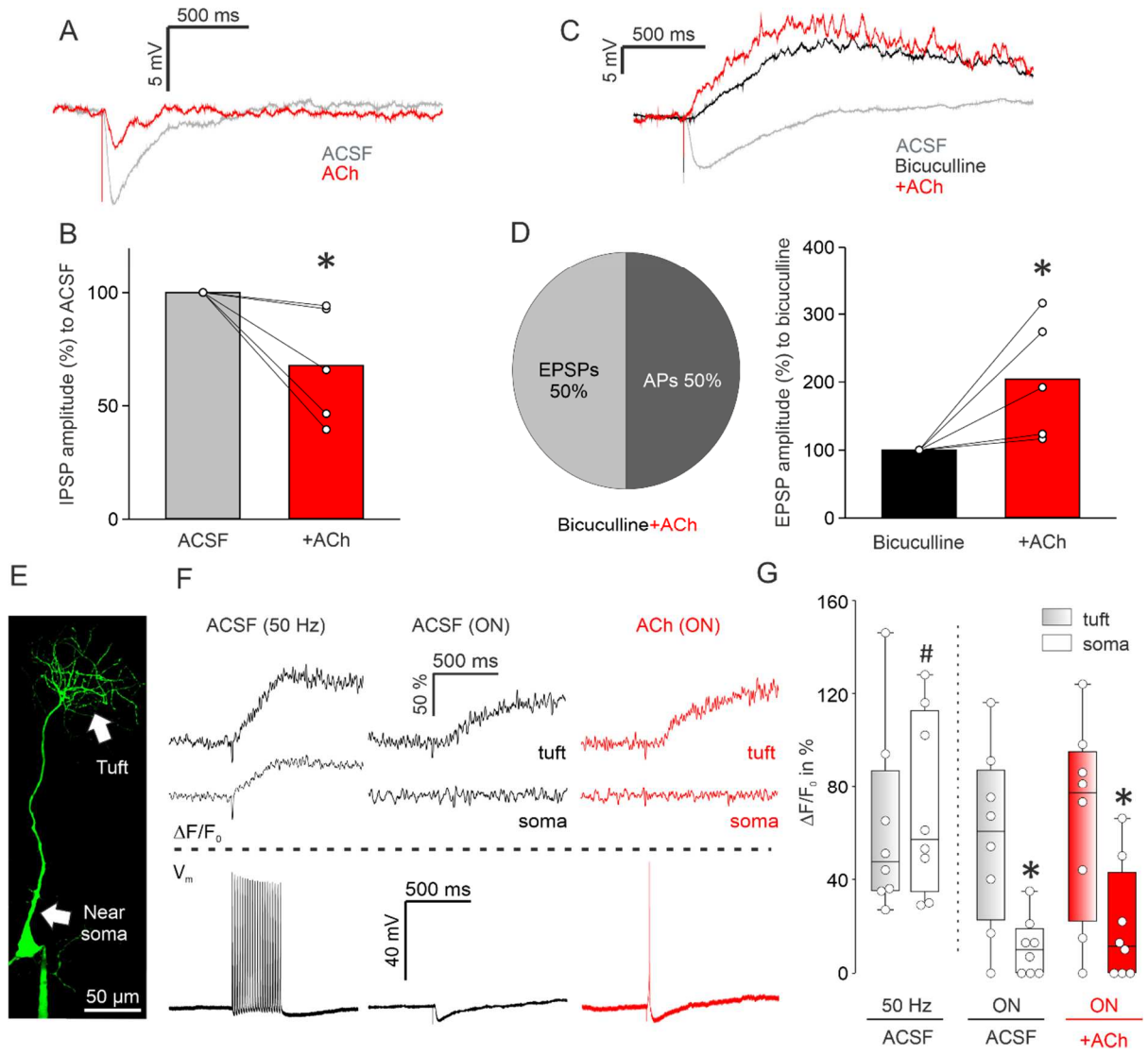

Fig. 17 **ACh modulates both ON-evoked inhibition and excitation via muscarinic receptors but does not increase intracellular Ca^{2+} influx**

Whole-cell patch-clamp recordings in 300 µm *in vitro* slices of responses from VPCs to electrical ON stimulation (50 µA, 100 µs, 30 s intervals). (A) Representative averaged traces of responses following ON stimulation in the ACSF condition (grey) and during bath application of ACh (acetylcholine, red) showing reduced IPSPs. (B) Cumulative analysis of normalized evoked IPSP amplitudes to the ACSF condition during bath application of ACh (n=5 cells). (C) Representative averaged traces of responses following ON stimulation in the ACSF condition (grey) and during bath application of bicuculline (50 µM, black) and additional application of ACh (100 µM, red).

(legend continued on next page)

(D) Pie-chart represents the proportion of cells showing either APs or EPSPs in the ACh condition (n=6 cells). Bar-charts represent cumulative analysis of normalized evoked EPSP amplitudes to the bicuculline condition during additional application of ACh (n=5 cells). Data are presented as means including distribution of single data points. Lines between data points represent related measurements. Related-Samples Wilcoxon Signed Rank Test, *p<0.05 vs. ACSF/bicuculline. (E) Representative picture of a VPC filled with OGB-1. Arrows indicate the tuft and the apical dendrite near the soma. Scale bar, 50 µm. (F) Representative averaged traces of Ca^{2+} influx in the tuft and the soma above the dot line. Representative averaged traces of responses following ON stimulation under the dot line (ACSF with 50 Hz somatic stimulation or ON stimulation, black; ACh with ON stimulation, red). (G) $\Delta F/F_0$ in % from baseline following different stimulation and pharmacology. Data are presented as box-plots including first, median, and third quartiles with whiskers representing the range of data points and distribution of single data points. (2) × (2) mixed model ANOVA (location [within subject] × treatment [within-subject]) with treatment being either 50 Hz vs. ON or ACSF vs. ACh, *p<0.05 vs. tuft within the condition. n=8 cells. #p<0.05 50 Hz in the ACSF (soma) vs. ON in the ACSF (soma). n=8/8 cells.

3.4.4 Muscarinic signaling is the major player in reducing inhibition of bulbar VPCs

To narrow down mechanisms of cholinergic excitation of VPCs, we next focused on ACh receptor subtypes. The selective agonists (nicotine, 100 µM; muscarine, 1 µM) or antagonists (mecamylamine, a nicotinic receptor antagonist, 20 µM; atropine, a muscarinic receptor antagonist, 10 µM) were bath-applied to examine changes of ON-evoked PSPs in VPCs. Unlike ACh application, nicotine application was not able to turn evoked IPSPs into excitation in any of the tested VPCs (Fig. 18B; n=8 from 5 rats). Moreover, the average amplitude of evoked IPSPs in nicotine was similar to control, even though variability across experiments was high (Fig. 18A+B; $p=0.327)_t$. Similar results were observed with ACh application following blockade of muscarinic signaling with atropine. Neither application of atropine alone nor the atropine-ACh condition showed any evoked excitation and/or reduction of evoked-IPSP amplitudes (Fig. 18C+D; p=0.156, Friedman test, $n=7$ from 4 rats)$_u$. Thus, nicotinic signaling is most likely not sufficient to turn evoked inhibition to excitation in VPCs.

Conversely, muscarine administration enabled excitation in 25 % of VPCs (Fig. 18F; APs and EPSPs in 1 cell each, n=8 from 5 rats). Furthermore, muscarine application significantly reduced the amplitudes of ON-evoked IPSPs in the remaining 75% of cells (Fig 18F; p=0.028, $n=6$ from 4 rats)$_v$. Intriguingly, application of mecamylamine followed by ACh, which isolates muscarinic signaling, also resulted in ON-evoked excitation in a similar amount of VPCs as

during muscarine application (Fig. 18G+H; APs 18 % and EPSPs 9 % of cells, n=11 from 9 rats). In addition, ACh following mecamylamine reduced evoked-IPSP amplitudes compared to control or mecamylamine alone (Fig. 18H; p=0.034, Friedman test, mecamylamine-ACh vs. ACSF p=0.024, mecamylamine-ACh vs. mecamylamine p=0.024, 73 % of cells, n=8 from 7 rats)$_w$ similar to muscarine application. Thus, these results indicate that the muscarinic pathway is the major player in reducing inhibition of ON-stimulated VPCs, even though we cannot entirely exclude the involvement of nicotinic signaling.

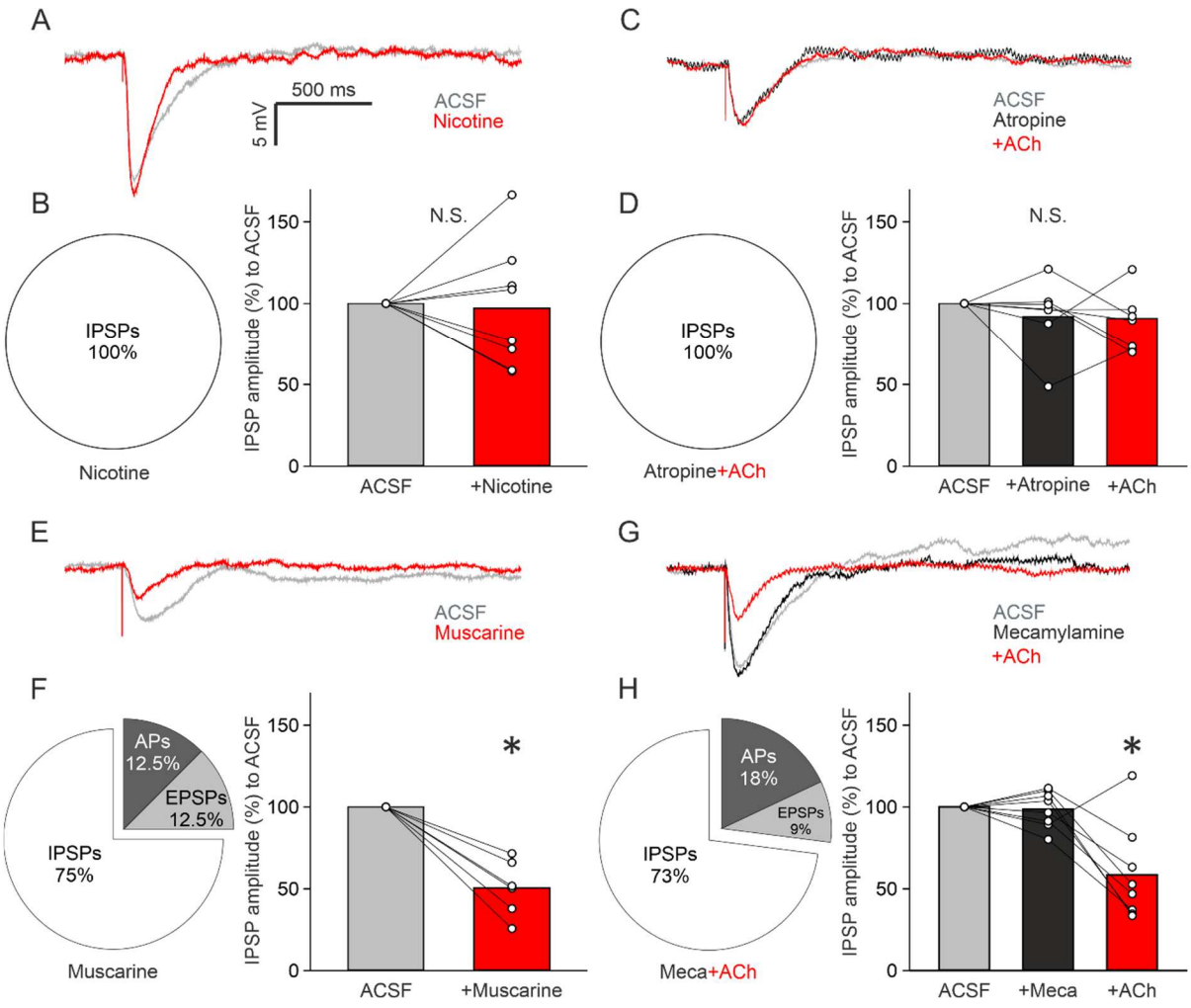

Fig. 18 **The muscarinic pathway is responsible for reduction of ON-evoked inhibition**

(A) Representative averaged traces of responses from VPCs following ON stimulation in the ACSF condition (grey) and during bath application of nicotine (100 µM, red). (B) Pie-chart represents the proportion of cells showing either APs, EPSPs or IPSPs (n=8 cells). Bar-charts represent cumulative analysis of normalized evoked IPSP amplitudes to the ASCF condition (n=8 cells without APs and EPSPs).

(legend continued on next page)

(C) Representative averaged traces of responses from VPCs following ON stimulation in the ACSF condition (grey) and during bath application of atropine (10 µM, black) and atropine+ACh (10 µM+100µM, red). (D) Pie-chart represents the proportion of cells showing either APs, EPSPs or IPSPs in the atropine+ACh condition (n=11 cells). Bar-charts represent cumulative analysis of normalized evoked IPSP amplitudes to the ASCF condition (n=8 cells without APs and EPSPs). (E) Representative averaged traces of responses from VPCs following ON stimulation in the ACSF condition (grey) and during bath application of muscarine (1 µM, red). (F) Pie-chart represents the proportion of cells showing either APs, EPSPs or IPSPs in the (n=8 cells). Bar-charts represent cumulative analysis of normalized evoked IPSP amplitudes to the ASCF condition (n=6 cells without APs and EPSPs). (G) Representative averaged traces of responses from VPCs following ON stimulation in the ACSF condition (grey) and during bath application of mecamylamine (20 µM, black) and mecamylamine+ACh (20 µM+100 µM, red). (H) Pie-chart represents the proportion of cells showing either APs, EPSPs or IPSPs in the mecamylamine+ACh condition (n=7 cells). Bar-charts represent cumulative analysis of normalized evoked IPSP amplitudes to the ASCF condition (n=7 cells without APs and EPSPs). Data are presented as means including distribution of single data points. Lines between data points represent related measurements. Related-Samples Wilcoxon Signed Rank Test, *p<0.05 vs. ACSF in agonist experiments. Friedman test, Dunn for single comparisons, *p<0.05 vs. Meca (mecamylamine) or vs. ACSF in antagonist experiments. N.S., not significant.

3.4.5 Cholinergic cells in the HDB are activated during social interaction

Our results reveal that ACh can flip ON-evoked inhibition of bulbar VPCs into excitation *in-vitro*. If this activating drive of ACh is indeed involved in triggering VPC excitation in behaving rats, we hypothesized that ACh should be released into the OB during social interaction. Thus, ACh neurons that are known to project to the OB from the horizontal limb of the diagonal band of Broca (HDB, Senut et al., 1989; Schwarz et al., 2020) should get activated by social interaction. Activity of the cholinergic system is correlated with changes in sensations or internal states such as arousal or attention (Imperato et al., 1992; Zhu et al., 1995; Butt et al., 1997; Linster and Hasselmo, 2000; Passetti et al., 2000; McKenna et al., 2009). Moreover, it was shown that stimulation of HDB ACh projections into the MOB can sharpen the odor responses of M/TCs (Rothermel et al., 2014; Bohm et al., 2020). Since we had obtained whole brains from a subset of the exposure experiments (water, rat urine, conspecific), we next investigated the activity of ACh neurons in the HDB. To visualize activated HDB neurons and specifically activated ACh neurons, we stained the HDB against pERK and choline acetyltransferase (ChAT, Fig. 19A). The total number of $pERK^+$ HDB cells was not significantly different between all groups (Fig. 19B; p=0.104, ANOVA, water n=5,

urine n=5, rat n=6)$_x$. However, the number of pERK$^+$ ACh neurons in the rat exposure group was significantly higher than that in the urine exposure group, even though the pERK$^+$ ACh neuron number in the rat exposure group was not higher than that in the water exposure group (Fig. 19C; p=0.034, ANOVA, rat vs. urine p=0.011, rat vs. water p=0.113, water vs. urine p=0.255)$_y$. The results indicate that HDB ACh neurons are activated more easily by social interactions than by investigating urine and thus more likely to excite VPCs specifically during social interactions.

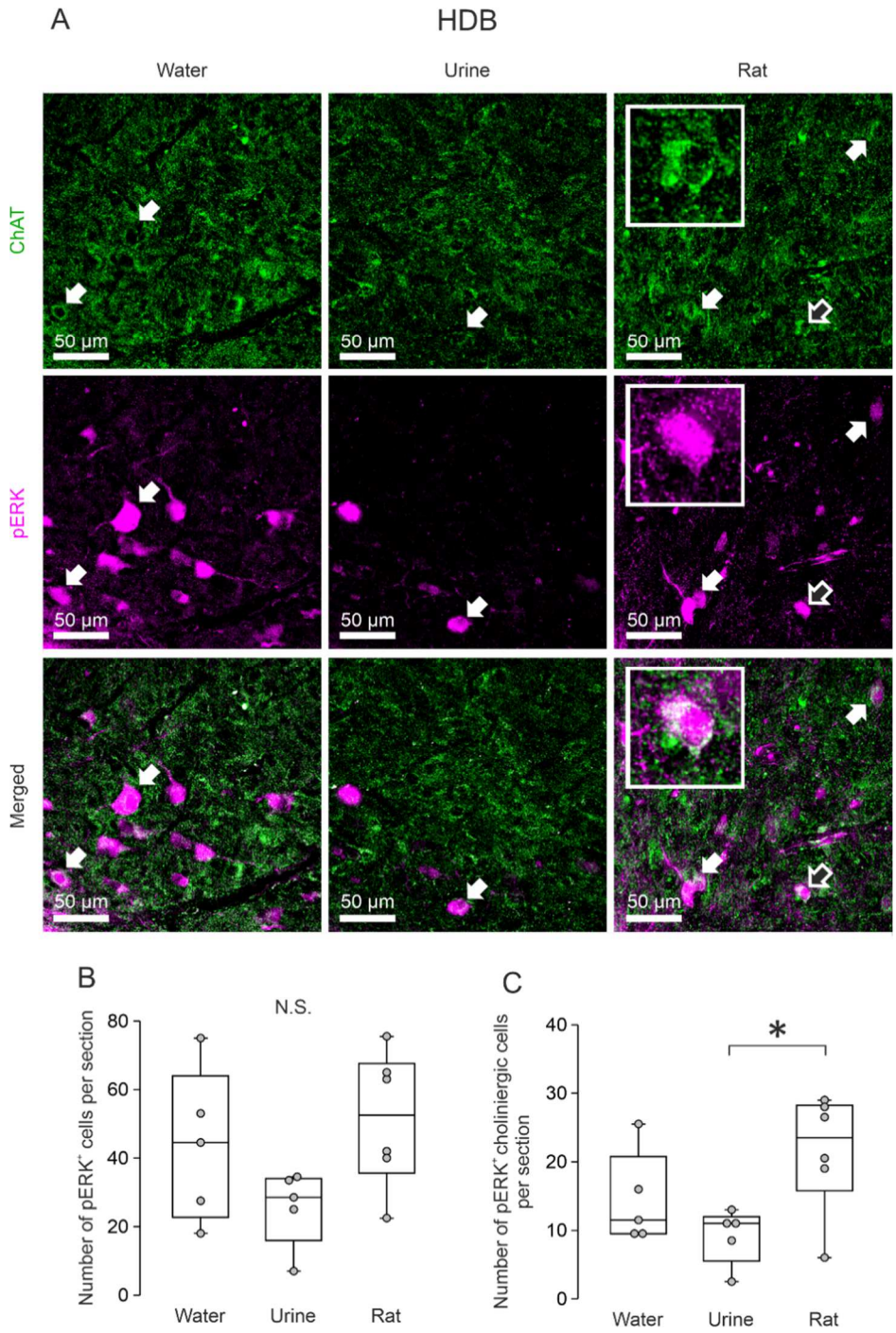

Fig. 19 **Cholinergic cells in the HDB are activated during social interaction**

(A) Representative average z-projections of the HDB (horizontal limb of the diagonal band of Broca) that were immune-stained for ChAT (choline-acetyltransferase, green, CF488) and pERK (magenta, CF 594) in the different experimental groups. Arrows indicate cells that are double-labeled for pERK and ChAT. Insets show enlarged pictures of the cell indicated by blank arrows. Scale bar, 50 µm valid for all images in the same panel. (B+C) Averaged number of pERK$^+$ cells or pERK$^+$ cholinergic cells per section in different experimental groups. Data are presented as box-plots including first, median, and third quartiles with whiskers representing the range of data points and distribution of single data points. One-way ANOVA, LSD for single comparisons, N.S., not significant, *p<0.05 Rat vs. Urine, n=5 rats (water), n=5 rats (urine), n=6 rats (rat).

3.4.6 Atropine-induced impairment of social discrimination is rescued by VP microinjection into the OB in male rats

Our data so far demonstrated a disinhibitory effect of bulbar ACh on ON-evoked VPC activity mainly via muscarinic receptors as well as the activation of both systems, intrinsic bulbar VP and HDB ACh, during social interaction. These observations are in line with behavioral studies that demonstrate that pharmacological blockade of bulbar V1a receptor or systemic ACh activity diminishes social discrimination abilities in rats (Anagnostaras et al., 2003; Tobin et al., 2010). To examine if the cellular mechanisms we observed in the OB indeed play a role for social discrimination in behaving rats, we tested (1) if the blockade of muscarinic ACh signaling in the OB impairs social discrimination and (2) if a later additional VP injection, mimicking potential ACh-facilitated VP release, can rescue a possibly impaired behavior. Thus, we performed microinjections of atropine (1 µg/ 1 µL per hemisphere) or vehicle (ACSF, 1 µL per hemisphere) followed by either VP (1 ng/ 1 µL per hemisphere) or vehicle before the sampling phase of a social discrimination test (Fig. 20A). In this test, the ability to discriminate two individuals is measured in terms of how long rats investigate a novel versus a known stimulus rat (Engelmann et al., 2011).

Control rats that received only vehicle investigated the novel stimulus rat significantly more than the known rat, indicating intact social discrimination (Fig. 20D; $p=0.033$, $n=13)_z$. In contrast, atropine-injected rats showed a similar duration of investigation towards both, novel and known stimulus rats (Fig. 20E; $p=0.240$, $n=14)_{a1}$. Thus, the blockade of muscarinic signaling in the OB indeed impaired social discrimination. Atropine-VP injected rats, however, significantly preferred investigating the novel stimulus rat over the known one (Fig. 20F; $p=0.031$, $n=14)_{b1}$. Hence, impairment of social discrimination by atropine is most likely caused by a disruption of the activation of the bulbar VP system, and in turn a reduced bulbar VP release during social interaction. Therefore, their ability to discriminate a known from a novel stimulus was rescued by additional VP injection.

To confirm that neither atropine nor VP microinjection into the OB induced unspecific behavioral effects, we demonstrated that these manipulations did not interfere with play behavior (Fig. 20G; $p=0.633$, $n=41)_{c1}$ and habituation to the juvenile rat (Fig. 20H; $p<0.001$, $n=41)_{d1}$ during the sampling phase. Further, also non-social investigatory behavior (Suppl. Fig. 4A; $p=0.843$, $n=41)_{e1}$ and habituation towards amyl acetate or (-)-carvone presented in a teaball (Suppl. Fig. 4B; $p<0.001$, $n=41)_{f1}$ was not changed by the pharmacological treatments. This final experiment thereby supports our hypothesis based on our findings *in-vitro* that the activity of the bulbar VP system (that is essential for social discrimination) is triggered by centrifugal ACh inputs during social interaction.

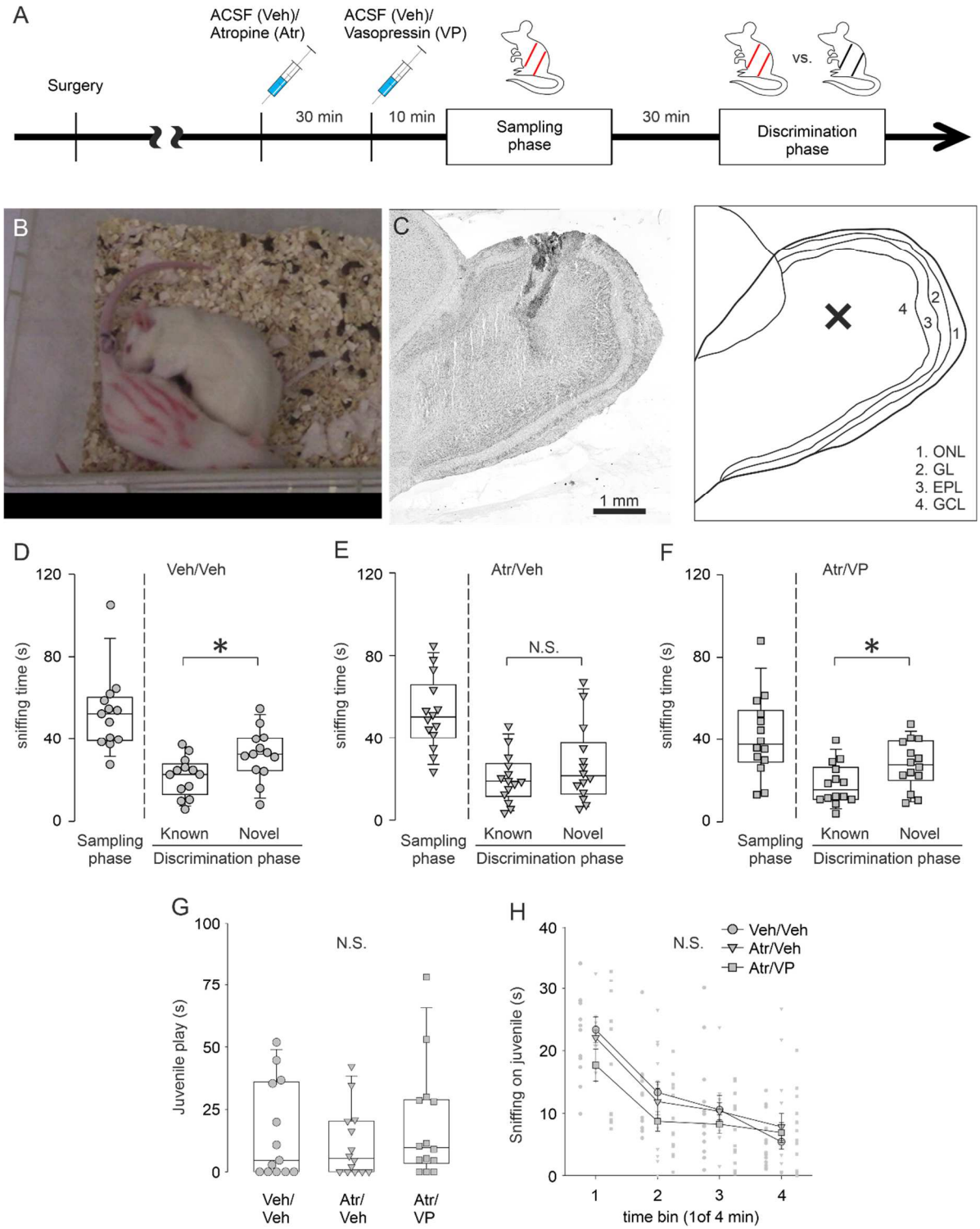

Fig. 20 **VP microinjection into the OB rescues atropine-induced impairment of social discrimination in male rats**

(A) Schematic time course of the experimental design. (B) Rat (5 weeks) without markings representing anogenital sniffing toward a stimulus rat (3 weeks) with red markings. (C) Representative picture of the OB with dye injection via drug injection system, counterstained with Cresyl violet and a schematic picture of the olfactory bulb. The cross in a schematic picture indicates the approximate injection position in the left picture. ONL, olfactory nerve layer; GL, glomerular layer; EPL, external plexiform layer; GCL, granule cell layer.

(legend continued on next page)

(D-F) Amount of time (s) that rats investigate stimulus rats in the sampling phase and in the discrimination phase (known or novel rat) following microinjection (1 µL per bulb) with only vehicle, atropine (1 µg/ 1 µL) and vehicle or atropine and VP (1 ng/ 1 µL). Data are presented as box-plots including first, median, and third quartiles with whiskers representing the range of data points and distribution of single data points. Paired Samples t-Test between known and novel, *$p<0.05$, n=13 rats (Veh/Veh), n=14 rats (Atr/Veh), n=14 rats (Atr/VP). (G) Amount of time (s) that rats are engaged in playing with the stimulus rat during the sampling phase. Data are presented as box-plots including first, median, and third quartiles with whiskers representing the range of data points and distribution of single data points. Kruskal-Wallis Test, n=13 rats (Veh/Veh), n=14 rats (Atr/Veh, 1µg), n=14 rats (Atr/VP, 1µg/1ng). (H) Amount of time (s) within time bins of 1 min that rats investigate the stimulus rat during the sampling phase following different drug application. Data are presented as means ± SEM including distribution of single data points. (4) × (3) mixed model ANOVA (time bin [within subject] × treatment [between-subject]), n=13 rats (Veh/Veh), n=14 rats (Atr/Veh, 1µg), n=14 rats (Atr/VP, 1 µg/1ng). N.S., not significant.

3.5 Discussion

Social discrimination in rats depends on the presence of endogenous VP in the OB (Tobin et al., 2010), which implies that social interaction can trigger VP release, via the activation of bulbar VPCs. A substantial background activity of VPCs (pERK) was found throughout all stimulation groups *in-vivo*, even though VPCs are inhibited by olfactory nerve input *in-vitro*. This background activity might be related to the circumstance that it is not realistic to deprive our experimental rats from all environmental sensory inputs, e.g., rat odors from other cages (Mirich et al., 2004). Nevertheless, we observed increased levels of bulbar VPC activation during social interaction (Fig. 15C+D). Thus, our results suggest that during social interaction VPC activity and hence the probability of bulbar VP release, are substantially increased. This finding is apparently at variance with others from Wacker et al. (2011), who reported that social interaction cannot trigger the expression of the immediate early genes c-Fos or Egr-1 in bulbar VPCs. However, as discussed by them, a missing expression signal of those genes might be explained by their general absence of expression in bulbar VPCs.

Since we know that VPCs are primarily inhibited by ON inputs *in-vitro* (Lukas et al., 2019), we hypothesized that additional inputs from outside of the OB are responsible for the activation of VPCs during social interaction.

Pheromones from conspecifics are detected by rodents during social interactions and were shown to directly influence social behaviors, such as sexual behavior or aggression between conspecifics (Haga et al., 2010; Hattori et al., 2016). Thus, pheromones would be an obvious way to provide social specificity via social interactions. Indeed, M/TCs in the AOB, the first pheromonal relay station in the brain, are known to innervate the dorsal MOB and therewith could also excite bulbar VPCs (Vargas-Barroso et al., 2016). In our hands, electric stimulation of the AOB failed to elicit any excitatory responses in MOB VPCs in *in-vitro* sagittal slice experiments (Supplementary Fig. 2D+E). Moreover, there was no significantly enhanced MOB VPC activation by urine, containing pheromones, compared to control.

However, we cannot entirely rule out this possibility because of the reduced connectivity *in-vitro* and the larger/different set of pheromonal cues accessible during investigation of a conspecific versus just urine. Moreover, although social interaction increases c-Fos expression in the AOB in general (Noack et al., 2010), we did not find any differences in the number of $pERK^+$ AOB M/TCs between the rat, urine, and water exposure group (Supplementary Fig. 1C+F). Also, we rarely observed $pERK^+$ VPCs in the AOB itself, neither following urine exposure nor social interaction (only 1 or even less cells on average per slice). In summary, pheromonal AOB signaling is rather unlikely to underlie VP-dependent individual social discrimination in the MOB.

Also, while removal of the vomeronasal organ initially prevents social recognition of same sex individuals, it is reinstated after 14 days, indicating that AOB functioning is not required for social recognition *per se* (Bluthe and Dantzer, 1993). Nevertheless, the AOB is crucial for individual discrimination in the context of reproduction. For example, the pheromonal memory of the stud male in female mice results in a pregnancy block induced by odors of male strangers. This consequence of social odor recognition, known as the Bruce effect, depends on pheromonal processing in the AOB (Kaba et al., 1989). Thus, the AOB may be essential for individual discrimination in certain situations, such as in a reproductive context, but not necessarily in social discrimination in general. Still, it is possible that modulatory top-down inputs to the MOB that are activated by AOB processing (Baum and Kelliher, 2009) is involved in the activation of MOB VPCs.

Cholinergic neurons in the HDB are the only known source that provides centrifugal neuromodulatory inputs to the GL of the OB, where VPCs are predominantly located (Senut et al., 1989; Lukas et al., 2019; Schwarz et al., 2020). Following social interaction, the number of $pERK^+$ cholinergic HDB neurons was significantly higher compared to rat urine exposure (Fig. 19C) indicating that cholinergic activation might be involved in bulbar VPC activation in the rat exposure group (Fig. 15C). Accordingly, we observed that ON-evoked

IPSPs are reversed into EPSPs/APs in 75 % of examined VPCs during ACh administration *in-vitro* (Fig. 16G). Moreover, we showed that ACh induces both, reduced inhibition, and stronger ON-driven excitation (Fig. 17A-D). Reduced GABAergic inhibition by ACh was already observed in hypothalamic VPCs, resulting in increased VP release *in-vitro* (Gregg, 1985; Li et al., 2001).

Non ACh-specific optogenetic silencing of all vesicular release from HDB projections in the OB reduces glomerular responses to odor stimulation *in-vivo* (Schwarz et al., 2020). In addition, optogenetic stimulation of specifically HDB cholinergic projections in the OB *in-vivo* increases odor responses in projection neurons (Rothermel et al., 2014; Bohm et al., 2020). Both results indicate overall excitatory effects of HDB cholinergic modulation in the OB during odor stimulation. Cells in the GL were reported to have a particularly high sensitivity for ACh, and direct application of ACh resulted in both, increase and decrease of spontaneous spiking rates in individual cells there (Ravel et al., 1990). These bidirectional effects may be explained by the presence of two different ACh receptor subtypes, nicotinic and muscarinic receptors, and their distinct effects on the various cell types of the OB (Matsutani and Yamamoto, 2008).

In our experiments, we demonstrated that muscarinic stimulation with either muscarine or mecamylamine-ACh application reversed evoked inhibition into excitation in some VPCs (Fig. 4E-H). At the level of the GL, it was shown that the muscarinic pathway enhances inhibitory inputs to GABAergic interneurons, i.e., periglomerular cells and short axon cells, hence possibly causing disinhibition of VPCs (Liu et al., 2015). According to our data, mainly muscarinic but not nicotinic stimulation reduced ON-evoked IPSP amplitudes in VPCs (Fig. 4A-H). In line with our observation, *in-vivo* Ca^{2+} imaging revealed that muscarinic stimulation increases glomerular sensitivity to odor presentation (Bendahmane et al., 2016).

All our pharmacological manipulations *in-vitro* were performed via bath application. Since nicotinic receptors are ionotropic and known to get desensitized (Quick and Lester, 2002), locally and temporally more precise administration, such as puff application or optical

uncaging, may be informative to investigate nicotinic mechanisms on a single cell level. Indeed, although we observed no statistical differences in nicotine effects on evoked-IPSP amplitudes, increasing and decreasing effects of nicotine application could be found across individual VPCs (Fig. 18A+B). In this context, D'Souza and Vijayaraghavan (D'Souza and Vijayaraghavan, 2012) described that nicotinic receptor signaling is involved in gain control mechanisms of excitatory projection neurons in the OB, which might explain the variable effects that we observed upon nicotine and atropine-ACh application. Moreover, muscarine application did not entirely replicate ACh effects (Fig. 16G, Fig. 18F+H). Thus, we cannot fully exclude nicotinic action in modulation of VPCs. Furthermore, the origin of the ON-driven excitation that is responsible for triggering APs during ACh application still needs to be identified. Possible candidates would be neurons providing somatic and lateral dendritic inputs to VPCs since ON-evoked Ca^{2+} signals in the tuft were not increased in ACh (Fig. 17G).

Although here we focused on the cholinergic system because of the strength of cholinergic effects, our *in-vitro* electrophysiology results indicate that increased VPC excitability could be triggered by synergistic cholinergic, serotonergic, and noradrenergic modulation; the possibility of such cooperative action should be accounted for in future studies.

If centrifugal cholinergic modulation from the HDB is indeed responsible for increasing VPC activity, the question remains how ACh is released in the OB in a context-dependent manner such as social interaction. Social perception is thought to be a multisensory process as diverse inputs from the whole stimulus animal are sampled and integrated (Engelmann et al., 2011; Bobrov et al., 2014; Rao et al., 2014). In support of this idea, Matsuo et al. (2015) showed that genetic ablation of dorsal MOB glomeruli impairs the expected emission of ultrasonic vocalization by male mice towards female urine, whereas these mice still emit ultrasonic vocalizations in the presence of a whole female mouse. This indicates that other sensory stimuli than those provided by olfaction can trigger this social behavior. Moreover, it

was shown that rats, which were exposed to just volatile odors of stimulus rats during the social discrimination paradigm cannot discriminate the different sources of these odors (Noack et al., 2010). According to our hypothesis, this impairment might be due to the absence of non-olfactory cues and lack of arousal.

Intriguingly, the HDB or the ACh system in general is activated by various sensations, such as olfactory, visual, and tactile stimuli (Zhu et al., 1995; Butt et al., 1997; Linster and Hasselmo, 2000). Stimulation of the HDB cholinergic projections or ACh application in turn can enhance as well as reduce neural activity in all primary sensory cortices (Metherate and Ashe, 1995; Kirkwood et al., 1999; Chaves-Coira et al., 2018). Also, especially if the sensation is associated with learning, ACh tends to be released in the respective sensory cortex, for example during conditioning of auditory or tactile cues with food as an unconditioned stimulus (Butt et al., 1997; Butt et al., 2009). Accordingly, our data demonstrates substantial HDB ACh activity during social interaction. Surprisingly, we were not able to find a significant difference between water stimulation and social interaction in ACh neurons of the HDB. It is not possible to determine from our data what may be the reason for this high activation in the water condition. However, water stimulation (with no or few olfactory cues) was not enough to increase pERK activity in MOB VPCs to the same level as social interaction, suggesting that both, ACh neuron activation in the HDB and olfactory inputs are needed for VPC activation. In support, our *in-vitro* electrophysiology results demonstrate that ACh modulation promotes especially excitation in VPCs following ON stimulation mimicking odor stimulation. Thus, it is tempting to speculate that the HDB cholinergic system could play a role as a multisensory integration center during complex contexts like social interaction that provides modulatory feedback to sensory processing, including but not limited to olfaction. Intriguingly, similar multi-sensory integration is also discussed to take place in the insular cortex which is responsible for coordinated behavioral output during social decision-making (Rogers-Carter and Christianson, 2019). From a translational point of view, it is interesting to note that also human research on social

behavior deficits suggests a social-context network that integrates social cues (frontal lobe), consolidates social-context associations (temporal lobe), and converges environmental and internal signals (insular lobe, Baez et al., 2017).

Moreover, ACh activity correlates with certain internal states in animals, e.g., arousal or attention (Imperato et al., 1992; Passetti et al., 2000; McKenna et al., 2009). This internal state-dependent ACh release is triggered by the sudden presence or novelty of stimuli (Acquas et al., 1996; Giovannini et al., 2001). Rats discriminate individuals according to their social novelty (Engelmann et al., 2011). Thus, we suggest that both multi-sensation and increased arousal and attention while assessing the novelty of rats in the context of social interaction can lead to increased HDB ACh activity and thereby cholinergic neurotransmission in the OB.

Our pERK and electrophysiological experiments imply a central role for ACh in VP-dependent social discrimination and accordingly social memory. The involvement of centrifugal ACh as a facilitator of olfactory learning or habituation has been investigated for decades (Wilson et al., 2004). The blockade of the muscarinic pathway in the OB impairs both aversive and appetitive learning (Ravel et al., 1994; Ross et al., 2019). Intriguingly, it was shown that the blockade of muscarinic neurotransmission in the OB by scopolamine does not impair single-molecule odor recognition (Mandairon et al., 2006a). However, non-ACh specific optogenetic silencing of overall release from HDB projections in the OB impairs social habituation to female conspecific mice (Schwarz et al., 2020). In addition, here we demonstrated that the injection of the muscarinic antagonist atropine in the OB efficiently blocks the recognition of a known rat in the social discrimination task. These findings indicate that social discrimination/habituation paradigms and simple odor discrimination/habituation paradigms differ from each other.

Regarding sensory complexity, social discrimination recruits multiple senses, whereas odor discrimination is limited to mostly mono-molecular odorants. As mentioned above,

multisensory stimulation is a known trigger for the activation of HDB ACh neurons. Atropine-induced impairment of social discrimination was rescued by additional VP injection in the OB (Fig. 20F). Therefore, we suggest that ACh facilitates social discrimination via enhancing bulbar VP release. Since bulbar VP signaling is essential for multisensory social discrimination but not for simple odor habituation (Tobin et al., 2010), we suggest that the probability of bulbar VP release is higher during social discrimination. This hypothesis is supported by a study with another social behavior-related neuropeptide, oxytocin, in which Martinon et al. (Martinon et al., 2019) demonstrated that oxytocin release in the bed nucleus of stria terminalis is not increased with a foot shock alone, but when the foot shock is paired with another sensory cue (condition stimulus). Intriguingly, multisensory integration was recently also implied in a context of social discrimination. Accordingly, rats and mice cannot recognize their cage mates if they are immobile due to anesthesia, and mice that are both whiskerless and deaf are not able to discriminate awake novel and known conspecifics anymore (de la Zerda et al., 2020).

We showed that social interaction as well as ACh activate bulbar VPCs, indicating that cholinergic activation contributes to increased activation of the bulbar VP system during social interaction. However, the pERK results also indicate that the entire neuronal population of the bulb shows increased activation, not just VPC neurons, upon social exposure. Thus, alternatively to a multisensory driven specific activation of bulbar VPCs, it is possible that a general arousal mechanism leads to an increased excitation of the entire bulbar network, including VPCs. Accordingly, this might also explain to a certain degree why urine, in contrast to a rat stimulus, did not activate significantly more VPCs than water, since urine might cause less general arousal than a hitherto unknown conspecific.

The absence of sensitivity to both, the muscarinic antagonist or a V1a receptor knock-down by siRNA in simple odor discrimination and habituation (Mandairon et al., 2006a; Tobin et al., 2010) implies that ACh-induced VP signaling is only necessary to differentiate difficult odor mixtures. Interestingly, ACh was reported to play a critical role in modulating olfactory

perceptual learning tasks (Wilson et al., 2004). Perceptual learning is a prerequisite for enhanced perceptual acuity during discrimination of previously experienced stimuli. Like social discrimination, perceptual learning is specific for trained stimuli (e.g., a conditioned odor, a previously sampled rat) and requires a certain attention/arousal of the learning animal. This enhancement of olfactory acuity is mediated by muscarinic signaling (Wilson et al., 2004). Thus, ACh-dependent VP neurotransmission might be involved not only in social discrimination, but also olfactory perceptual learning tasks in general, e.g., discrimination of closely related odor mixtures. Indeed, different body odors should be difficult to discriminate due to their complexity and similarity. Singer et al. (1997) showed that volatile MHC components in mouse urine contain similar compositions of compounds across strains suggesting that volatile MHCs are not distinguishable by the presence or absence of some unique compounds. However, the amplitudes of some prominent compound peaks in the gas chromatogram are different between strains, indicating that mice can recognize the differences of relative concentrations of certain compounds in body odor mixtures. Rats perceive not only volatile urinary odors but also volatile odors from other sources and even differentiate individuals from the same strain during the social discrimination task. Thus, it is likely that the olfactory cues that they can discriminate are even more complex. We therefore suggest that additional bulbar VP neuromodulation is needed to enhance the signal-to-noise ratio of complex odor inputs to allow better identification of individual body odors. Reduced activity of individual projection neurons via increased activity of interneurons is thought to act as a filtering mechanism (Yokoi et al., 1995; Cleland and Sethupathy, 2006).

Although social interaction increased pERK activation in MCs (Fig. 15E), inhibition of $pERK^{+}$ MCs, e.g., via a reduction of their firing frequency could still take place. E.g., pERK signaling could be not sensitive or fast enough to register this inhibition or pERK signaling is just gradually decreased but still higher than during baseline activity. Indeed, it was already shown that VP administration dampens odor-evoked firing of MCs in anesthetized rats (Tobin et al., 2010) and reduces ON-evoked EPSPs in external tufted cells *in-vitro* (Lukas et al.,

2019). Thus, we suggest that this filtering effect facilitated by bulbar VP can further reduce weak or quantitatively similar inputs, so that only quantitatively prominent inputs are transmitted to higher brain regions leading to more prominent differences in the neuronal representation of different social odor signatures. This reduction of noise could help the rats to discriminate similar mixtures of body odors during the social discrimination task, but also during social interaction in nature.

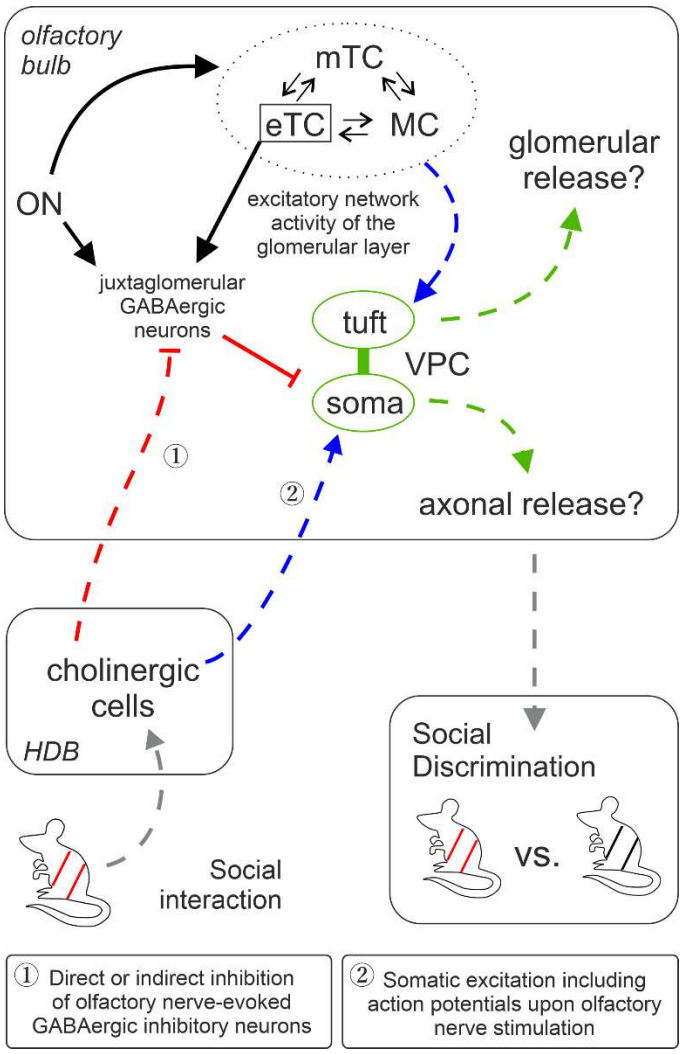

Fig. 21. **Graphic summary of OB pathways involved in social discrimination**

Blue, green, and grey arrows represent excitatory and red lines inhibitory pathways indicated by this study and our previous publication (Lukas et al., 2019). The cells within the dashed circle indicate the excitatory network within the same home glomerulus. Dashed pathways were confirmed but not fully dissected on the synaptic level. Green pathways are related to vasopressin signaling, grey pathways to sensory input or behavioral output and black pathways are based on findings from literature. Question marks indicate potential dendritic and axonal release of VP in the OB. Axonal projections innervate GL, EPL, MCL, and sGCL. EPL, external plexiform layer; eTC, external tufted cell; GL, glomerular layer; HDB, horizontal limb of the diagonal band of broca; MC, mitral cell; MCL, mitral cell layer; mTC, middle tufted cell; ON, olfactory nerve; sGCL, superficial granule cell layer; VPC, vasopressin cell.

Table 3 **Statistical overview**

	Figure	Type of statistic	Type of test	Test statistic	P-value	Effect size	Power
a	S1A	parametric	One-way ANOVA	$F_{(2,26)}$=0.406	p=0.670	*f*=0.176	0.115
b	15C	parametric	One-way ANOVA and post-hoc (LSD) rat vs water rat vs urine urine vs. water	$F_{(2,26)}$=3.713 - - -	p=0.038 p=0.011 p=0.197 p=0.195	*f*=0.463 *d*=1.147 *d*=0.604 *d*=0.663	0.548
c	15E	parametric	One-way ANOVA and post-hoc (LSD) rat vs water rat vs urine urine vs. water	$F_{(2,26)}$=3.586 - - -	p=0.042 p=0.025 p=0.034 p=0.949	*f*=0.525 *d*=1.117 *d*=0.824 *d*=0.232	0.663
d	S1C	parametric	One-way ANOVA	$F_{(2,24)}$=0.633	p=0.539	*f*=0.229	0.156
e	S1D	parametric	One-way ANOVA	$F_{(2,24)}$=0.746	p=0.485	*f*=0.237	0.164
f	S1E	parametric	One-way ANOVA	$F_{(2,24)}$=1.952	p=0.164	*f*=0.403	0.404
g	16C	non-parametric	Related samples Wilcoxon test	$W_{(8)}$=0; z=-2.521	p=0.012	*r*=0.891	0.995
h	16E	non-parametric	Related samples Wilcoxon test	$W_{(9)}$=1; z=-2.547	p=0.011	*r*=0.849	0.984
i	16G	non-parametric	Related samples Wilcoxon test	$W_{(20)}$=0; z=-3.920	p<0.001	*r*=0.876	1.000
j	16H	non-parametric	Mann-Whitney-U test	z=-4.652	p<0.001	*r*=0.736	1.000
k	16I	non-parametric	Kruskal Wallis and post-hoc (Bonferroni) 5-HT vs NA ACh vs 5-HAT ACh vs NA	H=17.439, df=2 z=0.003 z=-3.433 z=-3.291	p<0.001 p=1.000 p=0.003 p=0.002	- *r*=0.001 *r*=0.649 *r*=0.611	- 0.050 0.991 0.980
l	S2A	parametric	(4) × (2) mixed model ANOVA (intensity [within-subject] × treatment [within-subject])	$F_{(3, 54)}$=23.12 $F_{(1, 18)}$=0.647 $F_{(3,54)}$=0.562 (interaction)	p<0.001 p=0.432 p=0.604	*f*=1.132 *f*=0.176 *f*=0.255	1.000 0.119 0.158
m	S2B	parametric	(4) × (2) mixed model ANOVA (intensity [within-subject] × treatment [within-subject]) ACh vs. ACSF with 40 pA	$F_{(3, 54)}$=52.19 $F_{(1, 18)}$=3.228 $F_{(3,54)}$=6.346 (interaction) -	p<0.001 p=0.089 p=0.010 p=0.026	*f*=1.705 *f*=0.423 *f*=0.594 *d*=1.083	1.000 0.398 0.792
n	17B	non-parametric	Related samples Wilcoxon test	$W_{(5)}$=0; z=-2.023	p=0.043	*r*=0.905	0.872
o	17D	non-parametric	Related samples Wilcoxon test	$W_{(5)}$=0; z=2.023	p=0.043	*r*=0.905	0.872
p	-	non-parametric	Mann-Whitney-U test	z=3.121	p=0.002	*r*=0.716	0.988
q	17G	parametric	(2) × (2) mixed model ANOVA (location [within-subject] × treatment [within-subject])	$F_{(1,7)}$=17.8 $F_{(1,7)}$=1.98 $F_{(1,7)}$=0.014 (interaction)	p=0.004 p=0.203 p=0.910	*f*=1.596 *f*=0.531 *f*=0.045	1.000 1.000 0.081
r	17G	parametric	(2) × (2) mixed model ANOVA (stimulation [within-subject] × location [within-subject]) and post-hoc (Bonferroni) ON/soma vs. 50Hz/soma ON/soma vs. ON/tuft	$F_{(1, 7)}$=4.194 $F_{(1, 7)}$=7.446 $F_{(1,7)}$=15.01 (interaction) - -	p=0.080 p=0.029 p=0.006 p=0.014 p=0.002	*f=0.775* *f=1.030* *f=1.454* *dz=5.943* *dz=6.643*	0.424 0.650 0.911 - -
s	S3C	non-parametric	Mann-Whitney-U test	z=0.936	p=0.456	*r=0.209*	0.148
t	18B	non-parametric	Related samples Wilcoxon test	$W_{(8)}$=4; z=-0.420	p=0.327	*r=0.148*	0.065
u	18D	non-parametric	Friedman test	χ2=3.714, df=2	p=0.156	-	-
v	18F	non-parametric	Related samples Wilcoxon test	$W_{(6)}$=0; z=-2.201	p=0.028	*r=0.984*	1.000
w	18H	non-parametric	Friedman test and post-hoc (Dunn) Mecamylamine/ACh vs Mecamylamine Mecamylamine/ACh vs ACSF Mecamylamine vs ACSF	χ2=6.750, df=2 z=2.250 z=-2.250 z=0.000	p=0.034 p=0.024 p=0.024 p=1.000	- *r*=0.795 *r*=0.795 *r*=0.000	- 0.868 0.868 0.050
x	19B	parametric	One-way ANOVA	$F_{(2,13)}$=2.701	p=0.104	*f*=0.645	0.526
y	19C	parametric	One-way ANOVA and post-hoc	$F_{(2,13)}$=4.411	p=0.034	*f*=0.823	0.748

			(LSD) rat vs water rat vs urine urine vs. water	 - - -	 p=0.113 p=0.011 p=0.255	 *d*=0.918 *d*=1.826 *d*=0.933	
z	20D	parametric	Paired samples t-test	$t_{(12)}$=-2.411	p=0.033	*dz*=0.709	0.651
a1	20E	parametric	Paired samples t-test	$t_{(13)}$=-1.231	p=0.240	*dz*=0.202	0.208
b1	20F	parametric	Paired samples t-test	$t_{(13)}$=-2.420	p=0.031	*dz*=0.647	0.647
c1	20G	non-parametric	Kruskal-Wallis Test	H=0.915, df=2	p=0.633	-	-
d1	20H	parametric	(4) × (3) mixed model ANOVA (time bin [within-subject] × treatment [between-subject])	$F_{(3,114)}$=51.02 $F_{(2,38)}$=0.599 $F_{(6,114)}$=1.509 (interaction)	p<0.001 p=0.355 p=0.234	*f=1.161* *f=0.244* *f=0.283*	1.000 0.301 0.427
e1	S4A	non-parametric	Kruskal-Wallis Test	H=0.341, df=2	p=0.843	-	-
f1	S4B	parametric	(4) × (3) mixed model ANOVA (time bin [within-subject] × treatment [between-subject])	$F_{(3,114)}$=82.09 $F_{(2,38)}$=0.599 $F_{(6,114)}$=1.144 (interaction)	p<0.001 p=0.554 p=0.224	*f=1.147* *f=0.179* *f=0.274*	1.000 0.142 0.456

Type of statistic was determined using the Kolmogorov- Smirnov test in SPSS. Tests were performed using SPSS. Effect sizes for parametric statistics were determined using SPSS and G*Power (Cohen's *d, dz*, *f*). Effect sizes for non-parametric statistics were calculated from z-scores (Pearson's r = $|z|/\sqrt{n}$) (Rosenthal et al., 1994). Power (for α=0.05) was determined using G*Power.

3.6 Supplementary figures

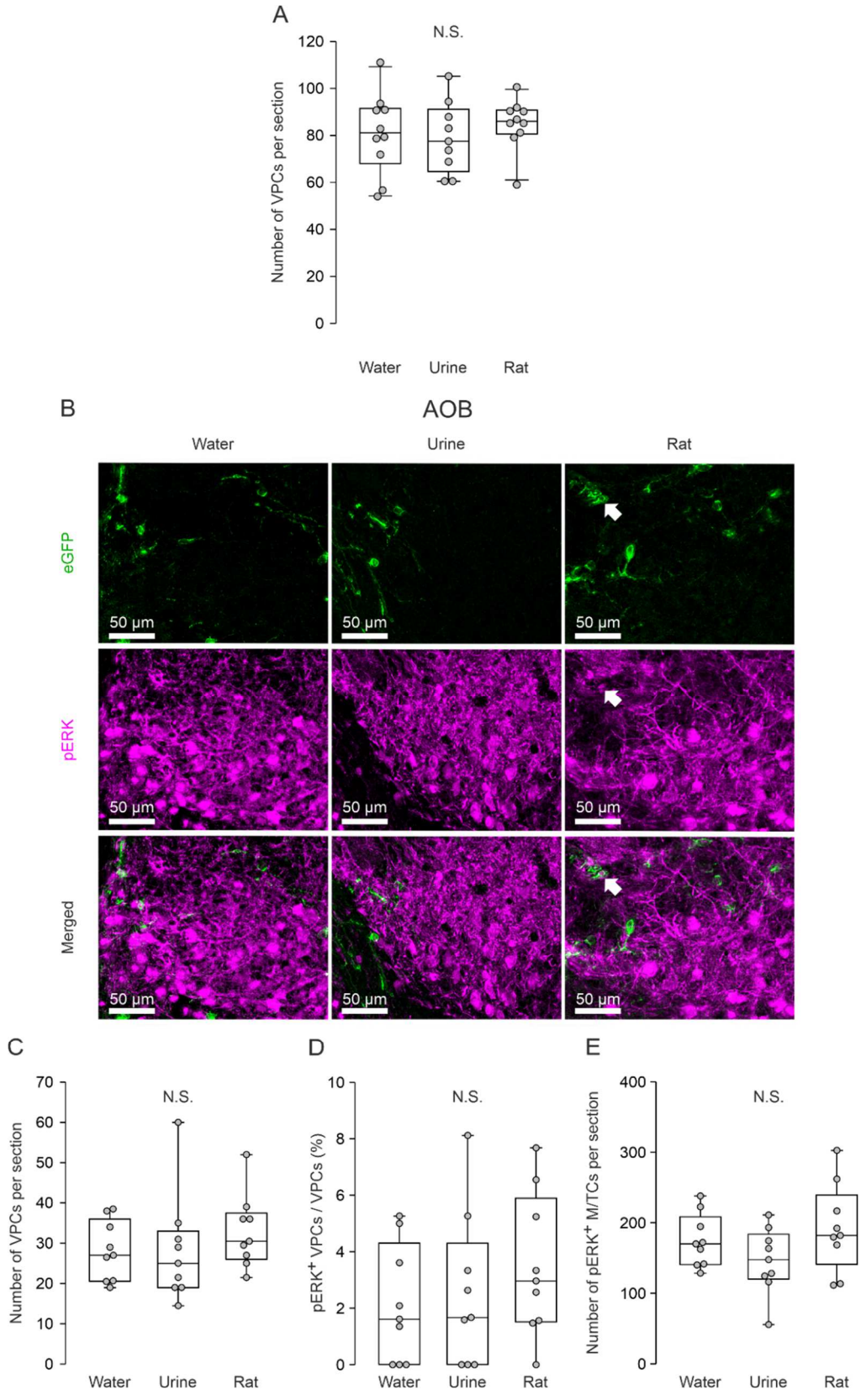

Supplementary Fig. 1 **VPC activation in the MOB and AOB**

(legend continued on next page)

(A) Averaged number of MOB VPCs per section in different stimulation groups. n=10 rats (water), n=9 rats (urine), n=10 rats (rat). Data are presented as box-plots including first, median, and third quartiles with whiskers representing the range of data points and distribution of single data points. One-way ANOVA, N.S., not significant. (B) Representative average z-projections of the accessory olfactory bulb that were immune-stained for eGFP (green, CF488) and pERK (magenta, CF 594) following water, urine, or rats stimulation. Arrows indicate a cell that is double-labeled for eGFP and pERK. Scale bar, 50 µm valid for all images in the panel. (C) Averaged number of AOB VPCs per section in different stimulation groups. (D) Averaged fraction of $pERK^+$ AOB VPCs of all AOB VPCs in different stimulation groups (%). (E) Averaged number of $pERK^+$ AOB M/TCs per section in different stimulation groups. Data are presented as box-plots including first, median, and third quartiles with whiskers representing the range of data points and distribution of single data points. One-way ANOVA, N.S., not significant. n=9 rats (water), n=9 rats (urine), n=9 rats (rat).

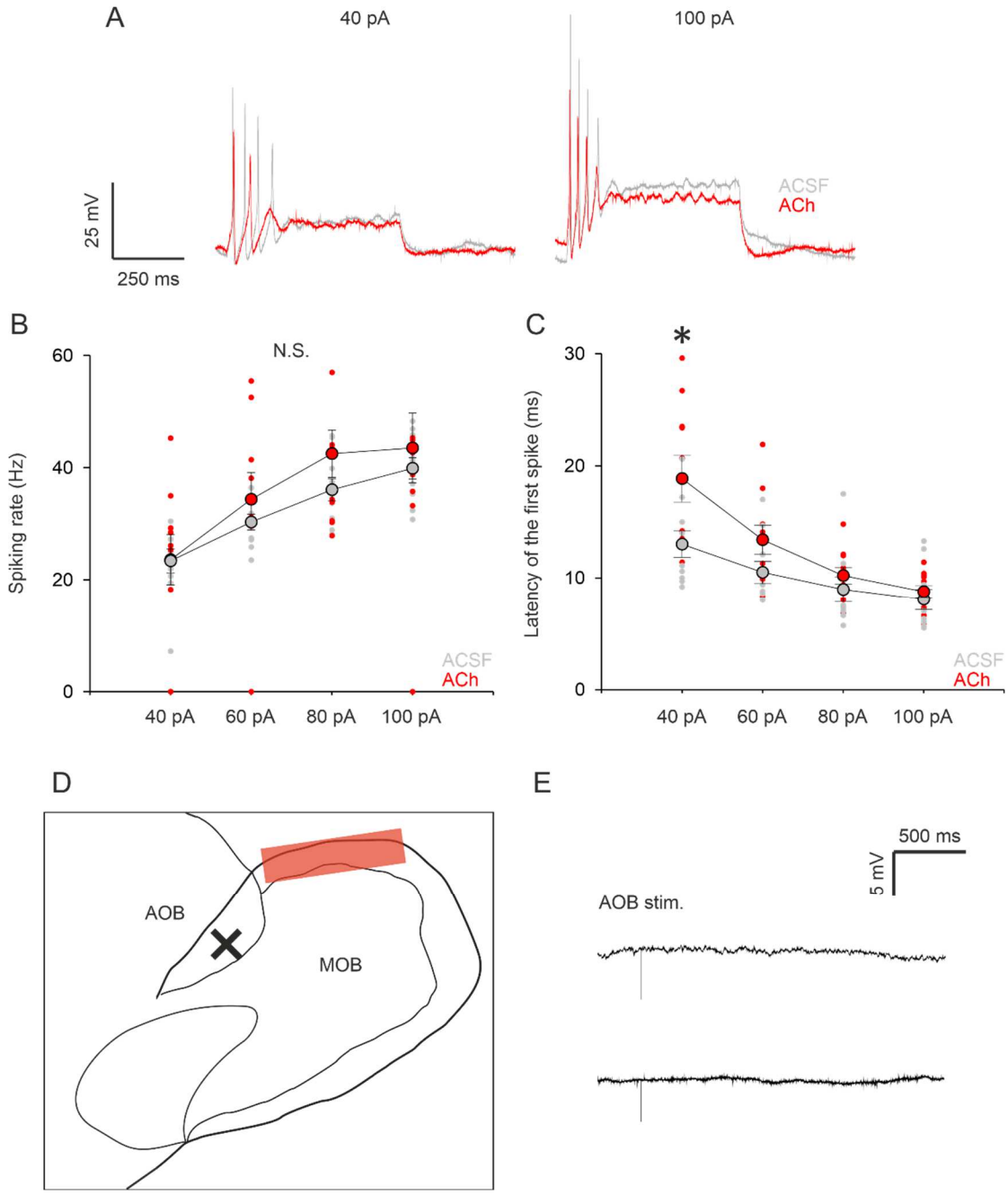

Supplementary Fig. 2 **ACh does not alter intrinsic excitability in VPCs and electrical AOB stimulation does not evoke excitatory responses in MOB VPCs**

(A) Representative traces of responses to somatically applied current steps in the ACSF condition (grey) and during bath application of ACh (100 µM, red). (B+C) Spiking rates of action potential trains and latency of the first spike evoked by somatic current injection (40-100 pA) in the ACSF condition (grey) and during bath application of ACh (100 µM, red). (2) × (2) mixed model ANOVA (intensity [within subject] × treatment [within-subject]). N.S., not significant. LSD for single comparison, *p<0.05 ACh (40pA) vs. ACSF (40pA). Data are means ± SEM including distribution of single data points. n=10 cells. (D) Schematic drawing of the sagittal OB. The cross indicates where the stimulation electrode was positioned. The red bar indicates the dorsal region of the MOB where patch-clamp recordings from MOB VPCs were performed. (E) Representative averaged trace of response from MOB VPCs to electrical vomeronasal nerve/ AOB stimulation (50-500 µA, 100 µs).

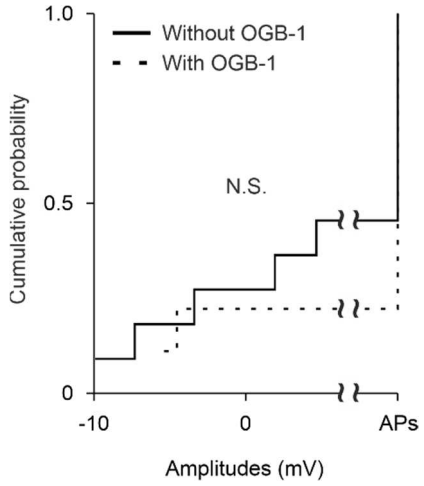

Supplementary Fig. 3 **Intracellular calcium indicator does not alter ACh effects on evoked PSP amplitudes in VPCs**

Cumulative probability of evoked PSP amplitudes in the ACh condition with or without OGB-1 in the intracellular solution (n=9/11 cells). The amplitudes of APs were set as 100 mV. Kruskal-Wallis test for variation comparison. N.S., not significant.

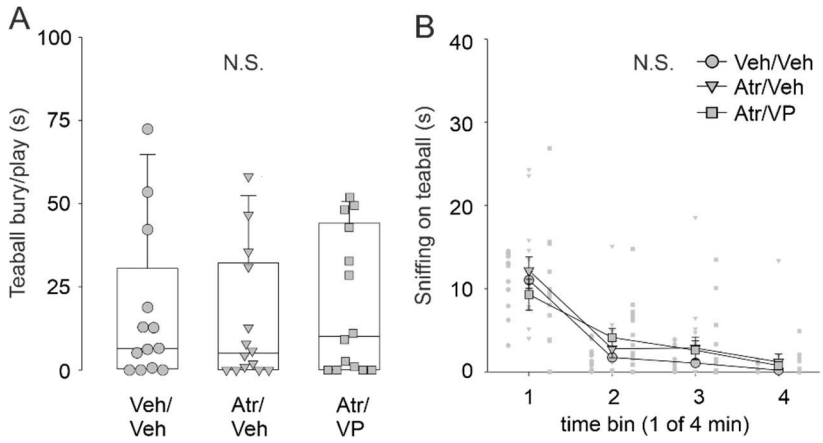

Supplementary Fig. 4 **Atropine and VP microinjection into the OB does not interfere with non-social investigatory/play behavior and habituation.**

(A) Amount of time (s) that rats are engaged in burying/playing with the teaball during neutral odor stimulation (amylacetate or carvone). Data are presented as box-plots including first, median, and third quartiles with whiskers representing the range of data points and distribution of single data points. Kruskal-Wallis Test, n=13 rats (Veh/Veh), n=14 rats (Atr/Veh, 1µg), n=14 rats (Atr/VP, 1µg/1ng). (B) Amount of time (s) within time bins of 1 min rats investigate the teaball during neutral odor presentation. Data are presented as means ± SEM including distribution of single data points. (4) × (3) mixed model ANOVA (time bin [within-subject] × treatment [between-subject]), n=13 rats (Veh/Veh), n=14 rats (Atr/Veh, 1µg), n=14 rats (Atr/VP, 1 µg/1ng). N.S., not significant.

Chapter 4: General discussion

This chapter aims to provide a comprehensive discussion of the data from both publications above (chapter 2+3). Moreover, some of the content in this chapter is an extension of the discussions found in the publications, due to the word number limitations of the journals. Therefore, there is some repetitions from the publications in this chapter for a better explanation.

4.1 Comparison of VPCs with other neurotransmitter systems in the OB

My PhD project aimed to characterize anatomical and physiological features of bulbar VPCs. Thus, chapter 2 described morphological and electrophysiological properties, and chapter 3 addressed the inputs to excite bulbar VPCs. Here, I would like to expand the comparison between VPCs and different neurotransmitter systems in the OB to better describe and understand the features of VPCs and the VP system.

4.1.1 Possible inhibitory and excitatory inputs to VPCs: insights from the classical intraglomerular microcircuit

MCs are the most abundant excitatory projection neuron type in the OB. Their somata are located in the MCL, and an apical dendrite usually projects to one glomerulus in which a dendritic tuft is formed. They receive excitatory inputs either directly from the ON or eTCs. I observed EPSPs following ON stimulation in MCs, whereas I observed only IPSPs in VPCs, even when those dendritic tufts were found in neighboring glomeruli (chapter 2). This contradiction is still not fully dissected. However, I obtained some knowledge to account for that. ON-evoked IPSPs in VPCs have relatively long onset latencies indicating polysynaptic transmission (12.6 ± 0.8 ms, chapter 2). In contrast, MCs usually show shorter latencies responding to the ON inputs (3-10 ms to the first ON-evoked AP in cell-attached configuration and ~6 ms to the ON-evoked IPSCs. De Saint Jan et al., 2009; Najac et al., 2011). This suggests that the origin of ON-evoked IPSPs in VPCs is probably not the same

population of inhibitory interneurons in MCs since their latencies of inhibition show a two-fold difference. Instead, inhibition would rather be relayed through several cells, hence several synapses. Thus, cells stimulated by eTCs or even MCs might be candidates to create longer onset latencies in VPCs. However, ON-evoked APs under ACh wash-in had onset latencies of 8.6 ± 0.7 ms (chapter 3) which is similar to the latency of ON-evoked APs in MCs (De Saint Jan et al., 2009) indicating that they might share excitatory sources, such as eTCs. eTCs are known as feed-forward excitatory sources for MCs. They mainly receive direct excitatory inputs from the ON (De Saint Jan et al., 2009). Therefore, their APs have a much shorter onset latencies responding to ON stimulation, 3-4 ms (De Saint Jan et al., 2009). Moreover, they activate inhibitory juxtaglomerular cells, e.g., PGCs (Hayar et al., 2004a; Shao et al., 2009; Kiyokage et al., 2010). PGCs are divided into two subtypes depending on their excitatory inputs, namely ON-driven cells that are excited by ON direct inputs and eTC-driven cells that are excited via eTCs. Since ON-driven PGCs have shorter onset latency of ON-evoked EPSCs (1.79-4.08 ms) than eTC-driven PGCs (2.16-8.20 ms, Shao et al., 2009), inhibitory inputs to VPCs might originate from eTC-driven PGCs (Fig. 22). If this would be the case, eTC-driven PGCs would show reduced evoked-EPSP amplitudes with VP wash-in, since evoked-IPSP amplitudes in VPCs decreased with VP application (chapter 2). Although PGCs might be responsible for ON-evoked inhibition in VPCs, this is not sufficient to explain how VPCs show evoked APs under the ACh condition. Bicuculline application blocked GABAergic inhibition and unveiled slow excitatory barrages with onset latencies of 46.1 ± 27.5 ms in VPCs following ON stimulation. However, fast EPSPs, e.g., with similar onset latencies to APs under the ACh condition, were not observed (chapter 2). Thus, it is unlikely that ACh effects to reduce ON-evoked GABAergic inhibition in VPCs are responsible for enabling firing with short latencies as observed (8.6 ± 0.7 ms). These results indicate that excitatory inputs enabling APs in VPCs with ACh are not only disinhibited via GABAergic interneurons under the ACh condition, but rather that they are more excited or less inhibited by the ACh signaling (Fig. 22).

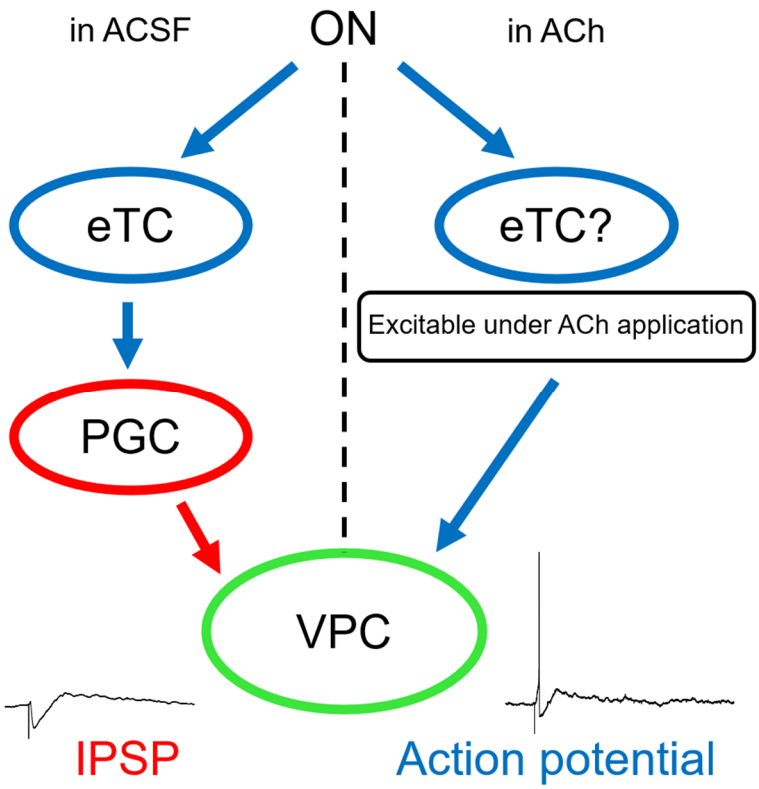

Fig. 22 **Schematic picture of possible inhibitory and excitatory microcircuits around VPCs**
The pathway left to the dotted line represents a possible inhibitory input to VPCs. The ON excites eTCs which in turn excite eTC-driven PGCs. Eventually, those PGCs inhibit VPCs resulting in IPSPs. The pathway right to the dotted line represents a possible excitatory input to VPCs under ACh application. The ON excites excitatory neurons, e.g., eTCs, that are more excitable under ACh administration. Activated excitatory neurons enable VPCs to fire action potentials. Blue arrows represent excitatory neurotransmission and a red arrow represents inhibitory neurotransmission.
ACSF, artificial cerebrospinal fluid; ACh, acetylcholine; ON, olfactory nerve; eTC, external tufted cell; PGC, periglomerular cell; VPC, vasopressin cell; IPSP, inhibitory postsynaptic potential.

4.1.2 Comparison of VPCs with other intrinsic neuromodulatory systems in the OB

4.1.2.1 Intrinsic neuropeptidergic systems

Many different neuropeptides are expressed in the OB including VP. Here, I chose intrinsic neuropeptidergic systems that have been studied at cellular and behavioral levels for comparison.

Cholecystokinin

Tavakoli et al. (2018) analyzed juxtaglomerular cells and categorized them according to their morphology. They suggested that VPCs are “horizontal superficial tufted cells”. However, our morphology analysis showed that VPCs have dissimilar morphological features (chapter 2), e.g., most VPCs (type 1) projected their neurites into inner layers (“vertically”). However, type 2 VPCs that have a single axon crossing the MCL might look morphologically similar to “horizontal superficial tufted cells, although they were found less often than type 1 VPCs (type 1 n=63, type 2 n=10). Type 2 VPCs project neurites laterally in the EPL and the GCL than type 1 VPCs. In terms of physiological properties, “horizontal superficial tufted cells” and VPCs are dissimilar, e.g., time constant; 21 ms vs. ~100 ms, input resistance; 0.33 GΩ vs. ~1 GΩ (horizontal superficial tufted cells vs. VPCs). However, “vertical superficial tufted cells” are rather similar to VPCs, e.g., vertical projections, time constant; 41 ms, input resistance; 0.65 GΩ. “Horizontal superficial tufted cells” could be CCK cells, instead. CCK cells are a subpopulation of superficial tufted cells like VPCs. They both usually innervate one glomerulus with their apical dendrites. However, unlike VPCs, ON-evoked EPSCs and APs are observed in CCK cells (Sun et al., 2020). Furthermore, both “horizontal superficial tufted cells” described in Tavakoli et al. (2018) and CCK cells excite PGCs.

CCK release has both, contradictory and similar effects on synaptic transmission in the OB compared to VP release. VP administration reduces the spontaneous spiking rate in MCs *in-vivo.* CCK application initially increases the spontaneous spiking rate followed by suppression mediated by glutamate and GABA in MCs *in-vitro* indicating that CCK directly excites MCs resulting in activation of GABAergic interneurons (Ma et al., 2013). Similarly, CCK excites selectively SACs, resulting in an increase of spontaneous IPSPs in eTCs, MCs, PGCs, and SACs themselves (Liu and Liu, 2018). In eTCs, ON-evoked EPSC amplitudes are reduced with CCK application via $GABA_B$ receptor activation, indicating that GABA released from SACs upon CCK application binds to $GABA_B$ receptors on the ON to reduce their glutamate release (Liu and Liu, 2018). We also observed inhibitory effects of VP on evoked

EPSPs in eTCs. Since VP receptors are widely expressed in the OB including the GL, inhibitory effects of VP on eTCs could be similar to that of CCK, i.e., via $GABA_B$ receptor activation.

CCK cells are known to project their axons to the IPL on the opposite side of the same OB (Liu and Shipley, 1994). Further, the ultrastructural analysis revealed that they synapse asymmetrically onto GC dendrites. Recently, it was shown that optogenetic activation of CCK cell projections originating from the opposite side of the OB excites GCs, interestingly, via glutamate not CCK (Sun et al., 2020). Paired-pulse optogenetic activation (10 Hz) of CCK cell projections in the IPL facilitates evoked-EPSP amplitudes in GCs, whereas paired-pulse activation of CCK cell dendrites in the EPL leads to depression of evoked-EPSP amplitudes. The authors hypothesized that the opposite effects of IPL and EPL activations might contribute to shifting inhibitory circuits on projection neurons from the EPL/GL to the IPL during sniffing. This shift of inhibitory circuits could make projection neurons more sensitive to ON inputs with less inhibition at the level of the GL. At the same time, enhanced inhibition by GCs may enable better signal processing, e.g., via lateral inhibition (Sun et al., 2020). This theory is indeed interesting since it is similar to our hypothesis that VP contributes to a better discrimination ability via activation of inhibitory interneurons. However, as most VPCs projected their neurites vertically (type 1) rather than horizontally (type 2) in the GCL indicating that most of them are unlikely to project to the opposite side of the same OB (chapter 2), VPC release may play a role mainly on the same side of the OB where they receive the ON inputs. Unfortunately, in our hands, optogenetic stimulation and double patching are not possible to perform yet to adopt their experimental design. However, investigation of VP effects on individual cell types presumably involved in inhibition, e.g., GCs and PGCs, should provide informative results upon understanding neural mechanisms of VP inhibitory effects on MCs (Tobin et al., 2010) and eTCs (chapter 2).

Interestingly, to my knowledge, there are only a few papers addressing CCK actions on olfactory-related behavior. A series of papers using i.p. injections of CCK or CCK-A/B

receptor antagonists demonstrated opposing effects on social recognition in rats (Lemaire et al., 1992; Lemaire et al., 1994). Activation of CCK-A receptor signaling prolongs social recognition, however activation of CCK-B receptor signaling impairs it. In this paper, social recognition was also shown to be influenced by projections from the entorhinal cortex to the hippocampus, as their dissection successfully impairs recognition. More importantly, the prolongation of memory by CCK-B receptor antagonists depends on the entorhinal cortex-hippocampus connection. The authors conclude that since the hippocampus is rich in CCK-B receptors (Köhler et al., 1987) and CCK-like immunoreactivity (Greenwood et al., 1981), CCK-B receptor signaling likely acts directly on the hippocampus. CCK-A receptor signaling, in contrast, seems to act via peripheral circuits. Thus, lesion of the peripheral vagus nerve block prolongation of memory by the CCK-A receptor agonist, whereas a sham operation did not alter effects of the agonist. it is unlikely that CCK acts in the OB to modulate social recognition, although local application of CCK into the OB would be necessary to confirm this hypothesis. Contrary to CCK, VP acts, beside in other brain regions, directly in the OB to establish social memory. This difference implies that the activity of CCK cells is not involved in social memory. CCK has been studied more extensively in different types of behaviors such as depressive-like behaviors or learning. For instance, CCK knockdown in the basolateral amygdala where it is known to be involved in anxiety and depressive-like behavior results in anxiolytic effects in the elevated plus maze test and reduces despair-like behavior in the forced swim test (Del Boca et al., 2012). Anxiety reduces rodent social motivation (File, 1985) and pharmacological behavior analysis suggests either hippocampal or peripheral effects of CCK. Thus, CCK effects on social recognition could be more internal-state dependent rather than directly altering sensory acuity. However, the electrophysiology data shown above and autoradiography (Saito et al., 1980) demonstrated that the OB is also rich in CCK receptors. Therefore, the CCK signaling in the OB might play a role in more general occasions. Accordingly, ON stimulation alone is able to excite bulbar CCK cells but not VPCs which indicates that CCK cell activity is less restricted than VPC activity.

Corticotropin releasing hormone

Corticotropin releasing hormone (CRH) is a neuropeptide generally known to act in the anterior pituitary to release corticotropin. In the axis, CRH is released from cells originating from the paraventricular nucleus of the hypothalamus (Antoni et al., 1983). In addition to hypothalamic CRH cells, a subpopulation of interneurons in the OB EPL is CRH expressing cells (Huang et al., 2013). Most interneurons in the EPL are GABAergic, contrary to VPCs (Tobin et al., 2010; Nagayama et al., 2014). They receive excitatory inputs from MCs, in return CRH neurons inhibit MCs with GABA (Huang et al., 2013). Further, *in-vivo* electrophysiology revealed that optogenetic activation of CRH neurons reduces spontaneous MC firing rates and MC responses to odor presentation in mice (Huang et al., 2013). Besides GABAergic neurotransmission, the CRH signaling is also suggested. First and most importantly, CRH cells are able to release CRH since their optogenetic activation increases the CRH concentration in the OB. CRH receptors (CRHR) are expressed dominantly in GCs, especially in adult-born GCs. The ratio of adult-born GCs that express CRHRs increases between 14 days (~35 %) and 28 days (~81 %). Moreover, CRH cells connect monosynaptically with adult-born GCs (Garcia et al., 2014). Those results indicate that the CRH signaling might be important for the development of adult-born GCs. Indeed, both, CRH KO and CRHR KO mouse lines have less adult-born GCs. Synaptic protein expression (e.g., synapsin) in the OB is reduced in those KO lines as well. In addition, transgenic constitutive activation of CRHRs elevates expression levels of the MC-specific GABA-Aα1 receptor, whereas it decreases expression levels of the AMPA receptor in the OB (Garcia et al., 2014). In line with these results, the frequency of miniature IPSCs in MCs is increased, however the amplitudes of miniature EPSCs in GCs are decreased in transgenic mice with constitutively activated CRHRs (Garcia et al., 2014). Therefore, CRH is likely involved in neuromodulation of MC-adult born GC synapses. As a behavioral output, the simple odor habituation-dishabituation task demonstrated that odor recognition is impaired in CRHR KO mice (Garcia et al., 2016). Although signaling pathways are different between CRHR and V1 receptors,

both receptors are G-protein coupled receptors (Birnbaumer, 2002; Grammatopoulos, 2012) that are known to modulate gene expression. Thus, VP effects on social discrimination could be mediated by neuromodulation of adult-born GCs.

Indeed, adult-born cells in the OB are suggested to play a role in social memory. Accordingly, Guarnieri et al. (2020) showed a possible involvement of bulbar neurogenesis in social memory in socially isolated mice that were treated with antidepressants. Social isolation impairs social memory in male mice, however a chronic treatment with an antidepressant rescues it. Moreover, decreased neurogenesis by social isolation is rescued in the chronically antidepressant-treated group. Interestingly, the increase of neurogenesis in the socially isolated mouse OB by antidepressant treatments is greater than in the hippocampus, another brain region involved in social memory (Guarnieri et al., 2020). However, since they analyzed only the number of adult-born cells, it is not clear how connections between adult-born cells and projection neurons are modified during social memory. Taken together, neurogenesis and, possibly, synaptic modulation of adult-born GCs might enhance social olfactory processing during social interaction, e.g., a social discrimination task with the VP system.

Somatostatin

Among other neuropeptides, somatostatin (SOM) plays a major role in the hypothalamus. However, SOM expressing cells are found in several other brain regions as well, e.g., the hippocampus and the amygdala (Martel et al., 2012). In the rodent OB, a subpopulation of PGCs in rats and subpopulations of EPL interneurons and GCL interneurons in mice are SOM immunopositive (Gutièrrez‐Mecinas et al., 2005; Lepousez et al., 2010a). Rat SOM cells are not GABAergic. However, like a subpopulation of PGCs, SOM cells receive asymmetric synaptic contacts from the ON. Further, they make asymmetric and symmetric synaptic contacts with dendrites of M/TCs (Gutièrrez‐Mecinas et al., 2005). Since SOM receptors are inhibitory Gi coupled receptors, they could inhibit principal cells more directly

than VP (V1 receptors are excitatory Gq coupled receptors, Birnbaumer, 2002; Martel et al., 2012). To my knowledge, there is no literature describing modulatory effects of the bulbar SOM system in rats. In mice, SOM cells in the GL are seldom found, instead they are in the deep EPL and the GCL and most SOM cells are GABAergic unlike in rats (Lepousez et al., 2010a). They make asymmetric and symmetric synaptic contacts with M/TCs and SOM receptors are expressed in MCs (Lepousez et al., 2010a; Lepousez et al., 2010b). *In-vivo* electrophysiology revealed that the SOM signaling is involved in the generation of gamma oscillations, which is believed to reflect synaptic interactions between M/TCs and GCs (Kay et al., 2009; Lepousez et al., 2010b). Thus, local injection of a SOM receptor agonist enhances gamma power and local injection of an antagonist decreases it (Lepousez et al., 2010b). Intriguingly, SOM effects on gamma power do not appear until 30 min after injection indicating that the SOM signaling is slow. Since social memory is already established with shorter inter-phase intervals (<30 min), this mechanism might be too slow to modulate olfactory processing during social interaction. The go/no-go task using mixtures of two similar odorants (e.g., (+)-carvone and (-)-carvone) was performed to examine SOM effects on behavior. Local injection of a SOM receptor antagonist impairs odor discrimination with similar binary odor mixtures (60/40). However injection of an agonist enables mice to discriminate more similar binary odor mixtures which control mice cannot discriminate (55/45, Lepousez et al., 2010b). Results indicate that SOM enhances odor discrimination with modulation of gamma oscillations. Improved sensory acuity by experiences (reinforcement with water reward in Lepousez et al. (2010b) study) is called perceptual learning. In chapter 3 (publication B), I suggested that VP effects on social discrimination might be involved in perceptual learning as well. If VP enhances olfactory acuity as shown here with SOM, a go/no-go task (e.g., with local injection of a V1 receptor antagonist) would confirm our hypothesis that VP effects on social memory are not restricted in “social” occasions but also in other contexts where animals need better olfactory acuity. As I introduced above, SOM effects in the rat OB are, to my knowledge, not shown yet. If SOM^+ PGCs express VP

receptors and they also contribute to improve olfactory acuity, the prolongation of social memory with VP could be mediated by SOM because of their slow onsets of effects.

4.1.2.2 Other intrinsic neuromodulatory systems

Dopamine

As mentioned in the general introduction, SACs located in the GL express both, GABA and dopamine (DA). Since they innervate several glomeruli (Kiyokage et al., 2010), they are thought to be involved in interglomerular inhibition. SACs receive excitatory inputs from either the ON or eTCs (Kiyokage et al., 2010) and inhibitory inputs from PGCs (Shao et al., 2019). Electrophysiological experiments revealed that both, GABA and DA released from SACs are involved in modulating excitatory bulbar neurons, e.g., eTCs or MCs. GABA released by SACs inhibits MCs and eTCs either directly or indirectly via $GABA_B$ receptors on the ON terminals (Liu et al., 2013; Liu et al., 2016; Vaaga et al., 2017). DA released simultaneously with GABA by SACs excites eTCs following GABAergic inhibition via D1-like receptors with increased hyperpolarization-induced inward-currents, which results in rebound spikes (Liu et al., 2013). DA is also involved in the inhibition of MCs via D2-like receptors on ON terminals (Ennis et al., 2001; Vaaga et al., 2017).

Interestingly, the DA transporter knock-out and D2-like receptor KO mice show olfactory deficits in some cases (Tillerson et al., 2006). In the habituation-dishabituation task, both KO lines successfully reduce investigation time towards the same odor (paprika or cinnamon) across subsequent trials. However, they did not show dishabituation towards the novel odor in the following trial. Moreover, both KO lines show a similar investigation time towards bedding odors from novel mice or own indicating that they cannot discriminate body odors (Tillerson et al., 2006). Results suggest that the DA system is important in odor processing in general, however it does not demonstrate the social-memory specificity like the VP system. Interestingly, the DA system in the OB is modulated by copulation in female mice (Serguera

et al., 2008). The authors found that the number of DA cells in the MOB and the DA level in the OB tissue are elevated 1.5 and 2.5 days after copulation, respectively, and later. The enhanced DA system seems to alter perception of conspecific urine. Accordingly, pregnant mice do not show preference towards the volatile fraction of male urine over of females. However, systemic injection of a D2 receptor antagonist rescues it (Serguera et al., 2008). The authors suggest that the elevated DA system in the OB inhibits the odor signaling resulting in impaired preference towards male urine. Although the bulbar DA system can be modulated in a context-dependent manner, elevation of the DA level starts 2.5 days after copulation. Thus, this modification is likely too slow to be involved in social discrimination since an interphase interval in the paradigm is only 30 min long. However, if VP increases SAC activity, DA may play a role as a filtering system via inhibition of OB neurons along with VP effects.

Nitric oxide

Nitric oxide (NO) synthase positive cells are widespread in bulbar layers, but primarily they are found within populations of inhibitory interneurons, such as PGCs, SACs, and GCs (Kosaka and Kosaka, 2007). NO is released by glutamate via NMDA receptor-mediated Ca^{2+} entry (Dawson and Snyder, 1994). In the OB, NO is released by odor presentation in mice (Lowe et al., 2008) and by noradrenaline via α1 receptors (González-Flores et al., 2007). NO is known to induce LTP (Zhuo et al., 1993). Therefore, NO is suggested to be involved in olfactory memory in ewes stored in the OB via facilitating MC-GC synapses. Thus, it is theorized that NO facilitates glutamate release from MCs which results in more reciprocal inhibition by GCs, leading to better processing of their own lamb odors (see general introduction, Kendrick et al., 1997a). Since social discrimination is often called social olfactory memory, similar mechanisms as for sheep olfactory memory are possible. Furthermore, it was shown that in the hypothalamus and the amygdala, ACh-induced VP

release is mediated by NO (Raber and Bloom, 1994), suggesting similar mechanisms of ACh-induced VP release in the OB as well.

ACh

In chapter 3, I demonstrated and discussed how ACh plays a role in exciting VPCs and enables social discrimination. VPCs were not excitable following ON stimulation alone in acute brain slices *in-vitro*. This result suggests that any neurotransmitter system in the OB which can be activated by ON inputs is not able to excite VPCs (chapter 2+3). Thus, ACh which modulates the VP system, is probably released mainly from projections from the HDB. However, there are subpopulations of interneurons in the OB expressing ACh (Krosnowski et al., 2012). A transgenic mouse line using the ChAT gene revealed subpopulations in all bulbar layers. Interestingly they are not immunoreactive to glutamate, GABA, or DA, but they are partially calbindin immunopositive. Further, after the cut of the olfactory peduncle to eliminate centrifugal projections, they found vesicular ACh transporter-immunoreactivity, which confirms that an intrinsic bulbar ACh system must exist. However, to my knowledge, there is no literature describing a functional role for the intrinsic ACh system in the MOB, yet. If ACh cells express AChRs or VP receptors, they might have enhancing effects on VPC activity via extra ACh release in the OB.

4.2 Possible mechanisms of VP effects enabling social discrimination

In chapter 3, social discrimination and olfactory perceptual learning were compared for their difficulties in discriminating stimuli used in both paradigms. Body odor mixtures in individuals are suggested to be not distinguishable by qualities, e.g., combinations of odorants, but by quantities of certain odor components (Singer et al., 1997). Odor pairs used in perceptual learning are not distinguishable for control animals, e.g., (+)-limonene and (-)-limonene (Mandairon et al., 2006b). Thus, the similarity of those paradigms is that animals improve their olfactory acuity by experiences of those stimuli, i.e., social interaction during the

sampling phase or previous experiences or learning with odors. Therefore, animals can successfully discriminate stimuli. Moreover, both paradigms are associated with the ACh signaling in the OB (chapter 3, Wilson et al., 2004). Taken together, it is suggested that ACh-induced VP effects may be involved not only in social discrimination but also in olfactory perceptual learning. To improve olfactory acuity, I hypothesized that bulbar VP enhances the signal-noise ratio in principal neuron activity. In line with this hypothesis, VP reduces firing rates in MCs (Tobin et al., 2010) and decreased the amplitudes of ON-evoked EPSPs in eTCs (chapter 2) indicating enhanced inhibition on them. Therefore, I suggest that only the most potent olfactory inputs can reach higher brain regions, hence a better odor representation can be expected there. Since other brain regions, e.g., the lateral septum, the medial amygdala, and the hippocampus, are involved in social memory (Bielsky et al., 2005; Lukas et al., 2013; Raam et al., 2017), memory might be stored and processed there. However, not higher brain regions but the AOB stores pheromonal memory in the context of the Bruce effect. Accordingly, Kaba et al. (1989) used local anesthesia with lidocaine following mating in the AOB or in the medial amygdala which is an output target of the AOB to examine the location of memory. Although lidocaine injection into the medial amygdala does not alter percentages of pregnancy block from control, lidocaine injection into the AOB results in high pregnancy block rates even in mice that were exposed to their stud males (Kaba et al., 1989). Results indicate that pheromonal memory is established in the AOB but not in the medial amygdala. This memory formation in the early olfactory brain regions is hypothesized to be mediated by LTP induction in MC-GC synapses. Therefore, MCs that are activated during mating receive enhanced inhibition (Kaba, 2010). Indeed *in-vivo* electrophysiology confirmed the hypothesis. Local field potentials in the MCL demonstrated that power in the 8-12 Hz band in response to stud male bedding is greater than that in response to novel male bedding indicating enhanced interactions between MCs and GCs. Moreover, single-unit recordings from the medial amygdala showed that the stud-male bedding exposure evokes a smaller number of spikes compared to the novel-male bedding

exposure (Binns and Brennan, 2005). Taken together, synaptic modulation on MC-GC synapses during mating results in different responses depending on stimuli already at the level of the AOB. Since social memory in rats lasts for a very short time of period (<120 min, Dluzen et al., 1998a) compared to the Bruce effect (at least for 30 days, Kaba et al., 1988), I suggest that it might be too short lasting to be mediated by LTP. Thus, an improvement of the signal-noise ratio by neuromodulation via the VP signaling is a more likely mechanism. However, local injection of VP into the OB prolongs social memory to at least 120 min (Dluzen et al., 1998a). In this case, it is hard to believe that VP still acts on OB neurons such as interneurons after such a long interval. Thus, I would tend to speculate that exogenous VP enhances connectivity between projection neurons and interneurons, e.g., via LTP, to elongate social discrimination ability. Intriguingly, a “sister neuropeptide” of VP, oxytocin induces LTP in MC-GC synapses by subthreshold retrograde stimulation of MCs in the mouse AOB (Fang et al., 2008). Since oxytocin receptors and V1 receptors are both Gq coupled receptors (Birnbaumer, 2002; Zingg and Laporte, 2003), the VP signaling might also be able to induce LTP in synapses between projection neurons and interneurons. Obviously, the VP dose used in that publication (Dluzen et al., 1998a) is likely to be higher than the physiological level as the control group was not able to discriminate between known and novel rats after 120 min intervals. Thus, I suggest that such hypothetical synaptic facilitation by VP must be weaker under physiological conditions. However, the weak synaptic facilitation could help to enhance inhibition specifically onto activated projection neurons since LTP is activity dependent.

4.3 Ethological advantages of the intrinsic bulbar VP system and centrifugal modulation

The following paragraph is based on knowledge obtained from “The Rat. A Study in Behavior” (Barnett, 1976). Wild rats live in any type of environment such as burrows, sewers, or basements of buildings. They seem to have rather stable groups so that only a few new rats

can be found between two-time population examinations in a mark-recapture study. In line with this finding, intruders are often found dead after a certain time in experimental conditions indicating that resident rats try to get rid of outsiders to maintain their own group. Thus, they have strict territories and when outsiders come in there, residents recognize them to either get rid of them or even kill them. To achieve this specificity against outsiders, they must discriminate between their territory mates and outsiders. This is presumably driven by olfactory cues, as the author described in the book "…they also sniff other rats, especially strangers and potential mates". This expression further implies that before showing aggression, rats discriminate individual odor signatures. In addition, removal of the OB indeed suppresses intermale aggression in laboratory rats (Bandler Jr and Chi, 1972). It could be that bulbectomized rats cannot get olfactory inputs from an intruder, hence those rats cannot recognize an intruder as a novel outsider. The results indicate that olfactory perception is important to show aggression. As far as I recognize, unlike mice (Novotny et al., 1985; Chamero et al., 2007; Hattori et al., 2016), there is no pheromone identified that directly induces intermale aggression in rats. This difference could be due to inbreeding of mouse strains which could emphasize pheromonal effects rather than differences in individual odor signatures. Indeed, males from an inbred mouse strain, i.e., Balb/c, do not show counter marking to unfamiliar male urine from the same strain, indicating that they cannot discriminate urine odors from themselves and others as long as they are the same strain (Nevison et al., 2000). Since most rat lines are outbred, individual body odors are likely to be varied, hence distinguishable even though from the same strain. In any cases, thus individual discrimination, hence aggression in male rats is likely to be mediated by more complex cognition rather than stimulated by only specific odorants, e.g., pheromones.
This hypothesis on complex cognition is supported by the importance of the lateral septum (LS) in social discrimination. The LS is believed to play a role as a sensory integrator conveying integrated information to brain regions responsible for initiating behavior, e.g., the hypothalamus (Sheehan et al., 2004). Accordingly, similar results were shown with

manipulation of the LS system compared to the OB in social discrimination. Blockade of the VP system in the LS disrupts social recognition/discrimination and exogenous VP local injection into the LS prolongs it (Dantzer et al., 1988; Terranova et al., 1994; Landgraf et al., 1995). These results suggest that even though olfactory processing is intact, rats need also other brain regions to discriminate individuals. Interestingly, the VP system in the LS is responsible for mediating aggression as well (Veenema et al., 2010; de Moura Oliveira et al., 2020). As mentioned above, wild rats tend to attack or even kill intruders (novel adults), however young male intruders are not attacked by residents (Barnett, 1976). This is a reason why researchers usually use juvenile rats as stimulus rats in social discrimination/recognition experiments to reduce aggression by subject rats during experiments. This further indicates that contexts of both individual discrimination and aggression are similar. Thus, VP effects in the LS on social discrimination and aggression might share similar neural circuits. Since VP is a neuropeptide highly conserved across vertebrates and invertebrates and is responsible for social behaviors in different species such as aggression or sexual behavior (Donaldson and Young, 2008), it could be that roles of VP are originally related to social contexts. Thus, it is rational that VP systems in the OB and the LS show similar effects on social discrimination from the evolutionary point of view. However, as discussed in chapter 3, the bulbar VP system helping identification of individual odor signatures could be extended to difficult non-social odor discrimination, e.g., olfactory perceptual learning. This hypothesis raises possible advantages of having the intrinsic bulbar VP system. Thus, whenever rats need to discriminate odors that are complex or too similar to others, VP can enhance olfactory acuity in an independent manner from VP systems in other brain regions, such as the LS. Interestingly, several brain regions connected with the LS also have intrinsic VP systems e.g., the medial amygdala and the bed nucleus of the stria terminalis (van Leeuwen and Caffé, 1983; Sheehan et al., 2004). Notably, the medial amygdala and the bed nucleus of the stria terminalis are involved in other social behavior, e.g., aggression, sexual behavior, or maternal behavior (Okabe et al., 2013; Hattori et al., 2016; Ishii et al., 2017). Therefore,

these local VP systems including the bulbar system might contribute to their independency, e.g., compared to the oxytocin system. Hence, VP systems can locally and independently modulate neurotransmission in different contexts.

Furthermore, bulbar VPCs need not only olfactory inputs but also centrifugal ACh modulation to be activated (chapter 3). I suggest that this is because the bulbar VP system is not always required, since most of the odors are easy to recognize, e.g., food, predators, or toxic chemicals. Thus, VPCs can be inactivated when VP is not required where arousal or attention in rats is not enough to activate top-down modulation to the OB (see discussion in chapter 3). Olfactory perceptual learning, which shows that olfactory acuity on experienced odors is improved, is mediated by centrifugal neuromodulators as well. It was shown that both, ACh and NA are involved in this type of odor discrimination (Fletcher and Wilson, 2002; Veyrac et al., 2009; Vinera et al., 2015). It is generally hypothesized that perceptual learning requires attention. Since perceptual learning can be found in different sensory modalities as well (Gilbert et al., 2001; Sale et al., 2011; Pacchiarini et al., 2017), it is logical that attention and arousal that are rather sensory-type unspecific internal states act as central mediators to enhance perceptual acuity in different sensations. Therefore, taking into account the results in chapter 3, I suggest that only when contexts (e.g., social interactions) that change internal states (e.g., attention or arousal) meet sensation (e.g., olfactory inputs), the local system that enhances sensory acuity (e.g., the bulbar VP system or synaptic plasticity) gets activated. Other examples of this context-sensation coupled mechanisms on enhancing sensory acuity are known. The female mouse auditory cortex becomes tuned to pup ultrasonic vocalizations when they are paired with oxytocin which would be a contextual factor (i.e., being a mother) in this case (Marlin et al., 2015). Olfactory perceptual learning using aversive conditioning also shows this relationship as the aversive conditioning is a context generating arousal (Critchley et al., 2002; Fletcher and Wilson, 2002).

Taken together, I suggest that the intrinsic bulbar VP system modulated by the cholinergic signaling is involved in improving olfactory acuity. Furthermore, the VP local distribution and centrifugal modulation of the VP system reflecting internal states may contribute to enhancing specificity in certain contexts where rats need to discriminate complex odors such as during a social discrimination task (Fig. 23).

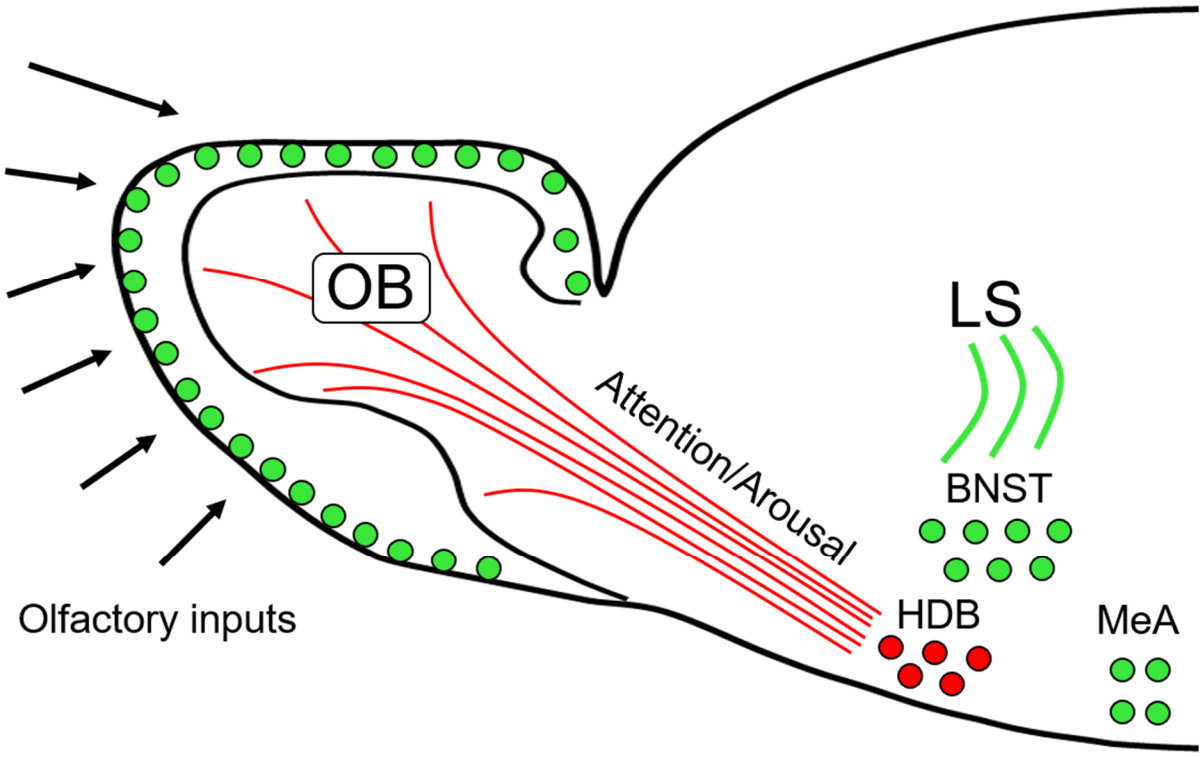

Fig. 23 **Graphic scheme of local VP systems and centrifugal cholinergic innervations to bulbar VP system**
Local vasopressin systems are distributed in social behavior-related brain regions, e.g., the OB, the LS, the BNST, or the MeA. Green dots and lines represent vasopressin expressing cells and their projections. The bulbar VP system is locally activated by olfactory inputs and centrifugal cholinergic innervations conveying internal states, e.g., attention or arousal. Red dots and lines represent cholinergic cells and their projections to the OB.
OB, olfactory bulb; HDB, horizontal limb of the diagonal band of Broca; LS, lateral septum; BNST, bed nucleus of the stria terminalis; MeA, medial amygdala.

5: Abbreviations

5-HT	Serotonin
ACh	Acetylcholine
AChR	Acetylcholine receptor
ACSF	Artificial cerebrospinal fluid
AHP	After hyperpolarization
AOB	Accessory olfactory bulb
AON	Anterior olfactory nucleus
AP	Action potential
Approx.	Approximately
Atr	Atropine
CCK	Cholecystokinin
ChAT	Choline acetyltransferase
CRH	Corticotropin releasing hormone
CRHR	Corticotropin releasing hormone receptor
CV	Coefficient of variance
DA	Dopamine
DAB	3,3'-diaminobenzidine
e.g.	For example (exempli gratia)
eFP	Evoked field potential
eGFP	Enhanced green fluorescent protein
EPL	External plexiform layer
EPSC	Excitatory postsynaptic current
EPSP	Excitatory postsynaptic potential
eTC	External tufted cell

Fig.	Figure
FWHM	Full width at half maximum
G in bulbar anatomy	Glomerulus
GABA	Gamma-aminobutyric acid
GC	Granule cell
GCL	Granule cell layer
GL	Glomerular layer
HDB	Horizontal limb of the diagonal band of Broca
i.e.	That is (id est)
i.p.	Intraperitoneal
I_h	Hyperpolarization activated current
IPL	Internal plexiform layer
IPSC	Inhibitory postsynaptic current
IPSP	Inhibitory postsynaptic potential
ISI	Inter spike interval
KO	Knock out
LS	Lateral septum
LTP	Long term potentiation
M/TC	Mitral and tufted cell
m1AChR	M1 muscarinic acetylcholine receptor
m2AChR	M2 muscarinic acetylcholine receptor
mAChR	Muscarinic acetylcholine receptor
MC	Mitral cell
MCL	Mitral cell layer
MeA	Medial amygdala
Meca	Mecamylamine

MHC	Major histocompatibility complex
MOB	Main olfactory bulb
mTC	Middle tufted cell
n	Number
N.S.	Not significant
NA	Noradrenaline
nAChR	Nicotinic acetylcholine receptor
NO	Nitric oxide
OB	Olfactory bulb
ON	Olfactory nerve
ONL	Olfactory nerve layer
PB	Phosphate buffer
PBS	Phosphate buffer-saline
PBST	Phosphate buffer-saline-Triton X
pERK	Phosphorylated extracellular signal-regulated kinase
PFA	Paraformaldehyde
PGC	Periglomerular cell
PSP	Postsynaptic potential
Ri	Input resistance
ROI	Region of interest
RT	Room temperature
s.c.	Subcutaneous
SAC	Short axon cell
sAP	Single action potential
SEM	Standard error of mean
SOM	Somatostatin

sTC	Superficial tufted cell
TC	Tufted cell
Veh	Vehicle
VGCC	Voltage-gated Ca^{2+} channel
Vm	Membrane potential
VP	Vasopressin
VPC	Vasopressin expressing cell
τ_m	Membrane time constant

6: References

Abraham, N.M., Egger, V., Shimshek, D.R., Renden, R., Fukunaga, I., Sprengel, R., et al. (2010). Synaptic Inhibition in the Olfactory Bulb Accelerates Odor Discrimination in Mice. *Neuron* 65(3), 399-411. doi: https://doi.org/10.1016/j.neuron.2010.01.009.

Acquas, E., Wilson, C., and Fibiger, H.C. (1996). Conditioned and unconditioned stimuli increase frontal cortical and hippocampal acetylcholine release: Effects of novelty, habituation, and fear. *Journal of Neuroscience* 16(9), 3089-3096. doi: 10.1523/JNEUROSCI.16-09-03089.1996.

Anagnostaras, S.G., Murphy, G.G., Hamilton, S.E., Mitchell, S.L., Rahnama, N.P., Nathanson, N.M., et al. (2003). Selective cognitive dysfunction in acetylcholine M-1 muscarinic receptor mutant mice. *Nature Neuroscience* 6(1), 51-58. doi: 10.1038/nn992.

Antal, M., Eyre, M., Finklea, B., and Nusser, Z. (2006). External tufted cells in the main olfactory bulb form two distinct subpopulations. *European Journal of Neuroscience* 24(4), 1124-1136.

Antoni, F.A., Palkovits, M., Makara, G.B., Linton, E.A., Lowry, P.J., and Kiss, J.Z. (1983). Immunoreactive Corticotropin-Releasing Hormone in the Hypothalamoinfundibular Tract. *Neuroendocrinology* 36(6), 415-423. doi: 10.1159/000123492.

Aroniadou-Anderjaska, V., Ennis, M., and Shipley, M.T. (1999). Dendrodendritic recurrent excitation in mitral cells of the rat olfactory bulb. *Journal of Neurophysiology* 82(1), 489-494.

Asaba, A., Hattori, T., Mogi, K., and Kikusui, T. (2014a). Sexual attractiveness of male chemicals and vocalizations in mice. *Front Neurosci* 8, 231. doi: 10.3389/fnins.2014.00231.

Asaba, A., Okabe, S., Nagasawa, M., Kato, M., Koshida, N., Osakada, T., et al. (2014b). Developmental social environment imprints female preference for male song in mice. *PloS one* 9(2), e87186.

Asaba, A., Osakada, T., Touhara, K., Kato, M., Mogi, K., and Kikusui, T. (2017). Male mice ultrasonic vocalizations enhance female sexual approach and hypothalamic kisspeptin neuron activity. *Hormones and Behavior* 94, 53-60.

Aungst, J., Heyward, P., Puche, A., Karnup, S., Hayar, A., Szabo, G., et al. (2003). Centre–surround inhibition among olfactory bulb glomeruli. *Nature* 426(6967), 623-629.

Bader, A., Klein, B., Breer, H., and Strotmann, J. (2012). Connectivity from OR37 expressing olfactory sensory neurons to distinct cell types in the hypothalamus. *Frontiers in Neural Circuits* 6(84). doi: 10.3389/fncir.2012.00084.

Baez, S., García, A.M., and Ibanez, A. (2017). "The Social Context Network Model in Psychiatric and Neurological Diseases," in *Social Behavior from Rodents to Humans: Neural Foundations and Clinical Implications,* eds. M. Wöhr & S. Krach. (Cham: Springer International Publishing), 379-396.

Bains, J.S., and Ferguson, A.V. (1999). Activation of N-methyl-d-aspartate receptors evokes calcium spikes in the dendrites of rat hypothalamic paraventricular nucleus neurons. *Neuroscience* 90(3), 885-891. doi: https://doi.org/10.1016/S0306-4522(98)00525-9.

Baldwin, B., and Shillito, E.E. (1974). The effects of ablation of the olfactory bulbs on parturition and maternal behaviour in Soay sheep. *Animal Behaviour* 22(1), 220-223. doi: 10.1016/S0003-3472(74)80072-2.

Bandler Jr, R.J., and Chi, C.C. (1972). Effects of olfactory bulb removal on aggression: A reevaluation. *Physiology & Behavior* 8(2), 207-211.

Barnett, S.A. (1976). *The rat: A study in behavior.* Transaction Publishers.
Baum, M.J., and Kelliher, K.R. (2009). Complementary Roles of the Main and Accessory Olfactory Systems in Mammalian Mate Recognition. *Annual Review of Physiology* 71(1), 141-160. doi: 10.1146/annurev.physiol.010908.163137.
Beach, F.A., and Jaynes, J. (1956). Studies of Maternal Retrieving in Rats. Iii. Sensory Cues Involved in the Lactating Female's Response To Her Young 1. *Behaviour* 10(1), 104-124.
Ben-Barak, Y., Russell, J., Whitnall, M., Ozato, K., and Gainer, H. (1985). Neurophysin in the hypothalamo-neurohypophysial system. I. Production and characterization of monoclonal antibodies. *The Journal of Neuroscience* 5(1), 81-97. doi: 10.1523/jneurosci.05-01-00081.1985.
Bendahmane, M., Ogg, M.C., Ennis, M., and Fletcher, M.L. (2016). Increased olfactory bulb acetylcholine bi-directionally modulates glomerular odor sensitivity. *Scientific reports* 6, 25808. doi: 10.1038/srep25808.
Bielsky, I.F., Hu, S.-B., Ren, X., Terwilliger, E.F., and Young, L.J. (2005). The V1a vasopressin receptor is necessary and sufficient for normal social recognition: a gene replacement study. *Neuron* 47(4), 503-513.
Bielsky, I.F., Hu, S.-B., Szegda, K.L., Westphal, H., and Young, L.J. (2004). Profound Impairment in Social Recognition and Reduction in Anxiety-Like Behavior in Vasopressin V1a Receptor Knockout Mice. *Neuropsychopharmacology* 29(3), 483-493. doi: 10.1038/sj.npp.1300360.
Binns, K.E., and Brennan, P.A. (2005). Changes in electrophysiological activity in the accessory olfactory bulb and medial amygdala associated with mate recognition in mice. *Eur J Neurosci* 21(9), 2529-2537. doi: 10.1111/j.1460-9568.2005.04090.x.
Birnbaumer, M. (2002). "58 - Vasopressin Receptors," in *Hormones, Brain and Behavior,* eds. D.W. Pfaff, A.P. Arnold, S.E. Fahrbach, A.M. Etgen & R.T. Rubin. (San Diego: Academic Press), 803-810.
Bluthe, R.M., and Dantzer, R. (1993). Role of the Vomeronasal System in Vasopressinergic Modulation of Social Recognition in Rats. *Brain Research* 604(1-2), 205-210. doi: 10.1016/0006-8993(93)90370-3.
Bobrov, E., Wolfe, J., Rao, R.P., and Brecht, M. (2014). The Representation of Social Facial Touch in Rat Barrel Cortex. *Current Biology* 24(1), 109-115. doi: 10.1016/j.cub.2013.11.049.
Bohm, E., Brunert, D., and Rothermel, M. (2020). Input dependent modulation of olfactory bulb activity by HDB GABAergic projections. *Scientific Reports* 10(1), 1-15. doi: 10.1038/s41598-020-67276-z.
Bosch, O.J. (2013). Maternal aggression in rodents: brain oxytocin and vasopressin mediate pup defence. *Philosophical Transactions of the Royal Society B: Biological Sciences* 368(1631), 20130085. doi: doi:10.1098/rstb.2013.0085.
Brennan, P., Kendrick, K., and Keverne, E. (1995). Neurotransmitter release in the accessory olfactory bulb during and after the formation of an olfactory memory in mice. *Neuroscience* 69(4), 1075-1086.
Brennan, P.A., and Kendrick, K.M. (2006). Mammalian social odours: attraction and individual recognition. *Philos Trans R Soc Lond B Biol Sci* 361(1476), 2061-2078. doi: 10.1098/rstb.2006.1931.
Brill, J., Shao, Z., Puche, A.C., Wachowiak, M., and Shipley, M.T. (2016). Serotonin increases synaptic activity in olfactory bulb glomeruli. *Journal of neurophysiology* 115(3), 1208-1219.
Bruce, H.M. (1959). An exteroceptive block to pregnancy in the mouse. *Nature* 184(4680), 105-105.
Bugbee, N.M., and Eichelman Jr, B.S. (1972). Sensory alterations and aggressive behavior in the rat. *Physiology & Behavior* 8(6), 981-985.

Buijs, R., De Vries, G., Van Leeuwen, F., and Swaab, D. (1983). "Vasopressin and oxytocin: distribution and putative functions in the brain," in *Progress in brain research*. Elsevier), 115-122.

Burton, S.D., and Urban, N.N. (2014). Greater excitability and firing irregularity of tufted cells underlies distinct afferent-evoked activity of olfactory bulb mitral and tufted cells. *J Physiol* 592(10), 2097-2118. doi: 10.1113/jphysiol.2013.269886.

Butt, A.E., Chavez, C.M., Flesher, M.M., Kinney-Hurd, B.L., Araujo, G.C., Miasnikov, A.A., et al. (2009). Association learning-dependent increases in acetylcholine release in the rat auditory cortex during auditory classical conditioning. *Neurobiology of Learning and Memory* 92(3), 400-409. doi: 10.1016/j.nlm.2009.05.006.

Butt, A.E., Testylier, G., and Dykes, R.W. (1997). Acetylcholine release in rat frontal and somatosensory cortex is enhanced during tactile discrimination learning. *Psychobiology* 25(1), 18-33. doi: 10.3758/BF03327024.

Bywalez, W.G., Ona-Jodar, T., Lukas, M., Ninkovic, J., and Egger, V. (2016). Dendritic Arborization Patterns of Small Juxtaglomerular Cell Subtypes within the Rodent Olfactory Bulb. *Front Neuroanat* 10, 127. doi: 10.3389/fnana.2016.00127.

Camats Perna, J., and Engelmann, M. (2017). "Recognizing Others: Rodent's Social Memories," in *Social Behavior from Rodents to Humans: Neural Foundations and Clinical Implications,* eds. M. Wöhr & S. Krach. (Cham: Springer International Publishing), 25-45.

Cardona, A., Saalfeld, S., Schindelin, J., Arganda-Carreras, I., Preibisch, S., Longair, M., et al. (2012). TrakEM2 Software for Neural Circuit Reconstruction. *PLOS ONE* 7(6), e38011. doi: 10.1371/journal.pone.0038011.

Carlson, G.C., Shipley, M.T., and Keller, A. (2000). Long-Lasting Depolarizations in Mitral Cells of the Rat Olfactory Bulb. *The Journal of Neuroscience* 20(5), 2011-2021. doi: 10.1523/jneurosci.20-05-02011.2000.

Castillo, P.E., Carleton, A., Vincent, J.-D., and Lledo, P.-M. (1999). Multiple and opposing roles of cholinergic transmission in the main olfactory bulb. *Journal of Neuroscience* 19(21), 9180-9191.

Cavalcante, L.E.S., Zinn, C.G., Schmidt, S.D., Saenger, B.F., Ferreira, F.F., Furini, C.R.G., et al. (2017). Modulation of the storage of social recognition memory by neurotransmitter systems in the insular cortex. *Behavioural Brain Research* 334, 129-134. doi: https://doi.org/10.1016/j.bbr.2017.07.044.

Chamero, P., Marton, T.F., Logan, D.W., Flanagan, K., Cruz, J.R., Saghatelian, A., et al. (2007). Identification of protein pheromones that promote aggressive behaviour. *Nature* 450(7171), 899-902. doi: 10.1038/nature05997.

Chatterjee, M., Perez de Los Cobos Pallares, F., Loebel, A., Lukas, M., and Egger, V. (2016). Sniff-Like Patterned Input Results in Long-Term Plasticity at the Rat Olfactory Bulb Mitral and Tufted Cell to Granule Cell Synapse. *Neural Plast* 2016, 9124986. doi: 10.1155/2016/9124986.

Chaudhury, D., Escanilla, O., and Linster, C. (2009). Bulbar acetylcholine enhances neural and perceptual odor discrimination. *J Neurosci* 29(1), 52-60. doi: 10.1523/JNEUROSCI.4036-08.2009.

Chaves-Coira, I., Rodrigo-Angulo, M.L., and Nunez, A. (2018). Bilateral Pathways from the Basal Forebrain to Sensory Cortices May Contribute to Synchronous Sensory Processing. *Frontiers in Neuroanatomy* 12, 5. doi: 10.3389/fnana.2018.00005.

Chen, W.R., Shen, G.Y., Shepherd, G.M., Hines, M.L., and Midtgaard, J. (2002). Multiple Modes of Action Potential Initiation and Propagation in Mitral Cell Primary Dendrite. *Journal of Neurophysiology* 88(5), 2755-2764. doi: 10.1152/jn.00057.2002.

Cilz, N.I., Cymerblit-Sabba, A., and Young, W.S. (2019). Oxytocin and vasopressin in the rodent hippocampus. *Genes, Brain and Behavior* 18(1), e12535. doi: https://doi.org/10.1111/gbb.12535.

Cleland, T.A., and Sethupathy, P. (2006). Non-topographical contrast enhancement in the olfactory bulb. *Bmc Neuroscience* 7(1), 1-18. doi: 10.1186/1471-2202-7-7.

Crespo, C., Blasco‐Ibáñez, J.M., Briñón, J.G., Alonso, J.R., Domínguez, M.I., and Martínez‐Guijarro, F.J. (2000). Subcellular localization of m2 muscarinic receptors in GABAergic interneurons of the olfactory bulb. *European Journal of Neuroscience* 12(11), 3963-3974.

Critchley, H.D., Mathias, C.J., and Dolan, R.J. (2002). Fear Conditioning in Humans: The Influence of Awareness and Autonomic Arousal on Functional Neuroanatomy. *Neuron* 33(4), 653-663. doi: https://doi.org/10.1016/S0896-6273(02)00588-3.

Curtis, J.T., Liu, Y., and Wang, Z. (2001). Lesions of the vomeronasal organ disrupt mating-induced pair bonding in female prairie voles (Microtus ochrogaster). *Brain research* 901(1-2), 167-174.

D'Souza, R.D., and Vijayaraghavan, S. (2012). Nicotinic receptor-mediated filtering of mitral cell responses to olfactory nerve inputs involves the α3β4 subtype. *Journal of Neuroscience* 32(9), 3261-3266.

Dantzer, R., Koob, G.F., Bluthe, R.M., and Lemoal, M. (1988). Septal Vasopressin Modulates Social Memory in Male-Rats. *Brain Research* 457(1), 143-147. doi: Doi 10.1016/0006-8993(88)90066-2.

Dantzer, R., Tazi, A., and Bluthe, R.M. (1990). Cerebral Lateralization of Olfactory-Mediated Affective Processes in Rats. *Behavioural Brain Research* 40(1), 53-60. doi: Doi 10.1016/0166-4328(90)90042-D.

Dawson, T., and Snyder, S. (1994). Gases as biological messengers: nitric oxide and carbon monoxide in the brain. *The Journal of Neuroscience* 14(9), 5147-5159. doi: 10.1523/jneurosci.14-09-05147.1994.

De Kock, C.P.J., Burnashev, N., Lodder, J.C., Mansvelder, H.D., and Brussaard, A.B. (2004). NMDA receptors induce somatodendritic secretion in hypothalamic neurones of lactating female rats. *The Journal of Physiology* 561(1), 53-64. doi: https://doi.org/10.1113/jphysiol.2004.069005.

de la Zerda, S.H., Netser, S., Magalnik, H., Briller, M., Marzan, D., Glatt, S., et al. (2020). Social recognition in rats and mice requires integration of olfactory, somatosensory and auditory cues. *bioRxiv*. doi: 10.1101/2020.05.05.078139.

de Moura Oliveira, V.E., Lukas, M., Wolf, H.N., Durante, E., Lorenz, A., Mayer, A.-L., et al. (2020). Concerted but segregated actions of oxytocin and vasopressin within the ventral and dorsal lateral septum determine female aggression. *bioRxiv*, 2020.2007.2028.224873. doi: 10.1101/2020.07.28.224873.

De Saint Jan, D., Hirnet, D., Westbrook, G.L., and Charpak, S. (2009). External tufted cells drive the output of olfactory bulb glomeruli. *Journal of Neuroscience* 29(7), 2043-2052.

de Vries, G.J., and Buijs, R.M. (1983). The origin of the vasopressinergic and oxytocinergic innervation of the rat brain with special reference to the lateral septum. *Brain Research* 273(2), 307-317. doi: https://doi.org/10.1016/0006-8993(83)90855-7.

Debarbieux, F., Audinat, E., and Charpak, S. (2003). Action Potential Propagation in Dendrites of Rat Mitral Cells In Vivo. *The Journal of Neuroscience* 23(13), 5553-5560. doi: 10.1523/jneurosci.23-13-05553.2003.

Del Boca, C., Lutz, P.E., Le Merrer, J., Koebel, P., and Kieffer, B.L. (2012). Cholecystokinin knock-down in the basolateral amygdala has anxiolytic and antidepressant-like effects in mice. *Neuroscience* 218, 185-195. doi: https://doi.org/10.1016/j.neuroscience.2012.05.022.

del Toro, E.D., Juiz, J.M., Peng, X., Lindstrom, J., and Criado, M. (1994). Immunocytochemical localization of the α7 subunit of the nicotinic acetylcholine receptor in the rat central nervous system. *Journal of comparative Neurology* 349(3), 325-342.

Devries, G.J., Buijs, R.M., Vanleeuwen, F.W., Caffe, A.R., and Swaab, D.F. (1985). The Vasopressinergic Innervation of the Brain in Normal and Castrated Rats. *Journal of Comparative Neurology* 233(2), 236-254. doi: DOI 10.1002/cne.902330206.

Dizinno, G., and Whitney, G. (1977). Androgen Influence on Male Mouse Ultrasounds during Courtship. *Hormones and Behavior* 8(2), 188-192. doi: Doi 10.1016/0018-506x(77)90035-6.

Dluzen, D.E., Muraoka, S., Engelmann, M., and Landgraf, R. (1998a). The effects of infusion of arginine vasopressin, oxytocin, or their antagonists into the olfactory bulb upon social recognition responses in male rats. *Peptides* 19(6), 999-1005. doi: 10.1016/S0196-9781(98)00047-3.

Dluzen, D.E., Muraoka, S., and Landgraf, R. (1998b). Olfactory bulb norepinephrine depletion abolishes vasopressin and oxytocin preservation of social recognition responses in rats. *Neuroscience Letters* 254(3), 161-164. doi: 10.1016/S0304-3940(98)00691-0.

Donaldson, Z.R., and Young, L.J. (2008). Oxytocin, Vasopressin, and the Neurogenetics of Sociality. *Science* 322(5903), 900-904. doi: 10.1126/science.1158668.

Dulac, C., O'Connell, L.A., and Wu, Z. (2014). Neural control of maternal and paternal behaviors. *Science* 345(6198), 765-770.

Egger, V., Nevian, T., and Bruno, R.M. (2007). Subcolumnar Dendritic and Axonal Organization of Spiny Stellate and Star Pyramid Neurons within a Barrel in Rat Somatosensory Cortex. *Cerebral Cortex* 18(4), 876-889. doi: 10.1093/cercor/bhm126.

Egger, V., and Stroh, O. (2009). Calcium buffering in rodent olfactory bulb granule cells and mitral cells. *The Journal of Physiology* 587(18), 4467-4479. doi: https://doi.org/10.1113/jphysiol.2009.174540.

Egger, V., Svoboda, K., and Mainen, Z.F. (2003). Mechanisms of lateral inhibition in the olfactory bulb: efficiency and modulation of spike-evoked calcium influx into granule cells. *Journal of Neuroscience* 23(20), 7551-7558.

Elaagouby, A., Ravel, N., and Gervais, R. (1991). Cholinergic modulation of excitability in the rat olfactory bulb: effect of local application of cholinergic agents on evoked field potentials. *Neuroscience* 45(3), 653-662.

Engelmann, M., Hadicke, J., and Noack, J. (2011). Testing declarative memory in laboratory rats and mice using the nonconditioned social discrimination procedure. *Nature Protocols* 6(8), 1152-1162. doi: 10.1038/nprot.2011.353.

Engelmann, M., Wotjak, C.T., and Landgraf, R. (1995). Social discrimination procedure: an alternative method to investigate juvenile recognition abilities in rats. *Physiology & behavior* 58(2), 315-321.

Ennis, M., Zhou, F.-M., Ciombor, K.J., Aroniadou-Anderjaska, V., Hayar, A., Borrelli, E., et al. (2001). Dopamine D2 Receptor–Mediated Presynaptic Inhibition of Olfactory Nerve Terminals. *Journal of Neurophysiology* 86(6), 2986-2997. doi: 10.1152/jn.2001.86.6.2986.

Fang, L.Y., Quan, R.D., and Kaba, H. (2008). Oxytocin facilitates the induction of long-term potentiation in the accessory olfactory bulb. *Neurosci Lett* 438(2), 133-137. doi: 10.1016/j.neulet.2007.12.070.

Ferguson, J.N., Young, L.J., Hearn, E.F., Matzuk, M.M., Insel, T.R., and Winslow, J.T. (2000). Social amnesia in mice lacking the oxytocin gene. *Nature genetics* 25(3), 284.

File, S.E. (1985). Animal Models for Predicting Clinical Efficacy of Anxiolytic Drugs: Social Behaviour. *Neuropsychobiology* 13(1-2), 55-62. doi: 10.1159/000118163.

Fletcher, M.L., and Wilson, D.A. (2002). Experience modifies olfactory acuity: acetylcholine-dependent learning decreases behavioral generalization between similar odorants. *Journal of Neuroscience* 22(2), RC201-RC201.

Fried, H.-U., Kaupp, U.B., and Müller, F. (2010). Hyperpolarization-activated and cyclic nucleotide-gated channels are differentially expressed in juxtaglomerular cells in the olfactory bulb of mice. *Cell and tissue research* 339(3), 463-479.

Garcia, I., Bhullar, P.K., Tepe, B., Ortiz-Guzman, J., Huang, L., Herman, A.M., et al. (2016). Local corticotropin releasing hormone (CRH) signals to its receptor CRHR1 during postnatal development of the mouse olfactory bulb. *Brain Structure and Function* 221(1), 1-20. doi: 10.1007/s00429-014-0888-4.

Garcia, I., Quast, Kathleen B., Huang, L., Herman, Alexander M., Selever, J., Deussing, Jan M., et al. (2014). Local CRH Signaling Promotes Synaptogenesis and Circuit Integration of Adult-Born Neurons. *Developmental Cell* 30(6), 645-659. doi: https://doi.org/10.1016/j.devcel.2014.07.001.

Ghatpande, A.S., Sivaraaman, K., and Vijayaraghavan, S. (2006). Store calcium mediates cholinergic effects on mIPSCs in the rat main olfactory bulb. *Journal of neurophysiology* 95(3), 1345-1355.

Gilbert, C.D., Sigman, M., and Crist, R.E. (2001). The Neural Basis of Perceptual Learning. *Neuron* 31(5), 681-697. doi: https://doi.org/10.1016/S0896-6273(01)00424-X.

Giovannini, M.G., Rakovska, A., Benton, R.S., Pazzagli, M., Bianchi, L., and Pepeu, G. (2001). Effects of novelty and habituation on acetylcholine, GABA, and glutamate release from the frontal cortex and hippocampus of freely moving rats. *Neuroscience* 106(1), 43-53. doi: 10.1016/S0306-4522(01)00266-4.

González-Flores, O., Beyer, C., Lima-Hernández, F.J., Gómora-Arrati, P., Gómez-Camarillo, M.A., Hoffman, K., et al. (2007). Facilitation of estrous behavior by vaginal cervical stimulation in female rats involves α1-adrenergic receptor activation of the nitric oxide pathway. *Behavioural Brain Research* 176(2), 237-243. doi: https://doi.org/10.1016/j.bbr.2006.10.007.

Grammatopoulos, D.K. (2012). Insights into mechanisms of corticotropin-releasing hormone receptor signal transduction. *British Journal of Pharmacology* 166(1), 85-97. doi: https://doi.org/10.1111/j.1476-5381.2011.01631.x.

Greenwood, R.S., Godar, S.E., Reaves Jr., T.A., and Hayward, J.N. (1981). Cholecystokinin in hippocampal pathways. *Journal of Comparative Neurology* 203(3), 335-350. doi: https://doi.org/10.1002/cne.902030303.

Gregg, C.M. (1985). The Compartmentalized Hypothalamo-Neurohypophysial System: Evidence for a NeurohypophysialAction of Acetylcholine on Vasopressin Release. *Neuroendocrinology* 40(5), 423-429. doi: 10.1159/000124108.

Guarnieri, L.O., Pereira-Caixeta, A.R., Medeiros, D.C., Aquino, N.S.S., Szawka, R.E., Mendes, E.M.A.M., et al. (2020). Pro-neurogenic effect of fluoxetine in the olfactory bulb is concomitant to improvements in social memory and depressive-like behavior of socially isolated mice. *Translational Psychiatry* 10(1), 33. doi: 10.1038/s41398-020-0701-5.

Gutièrrez‐Mecinas, M., Crespo, C., Blasco‐Ibáñez, J.M., Gracia‐Llanes, F.J., Marqués‐Marí, A.I., and Martínez‐Guijarro, F.J. (2005). Characterization of somatostatin‐ and cholecystokinin‐immunoreactive periglomerular cells in the rat olfactory bulb. *Journal of Comparative Neurology* 489(4), 467-479.

Haga, S., Hattori, T., Sato, T., Sato, K., Matsuda, S., Kobayakawa, R., et al. (2010). The male mouse pheromone ESP1 enhances female sexual receptive behaviour through a specific vomeronasal receptor. *Nature* 466(7302), 118-U136. doi: 10.1038/nature09142.

Halász , N. (1990). *The Vertebrate Olfactory System: Chemical neuroanatomy, function and development.* Budapest: Akadémiai Kiadó.

Hamilton, K.A., Heinbockel, T., Ennis, M., Szabó, G., Erdélyi, F., and Hayar, A. (2005). Properties of external plexiform layer interneurons in mouse olfactory bulb slices. *Neuroscience* 133(3), 819-829. doi: https://doi.org/10.1016/j.neuroscience.2005.03.008.

Hattori, T., Osakada, T., Matsumoto, A., Matsuo, N., Haga-Yamanaka, S., Nishida, T., et al. (2016). Self-Exposure to the Male Pheromone ESP1 Enhances Male Aggressiveness in Mice. *Current Biology* 26(9), 1229-1234. doi: 10.1016/j.cub.2016.03.029.

Hayar, A., Karnup, S., Ennis, M., and Shipley, M.T. (2004a). External Tufted Cells: A Major Excitatory Element That Coordinates Glomerular Activity. *The Journal of Neuroscience* 24(30), 6676-6685. doi: 10.1523/jneurosci.1367-04.2004.

Hayar, A., Karnup, S., Shipley, M.T., and Ennis, M. (2004b). Olfactory bulb glomeruli: external tufted cells intrinsically burst at theta frequency and are entrained by patterned olfactory input. *Journal of Neuroscience* 24(5), 1190-1199.

Hayar, A., Shipley, M.T., and Ennis, M. (2005). Olfactory Bulb External Tufted Cells Are Synchronized by Multiple Intraglomerular Mechanisms. *The Journal of Neuroscience* 25(36), 8197-8208. doi: 10.1523/jneurosci.2374-05.2005.

Heyward, P., Ennis, M., Keller, A., and Shipley, M.T. (2001). Membrane Bistability in Olfactory Bulb Mitral Cells. *The Journal of Neuroscience* 21(14), 5311-5320. doi: 10.1523/jneurosci.21-14-05311.2001.

Hill, J.A., Zoli, M., Bourgeois, J.-P., and Changeux, J.-P. (1993). Immunocytochemical localization of a neuronal nicotinic receptor: the beta 2-subunit. *Journal of Neuroscience* 13(4), 1551-1568.

Holderith, N.B., Shigemoto, R., and Nusser, Z. (2003). Cell type-dependent expression of HCN1 in the main olfactory bulb. *European Journal of Neuroscience* 18(2), 344-354. doi: https://doi.org/10.1046/j.1460-9568.2003.02756.x.

Huang, G.Z., Taniguchi, M., Zhou, Y.B., Zhang, J.J., Okutani, F., Murata, Y., et al. (2018). alpha2-Adrenergic receptor activation promotes long-term potentiation at excitatory synapses in the mouse accessory olfactory bulb. *Learn Mem* 25(4), 147-157. doi: 10.1101/lm.046391.117.

Huang, L., Garcia, I., Jen, H.-I., and Arenkiel, B. (2013). Reciprocal connectivity between mitral cells and external plexiform layer interneurons in the mouse olfactory bulb. *Frontiers in Neural Circuits* 7(32). doi: 10.3389/fncir.2013.00032.

Imperato, A., Puglisiallegra, S., Scrocco, M.G., Casolini, P., Bacchi, S., and Angelucci, L. (1992). Cortical and Limbic Dopamine and Acetylcholine-Release as Neurochemical Correlates of Emotional Arousal in Both Aversive and Non-Aversive Environmental-Changes. *Neurochemistry International* 20, S265-S270.

Ishii, K.K., Osakada, T., Mori, H., Miyasaka, N., Yoshihara, Y., Miyamichi, K., et al. (2017). A Labeled-Line Neural Circuit for Pheromone-Mediated Sexual Behaviors in Mice. *Neuron* 95(1), 123-137 e128. doi: 10.1016/j.neuron.2017.05.038.

Isogai, Y., Wu, Z., Love, M.I., Ahn, M.H.-Y., Bambah-Mukku, D., Hua, V., et al. (2018). Multisensory logic of infant-directed aggression by males. *Cell* 175(7), 1827-1841. e1817.

Kaba, H. (2010). Neurobiology of mammalian olfactory learning that occurs during sensitive periods. *Current Zoology* 56(6), 819-833.

Kaba, H., and Keverne, E.B. (1988). The Effect of Microinfusions of Drugs into the Accessory Olfactory-Bulb on the Olfactory Block to Pregnancy. *Neuroscience* 25(3), 1007-1011. doi: Doi 10.1016/0306-4522(88)90053-X.

Kaba, H., and Nakanishi, S. (1995). Synaptic mechanisms of olfactory recognition memory. *Reviews in the neurosciences* 6(2), 125-142.

Kaba, H., Rosser, A., and Keverne, B. (1989). Neural Basis of Olfactory Memory in the Context of Pregnancy Block. *Neuroscience* 32(3), 657-662. doi: 10.1016/0306-4522(89)90287-X.

Kaba, H., Rosser, A.E., and Keverne, E.B. (1988). Hormonal Enhancement of Neurogenesis and Its Relationship to the Duration of Olfactory Memory. *Neuroscience* 24(1), 93-98. doi: Doi 10.1016/0306-4522(88)90314-4.

Kanyshkova, T., Pawlowski, M., Meuth, P., Dubé, C., Bender, R.A., Brewster, A.L., et al. (2009). Postnatal Expression Pattern of HCN Channel Isoforms in Thalamic Neurons: Relationship to Maturation of Thalamocortical Oscillations. *The Journal of Neuroscience* 29(27), 8847-8857. doi: 10.1523/jneurosci.0689-09.2009.

Kay, L.M., Beshel, J., Brea, J., Martin, C., Rojas-Líbano, D., and Kopell, N. (2009). Olfactory oscillations: the what, how and what for. *Trends in Neurosciences* 32(4), 207-214. doi: https://doi.org/10.1016/j.tins.2008.11.008.

Kendrick, K., Guevara-Guzman, R., Zorrilla, J., Hinton, M., Broad, K., Mimmack, M.a., et al. (1997a). Formation of olfactory memories mediated by nitric oxide. *Nature* 388(6643), 670-674.

Kendrick, K., Keverne, E., Chapman, C., and Baldwin, B. (1988). Microdialysis measurement of oxytocin, aspartate, γ-aminobutyric acid and glutamate release from the olfactory bulb of the sheep during vaginocervical stimulation. *Brain research* 442(1), 171-174.

Kendrick, K., Lévy, F., and Keverne, E. (1991). Importance of vaginocervical stimulation for the formation of maternal bonding in primiparous and multiparous parturient ewes. *Physiology & behavior* 50(3), 595-600.

Kendrick, K., Lévy, F., and Keverne, E.B. (1992). Changes in the sensory processing of olfactory signals induced by birth in sleep. *Science* 256(5058), 833-836.

Kendrick, K.M., Da Costa, A.P., Broad, K.D., Ohkura, S., Guevara, R., Lévy, F., et al. (1997b). Neural control of maternal behaviour and olfactory recognition of offspring. *Brain research bulletin* 44(4), 383-395.

Kimoto, H., Haga, S., Sato, K., and Touhara, K. (2005). Sex-specific peptides from exocrine glands stimulate mouse vomeronasal sensory neurons. *Nature* 437(7060), 898-901. doi: 10.1038/nature04033.

Kirkwood, A., Rozas, C., Kirkwood, J., Perez, F., and Bear, M.F. (1999). Modulation of long-term synaptic depression in visual cortex by acetylcholine and norepinephrine. *Journal of Neuroscience* 19(5), 1599-1609. doi: 10.1523/JNEUROSCI.19-05-01599.1999.

Kiyokage, E., Pan, Y.-Z., Shao, Z., Kobayashi, K., Szabo, G., Yanagawa, Y., et al. (2010). Molecular identity of periglomerular and short axon cells. *Journal of Neuroscience* 30(3), 1185-1196.

Köhler, C., Hallman, H., and Radesäter, A.C. (1987). Distribution of [3h]cholecystokinin octapeptide binding sites in the hippocampal region of the rat brain as shown by in vitro receptor autoradiography. *Neuroscience* 21(3), 857-867. doi: https://doi.org/10.1016/0306-4522(87)90042-X.

Kosaka, T., and Kosaka, K. (2007). Heterogeneity of nitric oxide synthase-containing neurons in the mouse main olfactory bulb. *Neuroscience Research* 57(2), 165-178. doi: https://doi.org/10.1016/j.neures.2006.10.005.

Krosnowski, K., Ashby, S., Sathyanesan, A., Luo, W., Ogura, T., and Lin, W. (2012). Diverse populations of intrinsic cholinergic interneurons in the mouse olfactory bulb. *Neuroscience* 213, 161-178. doi: https://doi.org/10.1016/j.neuroscience.2012.04.024.

Landgraf, R., Gerstberger, R., Montkowski, A., Probst, J.C., Wotjak, C.T., Holsboer, F., et al. (1995). V1 vasopressin receptor antisense oligodeoxynucleotide into septum reduces vasopressin binding, social discrimination abilities, and anxiety-related behavior in rats. *Journal of Neuroscience* 15(6), 4250-4258.

Langdon, P.E., Harley, C.W., and McLean, J.H. (1997). Increased β adrenoceptor activation overcomes conditioned olfactory learning deficits induced by serotonin depletion. *Developmental Brain Research* 102(2), 291-293.

Le Jeune, H., Aubert, I., Jourdan, F., and Quirion, R. (1995). Comparative laminar distribution of various autoradiographic cholinergic markers in adult rat main

olfactory bulb. *Journal of chemical neuroanatomy* 9(2), 99-112. doi: 10.1016/0891-0618(95)00070-N.
Lemaire, M., Böhme, G.A., Piot, O., Roques, B.P., and Blanchard, J.C. (1994). CCK-A and CCK-B selective receptor agonists and antagonists modulate olfactory recognition in male rats. *Psychopharmacology* 115(4), 435-440. doi: 10.1007/BF02245565.
Lemaire, M., Piot, O., Roques, B.P., Böhme, G.A., and Blanchard, J.-C. (1992). Evidence for an endogenous cholecystokininergic balance in social memory. *NeuroReport* 3(10), 929-932.
Lepousez, G., Csaba, Z., Bernard, V., Loudes, C., Videau, C., Lacombe, J., et al. (2010a). Somatostatin interneurons delineate the inner part of the external plexiform layer in the mouse main olfactory bulb. *Journal of Comparative Neurology* 518(11), 1976-1994. doi: https://doi.org/10.1002/cne.22317.
Lepousez, G., Mouret, A., Loudes, C., Epelbaum, J., and Viollet, C. (2010b). Somatostatin Contributes to In Vivo Gamma Oscillation Modulation and Odor Discrimination in the Olfactory Bulb. *The Journal of Neuroscience* 30(3), 870-875. doi: 10.1523/jneurosci.4958-09.2010.
Lévy, F., Gervais, R., Kindermann, U., Orgeur, P., and Piketty, V. (1990). Importance of! b-noradrenergic receptors in the olfactory bulb of sheep for recognition of lambs. *Behavioral neuroscience* 104(3), 464.
Lévy, F., Guevara-Guzman, R., Hinton, M., Kendrick, K., and Keverne, E. (1993). Effects of parturition and maternal experience on noradrenaline and acetylcholine release in the olfactory bulb of sheep. *Behavioral neuroscience* 107(4), 662.
Lévy, F., Kendrick, K., Goode, J., Guevara-Guzman, R., and Keverne, E. (1995). Oxytocin and vasopressin release in the olfactory bulb of parturient ewes: changes with maternal experience and effects on acetylcholine, γ-aminobutyric acid, glutamate and noradrenaline release. *Brain research* 669(2), 197-206.
Lévy, F., Richard, P., Meurisse, M., and Ravel, N. (1997). Scopolamine impairs the ability of parturient ewes to learn to recognise their lambs. *Psychopharmacology* 129(1), 85-90.
Li, D.P., Pan, Y.Z., and Pan, H.L. (2001). Acetylcholine attenuates synaptic GABA release to supraoptic neurons through presynaptic nicotinic receptors. *Brain Research* 920(1-2), 151-158. doi: 10.1016/S0006-8993(01)03055-4.
Linster, C., and Hasselmo, M.E. (2000). Neural activity in the horizontal limb of the diagonal band of Broca can be modulated by electrical stimulation of the olfactory bulb and cortex in rats. *Neuroscience Letters* 282(3), 157-160. doi: 10.1016/S0304-3940(00)00885-5.
Liu, S., Aungst, J.L., Puche, A.C., and Shipley, M.T. (2011). Serotonin modulates the population activity profile of olfactory bulb external tufted cells. *Journal of neurophysiology* 107(1), 473-483. doi: 10.1152/jn.00741.2011.
Liu, S., Plachez, C., Shao, Z., Puche, A., and Shipley, M.T. (2013). Olfactory bulb short axon cell release of GABA and dopamine produces a temporally biphasic inhibition–excitation response in external tufted cells. *Journal of Neuroscience* 33(7), 2916-2926.
Liu, S., Puche, A.C., and Shipley, M.T. (2016). The interglomerular circuit potently inhibits olfactory bulb output neurons by both direct and indirect pathways. *Journal of Neuroscience* 36(37), 9604-9617.
Liu, S., and Shipley, M.T. (2008). Intrinsic conductances actively shape excitatory and inhibitory postsynaptic responses in olfactory bulb external tufted cells. *J Neurosci* 28(41), 10311-10322. doi: 10.1523/JNEUROSCI.2608-08.2008.
Liu, S.L., Shao, Z.Y., Puche, A., Wachowiak, M., Rothermel, M., and Shipley, M.T. (2015). Muscarinic Receptors Modulate Dendrodendritic Inhibitory Synapses to Sculpt

Glomerular Output. *Journal of Neuroscience* 35(14), 5680-5692. doi: 10.1523/Jneurosci.4953-14.2015.
Liu, W.L., and Shipley, M.T. (1994). Intrabulbar associational system in the rat olfactory bulb comprises cholecystokinin‐containing tufted cells that synapse onto the dendrites of GABAergic granule cells. *Journal of Comparative Neurology* 346(4), 541-558.
Liu, X., and Liu, S. (2018). Cholecystokinin selectively activates short axon cells to enhance inhibition of olfactory bulb output neurons. *The Journal of Physiology* 596(11), 2185-2207. doi: https://doi.org/10.1113/JP275511.
Longair, M.H., Baker, D.A., and Armstrong, J.D. (2011). Simple Neurite Tracer: open source software for reconstruction, visualization and analysis of neuronal processes. *Bioinformatics* 27(17), 2453-2454. doi: 10.1093/bioinformatics/btr390.
Lonstein, J.S., and Gammie, S.C. (2002). Sensory, hormonal, and neural control of maternal aggression in laboratory rodents. *Neuroscience & Biobehavioral Reviews* 26(8), 869-888.
Lowe, G., Buerk, D.G., Ma, J., and Gelperin, A. (2008). Tonic and stimulus-evoked nitric oxide production in the mouse olfactory bulb. *Neuroscience* 153(3), 842-850. doi: https://doi.org/10.1016/j.neuroscience.2008.03.003.
Ludwig, M., Bull, P.M., Tobin, V.A., Sabatier, N., Landgraf, R., Dayanithi, G., et al. (2005). Regulation of activity-dependent dendritic vasopressin release from rat supraoptic neurones. *The Journal of Physiology* 564(2), 515-522. doi: https://doi.org/10.1113/jphysiol.2005.083931.
Ludwig, M., Callahan, M.F., Neumann, I., Landgraf, R., and Morris, M. (1994). Systemic Osmotic Stimulation Increases Vasopressin and Oxytocin Release Within the Supraoptic Nucleus. *Journal of Neuroendocrinology* 6(4), 369-373. doi: https://doi.org/10.1111/j.1365-2826.1994.tb00595.x.
Ludwig, M., and Leng, G. (2006). Dendritic peptide release and peptide-dependent behaviours. *Nature Reviews Neuroscience* 7(2), 126.
Lukas, M., and de Jong, T.R. (2015). "Conspecific interactions in adult laboratory rodents: friends or foes?," in *Social Behavior from Rodents to Humans*. Springer), 3-24.
Lukas, M., Holthoff, K., and Egger, V. (2018). "Long-Term Plasticity at the Mitral and Tufted Cell to Granule Cell Synapse of the Olfactory Bulb Investigated with a Custom Multielectrode in Acute Brain Slice Preparations," in *Olfactory Receptors: Methods and Protocols,* eds. F.M. Simoes de Souza & G. Antunes. (New York, NY: Springer New York), 157-167.
Lukas, M., and Neumann, I.D. (2013). Oxytocin and vasopressin in rodent behaviors related to social dysfunctions in autism spectrum disorders. *Behav Brain Res* 251, 85-94. doi: 10.1016/j.bbr.2012.08.011.
Lukas, M., Suyama, H., and Egger, V. (2019). Vasopressin Cells in the Rodent Olfactory Bulb Resemble Non-Bursting Superficial Tufted Cells and Are Primarily Inhibited upon Olfactory Nerve Stimulation. *eneuro* 6(4), ENEURO.0431-0418.2019. doi: 10.1523/eneuro.0431-18.2019.
Lukas, M., Toth, I., Veenema, A.H., and Neumann, I.D. (2013). Oxytocin mediates rodent social memory within the lateral septum and the medial amygdala depending on the relevance of the social stimulus: male juvenile versus female adult conspecifics. *Psychoneuroendocrinology* 38(6), 916-926. doi: 10.1016/j.psyneuen.2012.09.018.
Luskin, M.B., and Price, J.L. (1983). The topographic organization of associational fibers of the olfactory system in the rat, including centrifugal fibers to the olfactory bulb. *Journal of Comparative Neurology* 216(3), 264-291. doi: https://doi.org/10.1002/cne.902160305.

Ma, J., Dankulich-Nagrudny, L., and Lowe, G. (2013). Cholecystokinin: an excitatory modulator of mitral/tufted cells in the mouse olfactory bulb. *PLoS One* 8(5), e64170.

Macrides, F., and Schneider, S.P. (1982). Laminar organization of mitral and tufted cells in the main olfactory bulb of the adult hamster. *Journal of Comparative Neurology* 208(4), 419-430. doi: https://doi.org/10.1002/cne.902080410.

Mandairon, N., Ferretti, C.J., Stack, C.M., Rubin, D.B., Cleland, T.A., and Linster, C. (2006a). Cholinergic modulation in the olfactory bulb influences spontaneous olfactory discrimination in adult rats. *European Journal of Neuroscience* 24(11), 3234-3244. doi: 10.1111/j.1460-9568.2006.05212.x.

Mandairon, N., Stack, C., Kiselycznyk, C., and Linster, C. (2006b). Enrichment to odors improves olfactory discrimination in adult rats. *Behavioral neuroscience* 120(1), 173.

Manning, M., Misicka, A., Olma, A., Bankowski, K., Stoev, S., Chini, B., et al. (2012). Oxytocin and Vasopressin Agonists and Antagonists as Research Tools and Potential Therapeutics. *Journal of Neuroendocrinology* 24(4), 609-628. doi: https://doi.org/10.1111/j.1365-2826.2012.02303.x.

Manning, M., Stoev, S., Chini, B., Durroux, T., Mouillac, B., and Guillon, G. (2008). "Peptide and non-peptide agonists and antagonists for the vasopressin and oxytocin V1a, V1b, V2 and OT receptors: research tools and potential therapeutic agents," in *Progress in Brain Research,* eds. I.D. Neumann & R. Landgraf. Elsevier), 473-512.

Markopoulos, F., Rokni, D., Gire, D.H., and Murthy, V.N. (2012). Functional properties of cortical feedback projections to the olfactory bulb. *Neuron* 76(6), 1175-1188.

Marlin, B.J., Mitre, M., D'amour, J.A., Chao, M.V., and Froemke, R.C. (2015). Oxytocin enables maternal behaviour by balancing cortical inhibition. *Nature* 520(7548), 499-504. doi: 10.1038/nature14402.

Martel, G., Dutar, P., Epelbaum, J., and Viollet, C. (2012). Somatostatinergic systems: an update on brain functions in normal and pathological aging. *Frontiers in Endocrinology* 3(154). doi: 10.3389/fendo.2012.00154.

Martinon, D., Lis, P., Roman, A.N., Tornesi, P., Applebey, S.V., Buechner, G., et al. (2019). Oxytocin receptors in the dorsolateral bed nucleus of the stria terminalis (BNST) bias fear learning toward temporally predictable cued fear. *Translational Psychiatry* 9(1), 140. doi: 10.1038/s41398-019-0474-x.

Marx, M., Günter, R.H., Hucko, W., Radnikow, G., and Feldmeyer, D. (2012). Improved biocytin labeling and neuronal 3D reconstruction. *Nature Protocols* 7(2), 394-407. doi: 10.1038/nprot.2011.449.

Matsuo, T., Hattori, T., Asaba, A., Inoue, N., Kanomata, N., Kikusui, T., et al. (2015). Genetic dissection of pheromone processing reveals main olfactory system-mediated social behaviors in mice. *P Natl Acad Sci USA* 112(3), E311-E320. doi: 10.1073/pnas.1416723112.

Matsuoka, M., Kaba, H., Moriya, K., Yoshida-Matsuoka, J., Costanzo, R.M., Norita, M., et al. (2004). Remodeling of reciprocal synapses associated with persistence of long-term memory. *Eur J Neurosci* 19(6), 1668-1672. doi: 10.1111/j.1460-9568.2004.03271.x.

Matsutani, S., and Yamamoto, N. (2008). Centrifugal innervation of the mammalian olfactory bulb. *Anatomical Science International* 83(4), 218-227. doi: 10.1111/j.1447-073X.2007.00223.x.

Matthews, G.A., Patel, R., Walsh, A., Davies, O., Martínez-Ricós, J., and Brennan, P.A. (2013). Mating increases neuronal tyrosine hydroxylase expression and selectively gates transmission of male chemosensory information in female mice. *PloS one* 8(7), e69943.

McKenna, J.T., Cordeira, J.W., Jeffrey, B.A., Ward, C.P., Winston, S., McCarley, R.W., et al. (2009). c-Fos protein expression is increased in cholinergic neurons of the rodent basal forebrain during spontaneous and induced wakefulness. *Brain Research Bulletin* 80(6), 382-388. doi: 10.1016/j.brainresbull.2009.08.015.

McLean, J.H., Darby-King, A., and Hodge, E. (1996). 5-HT_2 receptor involvement in conditioned olfactory learning in the neonate rat pup. *Behavioral neuroscience* 110(6), 1426.

McLean, J.H., Darby-King, A., Sullivan, R.M., and King, S.R. (1993). Serotonergic influence on olfactory learning in the neonate rat. *Behavioral and neural biology* 60(2), 152-162.

McLean, J.H., and Shipley, M.T. (1987). Serotonergic afferents to the rat olfactory bulb: I. Origins and laminar specificity of serotonergic inputs in the adult rat. *Journal of Neuroscience* 7(10), 3016-3028.

Mclean, J.H., Shipley, M.T., Nickell, W.T., Astonjones, G., and Reyher, C.K.H. (1989). Chemoanatomical Organization of the Noradrenergic Input from Locus Coeruleus to the Olfactory-Bulb of the Adult-Rat. *Journal of Comparative Neurology* 285(3), 339-349. doi: DOI 10.1002/cne.902850305.

Metherate, R., and Ashe, J.H. (1995). Synaptic-Interactions Involving Acetylcholine, Glutamate, and Gaba in Rat Auditory-Cortex. *Experimental Brain Research* 107(1), 59-72.

Meyer-Lindenberg, A., Domes, G., Kirsch, P., and Heinrichs, M. (2011). Oxytocin and vasopressin in the human brain: social neuropeptides for translational medicine. *Nature Reviews Neuroscience* 12(9), 524.

Migliore, M., Hines, M.L., and Shepherd, G.M. (2005). The role of distal dendritic gap junctions in synchronization of mitral cell axonal output. *J Comput Neurosci* 18(2), 151-161. doi: 10.1007/s10827-005-6556-1.

Mirich, J.M., Illig, K.R., and Brunjes, P.C. (2004). Experience‐dependent activation of extracellular signal‐related kinase (ERK) in the olfactory bulb. *Journal of comparative Neurology* 479(2), 234-241.

Nagayama, S., Homma, R., and Imamura, F. (2014). Neuronal organization of olfactory bulb circuits. *Front Neural Circuits* 8, 98. doi: 10.3389/fncir.2014.00098.

Nai, Q., Dong, H.-W., Hayar, A., Linster, C., and Ennis, M. (2009). Noradrenergic regulation of GABAergic inhibition of main olfactory bulb mitral cells varies as a function of concentration and receptor subtype. *Journal of neurophysiology* 101(5), 2472-2484.

Nai, Q., Dong, H.-W., Linster, C., and Ennis, M. (2010). Activation of α1 and α2 noradrenergic receptors exert opposing effects on excitability of main olfactory bulb granule cells. *Neuroscience* 169(2), 882-892.

Najac, M., De Saint Jan, D., Reguero, L., Grandes, P., and Charpak, S. (2011). Monosynaptic and Polysynaptic Feed-Forward Inputs to Mitral Cells from Olfactory Sensory Neurons. *The Journal of Neuroscience* 31(24), 8722-8729. doi: 10.1523/jneurosci.0527-11.2011.

Nevison, C.M., Barnard, C.J., Beynon, R.J., and Hurst, J.L. (2000). The consequences of inbreeding for recognizing competitors. *Proceedings of the Royal Society of London. Series B: Biological Sciences* 267(1444), 687-694. doi: doi:10.1098/rspb.2000.1057.

Nicoll, R.A. (1971). Recurrent Excitation of Secondary Olfactory Neurons: A Possible Mechanism for Signal Amplification. *Science* 171(3973), 824-826. doi: 10.1126/science.171.3973.824.

Noack, J., Richter, K., Laube, G., Haghgoo, H.A., Veh, R.W., and Engelmann, M. (2010). Different importance of the volatile and non-volatile fractions of an olfactory signature for individual social recognition in rats versus mice and short-term

versus long-term memory. *Neurobiology of Learning and Memory* 94(4), 568-575. doi: 10.1016/j.nlm.2010.09.013.
Novotny, M., Harvey, S., Jemiolo, B., and Alberts, J. (1985). Synthetic pheromones that promote inter-male aggression in mice. *Proceedings of the National Academy of Sciences* 82(7), 2059-2061. doi: 10.1073/pnas.82.7.2059.
Oettl, L.L., Ravi, N., Schneider, M., Scheller, M.F., Schneider, P., Mitre, M., et al. (2016). Oxytocin Enhances Social Recognition by Modulating Cortical Control of Early Olfactory Processing. *Neuron* 90(3), 609-621. doi: 10.1016/j.neuron.2016.03.033.
Ogg, M.C., Ross, J.M., Bendahmane, M., and Fletcher, M.L. (2018). Olfactory bulb acetylcholine release dishabituates odor responses and reinstates odor investigation. *Nature communications* 9(1), 1-11.
Ojima, H., Yamasaki, T., Kojima, H., and Akashi, A. (1988). Cholinergic Innervation of the Main and the Accessory Olfactory Bulbs of the Rat as Revealed by a Monoclonal-Antibody against Choline-Acetyltransferase. *Anatomy and Embryology* 178(6), 481-488. doi: Doi 10.1007/Bf00305035.
Okabe, S., Nagasawa, M., Kihara, T., Kato, M., Harada, T., Koshida, N., et al. (2013). Pup odor and ultrasonic vocalizations synergistically stimulate maternal attention in mice. *Behavioral neuroscience* 127(3), 432.
Olivier, J.D.A., Esquivel-Franco, D.C., Waldinger, M.D., and Olivier, B. (2019). "Chapter Seven - Serotonin and sexual behavior," in *The Serotonin System,* eds. M.D. Tricklebank & E. Daly. Academic Press), 117-132.
Ondrasek, N.R. (2016). Emerging Frontiers in Social Neuroendocrinology and the Study of Nonapeptides. *Ethology* 122(6), 443-455. doi: https://doi.org/10.1111/eth.12493.
Ostrowski, N., Lolait, S., and Young, W. (1994). Cellular localization of vasopressin V1a receptor messenger ribonucleic acid in adult male rat brain, pineal, and brain vasculature. *Endocrinology* 135(4), 1511-1528.
Pacchiarini, N., Fox, K., and Honey, R.C. (2017). Perceptual learning with tactile stimuli in rodents: Shaping the somatosensory system. *Learning & Behavior* 45(2), 107-114. doi: 10.3758/s13420-017-0269-y.
Pankevich, D.E., Baum, M.J., and Cherry, J.A. (2004). Olfactory sex discrimination persists, whereas the preference for urinary odorants from estrous females disappears in male mice after vomeronasal organ removal. *J Neurosci* 24(42), 9451-9457. doi: 10.1523/JNEUROSCI.2376-04.2004.
Passetti, F., Dalley, J.W., O'connell, M.T., Everitt, B.J., and Robbins, T.W. (2000). Increased acetylcholine release in the rat medial prefrontal cortex during performance of a visual attentional task. *European Journal of Neuroscience* 12(8), 3051-3058. doi: 10.1046/j.1460-9568.2000.00183.x.
Paxinos, G., and Watson, C. (2009). "The rat brain in stereotaxic coordinates: compact sixth edition". New York: Academic Press).
Perna, J.C., and Engelmann, M. (2015). "Recognizing others: rodent's social memories," in *Social Behavior from Rodents to Humans*. Springer), 25-45.
Petzold, G.C., Hagiwara, A., and Murthy, V.N. (2009). Serotonergic modulation of odor input to the mammalian olfactory bulb. *Nature neuroscience* 12(6), 784.
Phifer, C.B., and Terry, L.M. (1986). Use of hypothermia for general anesthesia in preweanling rodents. *Physiology & Behavior* 38(6), 887-890. doi: https://doi.org/10.1016/0031-9384(86)90058-2.
Pignatelli, A., and Belluzzi, O. (2008). Cholinergic modulation of dopaminergic neurons in the mouse olfactory bulb. *Chemical Senses* 33(4), 331-338. doi: 10.1093/chemse/bjm091.
Pinching, A.J., and Powell, T.P. (1971). The neuron types of the glomerular layer of the olfactory bulb. *J Cell Sci* 9(2), 305-345.
Popova, N.K., and Amstislavskaya, T.G. (2002). 5-HT2A and 5-HT2C serotonin receptors differentially modulate mouse sexual arousal and the hypothalamo-pituitary-

testicular response to the presence of a female. *Neuroendocrinology* 76(1), 28-34. doi: 10.1159/000063681.
Porter, R.H., Balogh, R.D., Cernoch, J.M., and Franchi, C. (1986). Recognition of kin through characteristic body odors. *Chemical Senses* 11(3), 389-395. doi: 10.1093/chemse/11.3.389.
Pow, D.V., and Morris, J.F. (1989). Dendrites of hypothalamic magnocellular neurons release neurohypophysial peptides by exocytosis. *Neuroscience* 32(2), 435-439. doi: https://doi.org/10.1016/0306-4522(89)90091-2.
Prado, V.F., Martins-Silva, C., de Castro, B.M., Lima, R.F., Barros, D.M., Amaral, E., et al. (2006). Mice deficient for the vesicular acetylcholine transporter are myasthenic and have deficits in object and social recognition. *Neuron* 51(5), 601-612. doi: 10.1016/j.neuron.2006.08.005.
Purvis, E.M., Klein, A.K., and Ettenberg, A. (2018). Lateral habenular norepinephrine contributes to states of arousal and anxiety in male rats. *Behavioural Brain Research* 347, 108-115. doi: 10.1016/j.bbr.2018.03.012.
Quick, M.W., and Lester, R.A.J. (2002). Desensitization of neuronal nicotinic receptors. *Journal of Neurobiology* 53(4), 457-478. doi: https://doi.org/10.1002/neu.10109.
Raam, T., McAvoy, K.M., Besnard, A., Veenema, A.H., and Sahay, A. (2017). Hippocampal oxytocin receptors are necessary for discrimination of social stimuli. *Nature communications* 8(1), 1-14.
Raber, J., and Bloom, F. (1994). IL-2 induces vasopressin release from the hypothalamus and the amygdala: role of nitric oxide-mediated signaling. *The Journal of Neuroscience* 14(10), 6187-6195. doi: 10.1523/jneurosci.14-10-06187.1994.
Rao, R.P., Mielke, F., Bobrov, E., and Brecht, M. (2014). Vocalization–whisking coordination and multisensory integration of social signals in rat auditory cortex. *Elife* 3, e03185. doi: 10.7554/eLife.03185.
Ravel, N., Akaoka, H., Gervais, R., and Chouvet, G. (1990). The Effect of Acetylcholine on Rat Olfactory-Bulb Unit-Activity. *Brain Research Bulletin* 24(2), 151-155. doi: 10.1016/0361-9230(90)90199-A.
Ravel, N., Elaagouby, A., and Gervais, R. (1994). Scopolamine Injection into the Olfactory-Bulb Impairs Short-Term Olfactory Memory in Rats. *Behavioral Neuroscience* 108(2), 317-324. doi: 10.1037/0735-7044.108.2.317.
Rogers-Carter, M.M., and Christianson, J.P. (2019). An insular view of the social decision-making network. *Neurosci Biobehav R* 103, 119-132. doi: 10.1016/j.neubiorev.2019.06.005.
Rosenthal, R., Cooper, H., and Hedges, L. (1994). Parametric measures of effect size. *The handbook of research synthesis* 621(2), 231-244.
Ross, J.M., Bendahmane, M., and Fletcher, M.L. (2019). Olfactory Bulb Muscarinic Acetylcholine Type 1 Receptors Are Required for Acquisition of Olfactory Fear Learning. *Frontiers in Behavioral Neuroscience* 13. doi: 10.3389/fnbeh.2019.00164.
Rosser, A.E., and Keverne, E. (1985). The importance of central noradrenergic neurones in the formation of an olfactory memory in the prevention of pregnancy block. *Neuroscience* 15(4), 1141-1147.
Rosser, A.E., Remfry, C.J., and Keverne, E.B. (1989). Restricted Exposure of Mice to Primer Pheromones Coincident with Prolactin Surges Blocks Pregnancy by Changing Hypothalamic Dopamine Release. *Journal of Reproduction and Fertility* 87(2), 553-559.
Rothermel, M., Carey, R.M., Puche, A., Shipley, M.T., and Wachowiak, M. (2014). Cholinergic Inputs from Basal Forebrain Add an Excitatory Bias to Odor Coding in the Olfactory Bulb. *Journal of Neuroscience* 34(13), 4654-4664. doi: 10.1523/Jneurosci.5026-13.2014.

Rothermel, M., and Wachowiak, M. (2014). Functional imaging of cortical feedback projections to the olfactory bulb. *Front Neural Circuits* 8, 73. doi: 10.3389/fncir.2014.00073.

Sabatier, N., Richard, P., and Dayanithi, G. (1997). L-, N- and T- but neither P- nor Q-type Ca2+ Channels Control Vasopressin-Induced Ca2+ Influx in Magnocellular Vasopressin Neurones Isolated from the Rat Supraoptic Nucleus. *The Journal of Physiology* 503(2), 253-268. doi: https://doi.org/10.1111/j.1469-7793.1997.253bh.x.

Saboory, E., Gholami, M., Zare, S., and Roshan‐Milani, S. (2014). The long‐term effects of neonatal morphine administration on the pentylenetetrazol seizure model in rats: The role of hippocampal cholinergic receptors in adulthood. *Developmental psychobiology* 56(3), 498-509. doi: 10.1002/dev.21117.

Saito, A., Sankaran, H., Goldfine, I., and Williams, J. (1980). Cholecystokinin receptors in the brain: characterization and distribution. *Science* 208(4448), 1155-1156. doi: 10.1126/science.6246582.

Sale, A., De Pasquale, R., Bonaccorsi, J., Pietra, G., Olivieri, D., Berardi, N., et al. (2011). Visual perceptual learning induces long-term potentiation in the visual cortex. *Neuroscience* 172, 219-225. doi: https://doi.org/10.1016/j.neuroscience.2010.10.078.

Schaefer, M.L., Yamazaki, K., Osada, K., Restrepo, D., and Beauchamp, G.K. (2002). Olfactory Fingerprints for Major Histocompatibility Complex-Determined Body Odors II: Relationship among Odor Maps, Genetics, Odor Composition, and Behavior. *The Journal of Neuroscience* 22(21), 9513-9521. doi: 10.1523/jneurosci.22-21-09513.2002.

Schindelin, J., Arganda-Carreras, I., Frise, E., Kaynig, V., Longair, M., Pietzsch, T., et al. (2012). Fiji: an open-source platform for biological-image analysis. *Nature Methods* 9(7), 676-682. doi: 10.1038/nmeth.2019.

Schwarz, I., Müller, M., Pavlova, I., Schweihoff, J., Musacchio, F., Mittag, M., et al. (2020). The diagonal band of broca continually regulates olfactory-mediated behaviors by modulating odor-evoked responses within the olfactory bulb. *bioRxiv*, 2020.2011.2007.372649. doi: 10.1101/2020.11.07.372649.

Searby, A., and Jouventin, P. (2003). Mother-lamb acoustic recognition in sheep: a frequency coding. *Proceedings of the Royal Society of London. Series B: Biological Sciences* 270(1526), 1765-1771.

Senut, M., Menetrey, D., and Lamour, Y. (1989). Cholinergic and peptidergic projections from the medial septum and the nucleus of the diagonal band of Broca to dorsal hippocampus, cingulate cortex and olfactory bulb: a combined wheatgerm agglutinin-apohorseradish peroxidase-gold immunohistochemical study. *Neuroscience* 30(2), 385-403. doi: 10.1016/0306-4522(89)90260-1.

Serguera, C., Triaca, V., Kelly-Barrett, J., Banchaabouchi, M.A., and Minichiello, L. (2008). Increased dopamine after mating impairs olfaction and prevents odor interference with pregnancy. *Nat Neurosci* 11(8), 949-956. doi: 10.1038/nn.2154.

Shao, Z., Liu, S., Zhou, F., Puche, A.C., and Shipley, M.T. (2019). Reciprocal Inhibitory Glomerular Circuits Contribute to Excitation–Inhibition Balance in the Mouse Olfactory Bulb. *eNeuro* 6(3).

Shao, Z., Puche, A.C., Kiyokage, E., Szabo, G., and Shipley, M.T. (2009). Two GABAergic Intraglomerular Circuits Differentially Regulate Tonic and Phasic Presynaptic Inhibition of Olfactory Nerve Terminals. *Journal of Neurophysiology* 101(4), 1988-2001. doi: 10.1152/jn.91116.2008.

Sheehan, T.P., Chambers, R.A., and Russell, D.S. (2004). Regulation of affect by the lateral septum: implications for neuropsychiatry. *Brain Research Reviews* 46(1), 71-117. doi: https://doi.org/10.1016/j.brainresrev.2004.04.009.

Shipley, M.T., and Ennis, M. (1996). Functional organization of olfactory system. *Journal of Neurobiology* 30(1), 123-176. doi: 10.1002/(sici)1097-4695(199605)30:1<123::aid-neu11>3.0.co;2-n.

Shipley, M.T., Halloran, F.J., and Delatorre, J. (1985). Surprisingly Rich Projection from Locus Coeruleus to the Olfactory-Bulb in the Rat. *Brain Research* 329(1-2), 294-299. doi: Doi 10.1016/0006-8993(85)90537-2.

Singer, A.G., Beauchamp, G.K., and Yamazaki, K. (1997). Volatile signals of the major histocompatibility complex in male mouse urine. *P Natl Acad Sci USA* 94(6), 2210-2214. doi: 10.1073/pnas.94.6.2210.

Smotherman, W.P., Bell, R.W., Starzec, J., Elias, J., and Zachman, T.A. (1974). Maternal Responses to Infant Vocalizations and Olfactory Cues in Rats and Mice. *Behavioral Biology* 12(1), 55-66. doi: Doi 10.1016/S0091-6773(74)91026-8.

Soffie, M., and Lamberty, Y. (1988). Scopolamine Effects on Juvenile Conspecific Recognition in Rats - Possible Interaction with Olfactory Sensitivity. *Behavioural Processes* 17(3), 181-190. doi: Doi 10.1016/0376-6357(88)90001-0.

Son, S.J., Filosa, J.A., Potapenko, E.S., Biancardi, V.C., Zheng, H., Patel, K.P., et al. (2013). Dendritic peptide release mediates interpopulation crosstalk between neurosecretory and preautonomic networks. *Neuron* 78(6), 1036-1049. doi: 10.1016/j.neuron.2013.04.025.

Spindle, M.S., Parsa, P.V., Bowles, S.G., D'Souza, R.D., and Vijayaraghavan, S. (2018). A dominant role for the beta 4 nicotinic receptor subunit in nicotinic modulation of glomerular microcircuits in the mouse olfactory bulb. *J Neurophysiol* 120(4), 2036-2048. doi: 10.1152/jn.00925.2017.

Sterba, G. (1974). "Ascending Neurosecretory Pathways of the Peptidergic Type," in *Neurosecretion — The Final Neuroendocrine Pathway: VI International Symposium on Neurosecretion, London 1973,* eds. F. Knowles & L. Vollrath. (Berlin, Heidelberg: Springer Berlin Heidelberg), 38-47.

Stowers, L., and Kuo, T.-H. (2016). "Chapter 1 - Specialized Chemosignaling that Generates Social and Survival Behavior in Mammals," in *Chemosensory Transduction,* eds. F. Zufall & S.D. Munger. Academic Press), 3-27.

Stuart, G., Spruston, N., Sakmann, B., and Häusser, M. (1997). Action potential initiation and backpropagation in neurons of the mammalian CNS. *Trends in Neurosciences* 20(3), 125-131. doi: https://doi.org/10.1016/S0166-2236(96)10075-8.

Sullivan, R.M., McGaugh, J.L., and Leon, M. (1991). Norepinephrine-induced plasticity and one-trial olfactory learning in neonatal rats. *Developmental Brain Research* 60(2), 219-228.

Sun, X., Liu, X., Starr, E.R., and Liu, S. (2020). CCKergic tufted cells differentially drive two anatomically segregated inhibitory circuits in the mouse olfactory bulb. *Journal of Neuroscience*.

Sun, Y.G., Pita-Almenar, J.D., Wu, C.S., Renger, J.J., Uebele, V.N., Lu, H.C., et al. (2013). Biphasic cholinergic synaptic transmission controls action potential activity in thalamic reticular nucleus neurons. *J Neurosci* 33(5), 2048-2059. doi: 10.1523/JNEUROSCI.3177-12.2013.

Takayanagi, Y., Yoshida, M., Bielsky, I.F., Ross, H.E., Kawamata, M., Onaka, T., et al. (2005). Pervasive social deficits, but normal parturition, in oxytocin receptor-deficient mice. *P Natl Acad Sci USA* 102(44), 16096-16101. doi: 10.1073/pnas.0505312102.

Tavakoli, A., Schmaltz, A., Schwarz, D., Margrie, T.W., Schaefer, A.T., and Kollo, M. (2018). Quantitative association of anatomical and functional classes of olfactory bulb neurons. *Journal of Neuroscience* 38(33), 7204-7220.

Terranova, J.P., Pério, A., Worms, P., Fur, G.L., and Soubrié, P. (1994). Social olfactory recognition in rodents: deterioration with age, cerebral ischaemia and septal lesion. *Behavioural Pharmacology* 5(1), 90-98.

Tillerson, J.L., Caudle, W.M., Parent, J.M., Gong, C., Schallert, T., and Miller, G.W. (2006). Olfactory discrimination deficits in mice lacking the dopamine transporter or the D2 dopamine receptor. *Behavioural Brain Research* 172(1), 97-105. doi: https://doi.org/10.1016/j.bbr.2006.04.025.

Tobin, V.A., Hashimoto, H., Wacker, D.W., Takayanagi, Y., Langnaese, K., Caquineau, C., et al. (2010). An intrinsic vasopressin system in the olfactory bulb is involved in social recognition. *Nature* 464(7287), 413-U110. doi: 10.1038/nature08826.

Tricklebank, M.D., and Petrinovic, M.M. (2019). "Chapter Nine - Serotonin and aggression," in *The Serotonin System,* eds. M.D. Tricklebank & E. Daly. Academic Press), 155-180.

Tschanz, B. (1962). Über die Beziehung zwischen Muttertier und Jungen beim Mufflon (Ovis aries musimon, Pall.). *Experientia* 18(4), 187-190. doi: 10.1007/bf02151723.

Ueta, Y., Fujihara, H., Serino, R., Dayanithi, G., Ozawa, H., Matsuda, K., et al. (2005). Transgenic expression of enhanced green fluorescent protein enables direct visualization for physiological studies of vasopressin neurons and isolated nerve terminals of the rat. *Endocrinology* 146(1), 406-413. doi: 10.1210/en.2004-0830.

Vaaga, C.E., Yorgason, J.T., Williams, J.T., and Westbrook, G.L. (2017). Presynaptic gain control by endogenous cotransmission of dopamine and GABA in the olfactory bulb. *Journal of Neurophysiology* 117(3), 1163-1170. doi: 10.1152/jn.00694.2016.

Vaccari, C., Lolait, S.J., and Ostrowski, N.L. (1998). Comparative Distribution of Vasopressin V1b and Oxytocin Receptor Messenger Ribonucleic Acids in Brain** Portions of the OTR mRNA distribution data were presented at the Wenner-Gren Conference, Stockholm, Sweden, 1996. This work was funded by the NIMH, NIH and by grant no. MH-01050 to CS Carter that provided partial support to C. Vaccari and E. Gournelos, who were also recipients of Howard Hughes Undergraduate Fellowships from the University of Maryland, College Park. *Endocrinology* 139(12), 5015-5033.

van Leeuwen, F., and Caffé, R. (1983). Vasopressin-immunoreactive cell bodies in the bed nucleus of the stria terminalis of the rat. *Cell and tissue research* 228(3), 525-534.

Vargas-Barroso, V., Ordaz-Sánchez, B., Peña-Ortega, F., and Larriva-Sahd, J.A. (2016). Electrophysiological Evidence for a Direct Link between the Main and Accessory Olfactory Bulbs in the Adult Rat. *Frontiers in Neuroscience* 9, 518. doi: 10.3389/fnins.2015.00518.

Veenema, A.H., Beiderbeck, D.I., Lukas, M., and Neumann, I.D. (2010). Distinct correlations of vasopressin release within the lateral septum and the bed nucleus of the stria terminalis with the display of intermale aggression. *Horm Behav* 58(2), 273-281. doi: 10.1016/j.yhbeh.2010.03.006.

Veyrac, A., Sacquet, J., Nguyen, V., Marien, M., Jourdan, F., and Didier, A. (2009). Novelty determines the effects of olfactory enrichment on memory and neurogenesis through noradrenergic mechanisms. *Neuropsychopharmacology* 34(3), 786-795.

Vinera, J., Kermen, F., Sacquet, J., Didier, A., Mandairon, N., and Richard, M. (2015). Olfactory perceptual learning requires action of noradrenaline in the olfactory bulb: comparison with olfactory associative learning. *Learning & memory* 22(3), 192-196.

Wacker, D.W., Engelmann, M., Tobin, V.A., Meddle, S.L., and Ludwig, M. (2011). Vasopressin and social odor processing in the olfactory bulb and anterior olfactory nucleus. *Ann Ny Acad Sci* 1220, 106-116. doi: 10.1111/j.1749-6632.2010.05885.x.

Wamsley, J.K., Zarbin, M.A., and Kuhar, M.J. (1984). Distribution of Muscarinic Cholinergic High and Low Affinity Agonist Binding-Sites - a Light Microscopic Autoradiographic Study. *Brain Research Bulletin* 12(3), 233-243. doi: Doi 10.1016/0361-9230(84)90051-0.

Wersinger, S.R., Temple, J.L., Caldwell, H.K., and Young, W.S., 3rd (2008). Inactivation of the oxytocin and the vasopressin (Avp) 1b receptor genes, but not the Avp 1a receptor gene, differentially impairs the Bruce effect in laboratory mice (Mus musculus). *Endocrinology* 149(1), 116-121. doi: 10.1210/en.2007-1056.

Willhite, D.C., Nguyen, K.T., Masurkar, A.V., Greer, C.A., Shepherd, G.M., and Chen, W.R. (2006). Viral tracing identifies distributed columnar organization in the olfactory bulb. *Proceedings of the National Academy of Sciences* 103(33), 12592-12597.

Williams, J.R., Slotnick, B.M., Kirkpatrick, B.W., and Carter, C.S. (1992). Olfactory-Bulb Removal Affects Partner Preference Development and Estrus Induction in Female Prairie Voles. *Physiology & Behavior* 52(4), 635-639. doi: 10.1016/0031-9384(92)90390-N.

Wilson, D.A., Fletcher, M.L., and Sullivan, R.M. (2004). Acetylcholine and olfactory perceptual learning. *Learning & Memory* 11(1), 28-34. doi: 10.1101/lm.66404.

Winslow, J.T. (2003). Mouse Social Recognition and Preference. *Current Protocols in Neuroscience* 22(1), 8.16.11-18.16.16. doi: https://doi.org/10.1002/0471142301.ns0816s22.

Xiong, W., and Chen, W.R. (2002). Dynamic Gating of Spike Propagation in the Mitral Cell Lateral Dendrites. *Neuron* 34(1), 115-126. doi: https://doi.org/10.1016/S0896-6273(02)00628-1.

Yokoi, M., Mori, K., and Nakanishi, S. (1995). Refinement of Odor Molecule Tuning by Dendrodendritic Synaptic Inhibition in the Olfactory-Bulb. *P Natl Acad Sci USA* 92(8), 3371-3375. doi: 10.1073/pnas.92.8.3371.

Yuan, Q., Harley, C.W., and McLean, J.H. (2003). Mitral cell β1 and 5-HT2A receptor colocalization and cAMP coregulation: A new model of norepinephrine-induced learning in the olfactory bulb. *Learning & memory* 10(1), 5-15. doi: 10.1101/lm.54803.

Zaborszky, L., Carlsen, J., Brashear, H., and Heimer, L. (1986). Cholinergic and GABAergic afferents to the olfactory bulb in the rat with special emphasis on the projection neurons in the nucleus of the horizontal limb of the diagonal band. *Journal of Comparative Neurology* 243(4), 488-509.

Zhou, Z., Xiong, W., Zeng, S., Xia, A., Shepherd, G.M., Greer, C.A., et al. (2006). Dendritic excitability and calcium signalling in the mitral cell distal glomerular tuft. *European Journal of Neuroscience* 24(6), 1623-1632. doi: https://doi.org/10.1111/j.1460-9568.2006.05076.x.

Zhu, X.O., Brown, M.W., Mccabe, B.J., and Aggleton, J.P. (1995). Effects of the Novelty or Familiarity of Visual-Stimuli on the Expression of the Immediate-Early Gene C-Fos in Rat-Brain. *Neuroscience* 69(3), 821-829. doi: 10.1016/0306-4522(95)00320-I.

Zhuo, M., Small, S., Kandel, E., and Hawkins, R. (1993). Nitric oxide and carbon monoxide produce activity-dependent long-term synaptic enhancement in hippocampus. *Science* 260(5116), 1946-1950. doi: 10.1126/science.8100368.

Zimnik, N.C., Treadway, T., Smith, R.S., and Araneda, R.C. (2013). α 1A - Adrenergic regulation of inhibition in the olfactory bulb. *The Journal of physiology* 591(7), 1631-1643. doi: 10.1113/jphysiol.2012.248591.

Zingg, H.H., and Laporte, S.A. (2003). The oxytocin receptor. *Trends in Endocrinology & Metabolism* 14(5), 222-227. doi: https://doi.org/10.1016/S1043-2760(03)00080-8.

7: Acknowledgements

First and foremost, I would love to thank my PhD supervisor, Dr. Michael Lukas for everything he did for me since I came to Regensburg. He supported and guided me throughout my work. Importantly, he has been there as a friend outside of the lab as well. That helped me a lot for work in a totally new environment. Therefore, I could focus on my work and actively ask him for comments or discuss my data with him, and now successfully finish my thesis.

I also thank everyone in our group AG Egger, Prof. Dr. Veronica Egger, Dr. Max Müller, and Dr. Luna Jammal for valuable conversations about science in office and lab meetings and for creating a good atmosphere in our working place. I cannot thank Anne Pietryga-Krieger enough for her warm support for us, including animal care and preparing the solutions that are essential for our work.

I would like to thank my PhD mentors, Prof. Dr. Veronica Egger and Dr. Wolfgang Kelsch for their guidance during the PhD program of the Regensburg International Graduate School of Life Sciences. I sincerely appreciate their comments and advice, especially in the annual progress reports.

I wish to thank the whole AG Neumann and AG Flor for friendly conversations in and outside of the lab.

I especially thank my father, mother, and sister for their support throughout my PhD work from the other side of the continent.

日本にいる父、母、妹に心より感謝を申しあげます。ドイツへ来ることを後押ししてくれたこと、ドイツでも日本でもサポートしてくれたこと、ありがとうございました。

最後に、実験に供された動物達に心よりの感謝を表するとともに、ご冥福をお祈りいたします。